ELECTROCHEMICALLY CONTROLLED DETECTION OF CATECHOLAMINES ON POLY(2-AMINOBENZYLAMINE) THIN FILMS BY SURFACE PLASMON RESONANCE SPECTROSCOPY

SOPIS CHUEKACHANG

DOCTORAL PROGRAM IN ELECTRICAL AND INFORMATION ENGINEERING

GRADUATE SCHOOL OF SCIENCE AND TECHNOLOGY

NIIGATA UNIVERSITY

Thesis Title	Electrochemically Controlled Detection of Catecholamines on Poly(2-aminobenzylamine) Thin Films by Surface Plasmon Resonance Spectroscopy
Author	Mr. Sopis Chuekachang
Degree	Doctor of Philosophy (Electrical and Information Engineering)

ABSTRACT

In this study, we present an electrochemically controlled surface plasmon resonance (EC-SPR) biosensor to detect some biomolecules on poly(2-aminobenzylamine) (P2ABA) thin films. The P2ABA thin films are stable and display electroactivity in a neutral PBS solution. Specific detection of adrenaline was performed on P2ABA thin films because the benzylamine groups in the P2ABA structure could specifically react with adrenalines. Adrenaline was detected in real time by EC-SPR spectroscopy, which provides an electrochemically controlled SPR reflectivity change on the P2ABA thin film upon adrenaline injection. The measured responses were quite different from those for uric acid and ascorbic acid, which are

major interferences in adrenaline detection. The electrochemically applied potential facilitates the specific detection of adrenaline. In addition, the detection of adrenaline on the P2ABA thin films was investigated by a quartz crystal microbalance technique. The detection limit for adrenaline at open circuit potential was 10 pM.

Moreover, the P2ABA thin films were characterized by UV-vis absorption spectroscopy, FTIR/ATR, AFM and QCM-D techniques**.**

TABLE OF CONTENTS

Page

Acknowledgements iii

Abstract v

List of tables xii

List of figures xiii

Abbreviations and Symbols xx

Chapter 1 Introduction 1

1.1 Conducting polymers 1

1.1.1 Conduction mechanisms 3

1.1.2 Synthesis of conducting polymers 5

1.1.3 Step-growth polymerization 6

1.1.4 Chain-growth polymerizations 7

1.1.5 Ring-opening metathesis polymerization 7

1.1.6 Electrochemical synthesis 8

1.1.7 Polyaniline 10

1.1.8 Electrochemical set up 13

1.1.8.1 Working electrodes or indicator electrodes 14

1.1.8.2 Counter or auxiliary electrode 15

TABLE OF CONTENTS (Continued)

Page

1.1.8.3 Reference electrodes 15

1.1.8.4 Silver/silver chloride reference electrode 16

1.1.8.5 Saturated calomel reference electrode 16

1.1.8.6 Pseudo-reference electrode 17

1.1.8.7 Silver/silver ion electrode 17

1.1.8.8 Electrolyte solution 18

1.2 Cyclic voltammetry 19

1.2.1 Cyclic voltammetry primer 20

1.2.2 Mechanistic complications 23

1.2.2.1 Nernstian (reversible) behavior 23

1.2.2.2 The Electrochemical Chemical (EC) mechanism 26

1.2.2.3 Dealing with an EC mechanism 27

1.3 Surface Plasmon Resonance Spectroscopy 29

1.3.1 Theoretical background 29

1.3.2 The architecture of experimental setup 30

1.3.3 SPR for investigation of the adsorption processes 32

1.3.4 Electrochemical-Surface Plasmon Resonance Spectroscopy (EC-SPR) 35

TABLE OF CONTENTS (Continued)

Page

1.4 Biomolecules (such as catecholamine, uric acid and ascorbic acid) 36

1.4.1 Catecholamine 36

1.4.2 Adrenaline 40

1.4.3 Uric acid 42

1.4.4 Ascorbic acid 44

1.5 Literature review 46

1.8 Research objectives 65

Chapter 2 Experimental 66

2.1 Chemicals 66

2.2 Instruments 67

2.2.1 Thermal evaporator 69

2.3 Electropolymerization of 2ABA on gold electrode 70

2.4 Characterization of the P2ABA thin films 71

2.4.1 Quartz crystal microbalance with dissipation (QCM-D) measurement 71

2.4.2 UV-vis absorption properties of P2ABA thin film 72

2.4.3 Fourier transforms infrared spectroscopy attenuated total reflectance (FTIR/ATR) 72

TABLE OF CONTENTS (Continued)

Page

2.4.3.1 KBr Spectra determinations 73

2.4.3.2 ATR Spectra determinations 74

2.4.4 Atomic Force Microscopy (AFM) Analysis 74

2.5 Detection of adrenaline on the P2ABA thin films 75

2.6 Detection of adrenaline in the presence of UA and AA 76

2.7 Method 76

Chapter 3 Results and discussion 77

3.1 Fabrication of P2ABA thin film by EC-SPR 77

3.1.1 EC-SPR measurement for electropolymerization of 2ABA 77

3.1.2 Electrochemical behavior of P2ABA thin film 79

3.1.3 Study of an active surface P2ABA film 81

3.1.4 Detection of adrenaline on the P2ABA thin film 83

3.1.5 Detection limit 91

3.1.6 Efficiency of P2ABA thin film 93

3.1.7 SPR reflectivity change of P2ABA film before and after detection of adrenaline, UA and AA 94

TABLE OF CONTENTS (Continued)

Page

3.2 Characterization of P2ABA thin films 97

3.2.1 QCM-D measurement 97

3.2.2 UV-vis absorption properties of P2ABA thin film before and after adsorption of adrenaline 100

3.2.3 Atomic force microscopy (AFM) analysis 102

3.2.4 Fourier transforms infrared spectroscopy attenuated total reflectance (FTIR/ATR) analysis 103

Chapter 4 Conclusion 106

References 110

Curriculum Vitae 123

LIST OF TABLES

Table		Page
1.1	Chemical structures of some of the most common conjugated polymers	2
1.2	Comparison of chemical and electrochemical CPs polymerization	6
2.1	Chemical, purity, molecular formula, molecular weight and company	66

LIST OF FIGURES

Figure		Page
1.1	Band structure in an electronically conducting polymer	3
1.2	General schemes for a ring-opening polymerization	8
1.3	Mechanism for heterocycle polymerization via electrochemical synthesis X= NH, S, or O. This pathway is initiated by the oxidation of a monomer at the working electrode to give a cation species, which can react with a neutral monomer species or radical cation oligomeric species to generate the polymer Common vinyl polymers synthesized by chain-growth polymerization	10
1.4	Main PANI structure n + m = 1, x = degree of polymerization	10
1.5	PANI (emeraldine) salt in the alkaline medium convert to PANI (emeraldine) base. A^- is an alkali ion	11
1.6	Electropolymerization setup	14
1.7	Normal wave form of cyclic voltammetry	21
1.8	The basic shape of the current response for a cyclic voltammetry	22
1.9	Cyclic voltammograms for ferrocene carboxylic acid at different scan rate	24
1.10	The basic shape of cyclic voltammograms of EC mechanism with different different first-order rate constant (k_f)	25

LIST OF FIGURES (Continued)

Figure		Page
1.11	The basic shape of cyclic voltammograms of EC mechanism with different scan rates	27
1.12	The basic shape of cyclic voltammograms of EC mechanism with different scan rates	29
1.13	Two concept for experimental setup of surface plasmon resonance spectroscopy (a) The Otto-configuration (b) Kretschman configuration with attenuated total internal reflection (ATR) construction	32
1.14	Schematic of the experimental system for SPS reflectivity curve obtained from a bare Au-film and self-assembled monolayer	34
1.15	Schematic diagram showing the experimental set up of EC-SPR	35
1.16	Chemical structure of catechol and catecholamines	37
1.17	Synthesis of catecholamines (adrenaline, noradrenaline, dopamine) from tyrosine	38
1.18	Chemical structure of uric acid	42
1.19	Chemical structure of ascorbic acid	45
1.20	Chemical structure of (a) ascorbic acid (reduced form of Vitamin C) and (b) dehydroascorbic acid (oxidized form of Vitamin C)	46

LIST OF FIGURES (Continued)

Figure		Page
2.1	EC-SPR instrument setup	68
2.2	Schematic diagram showing vacuum evaporation device	69
2.3	Immobilization of P2ABA thin film on gold film electrode by electropolymerization of 50 mM 2ABA monomer in 0.5 M H_2SO_4 followed by cycling the potential between –0.2 and 0.1 V vs. Ag/AgCl for 10 cycles at a scan rate 20 mV/s	70
2.4	QCM-D instrument	71
2.5	V-650 UV-vis Spectrophotometer	72
2.6	FTIR/ATR instrument	73
2.7	ATR measurement	74
2.8	Block diagram of AFM	75
3.1	Cyclic voltammograms of 50 mM 2ABA monomer on gold electrode by cycling the potential between –0.2 and 0.1 V vs. Ag/AgCl for 10 cycles at a scan rate of 20 mV/s to form P2ABA film	78
3.2	Angular-reflectivity curves before and after electropolymerization of P2ABA thin film on gold-coated high reflective index glass substrate	78

LIST OF FIGURES (Continued)

Figure		Page
3.3	(a) CV of P2ABA film at a different scan rates in PBS solution and (b) the plots of anodic peak currents with scan rate	79
3.4	SPR angular curves of P2ABA film in PBS solution at several constant applied potentials	80
3.5	SPR reflectivity response upon injection of 1 mM adrenaline into P2ABA film at constant applied potentials of –0.2 V and 0.5 V	81
3.6	CV traces after completing detection adrenaline at constant applied potentials of (a) –0.2 V and (b) 0.5 V	83
3.7	The specific reaction of adrenaline to P2ABA film	84
3.8	SPR reflectivity responses upon injection of 1 mM adrenaline into P2ABA and PANI thin film at (a) constant potentials of 0.5 V and (b) an open circuit potential	85
3.9	The current response upon injection of 1 mM adrenaline into P2ABA and PANI thin film at a constant applied potential of 0.5 V	86
3.10	SPR reflectivity and current response upon injection of 1 mM adrenaline into P2ABA and PANI thin film at a constant applied potential of –0.2 V	87

LIST OF FIGURES (Continued)

Figure		Page
3.11	SPR reflectivity response after injection 1 mM each of adrenaline, UA and AA into P2ABA thin film at a constant applied potential of 0.5 V	88
3.12	The SPR reflectivity result of P2ABA film after reaction with 1 mM each of adrenaline, UA and AA at constant applied potentials of (a) –0.2 V and (b) an open circuit potential	90
3.13	SPR reflectivity responses upon injection of 1 mM adrenaline into P2ABA thin film at −0.2, open circuit potential, and 0.5 V	91
3.14	SPR reflectivity response upon injection of 1 mM to 10 pM adrenaline into P2ABA thin film at an open circuit	92
3.15	Calibrated double-logarithmic plots of the change of the reflectivity as a function of adrenaline concentration	93
3.16	Simultaneous observation of SPR reflectivity response upon injection of 1 mM adrenaline, AA and UA into P2ABA thin film at an open circuit potential	94
3.17	SPR reflectivity of P2ABA film before and after injection of 1mM adrenaline at a constant applied potential of 0.5V	95

LIST OF FIGURES (Continued)

Figure		Page
3.18	SPR reflectivity of P2ABA film before and after injection of 1mM UA at a constant applied potential of 0.5V	95
3.19	SPR reflectivity of P2ABA film before and after injection of 1mM AA at a constant applied potential of 0.5V	96
3.20	The plot of SPR reflectivity change of P2ABA film in PBS solution after the injection of 1mM adrenaline at constant applied potentials of –0.2, open circuit, 0.2, 0.3 and 0.5V	97
3.21	QCM-D response upon injection of 1 mM, 100 µM, 10 µM, and1 µM adrenaline into P2ABA thin film at an open circuit potential	98
3.22	QCM-D response upon injection of 1 mM adrenaline into P2ABA thin film compared with UA and AA at an open circuit potential	99
3.23	Plots the change of the QCM frequency as a function of concentration	99
3.24	(a) UV-vis spectrum of each material in PBS solution and (b) UV-vis spectrum of P2ABA after the reaction with 1mM each of adrenaline, UA and AA at a constant applied potential of 0.5 V	101
3.25	AFM images of P2ABA film (a) after binding reaction with adrenaline at constant applied potentials of (b) –0.2 V, (c) open circuit and (d) 0.5 V	103

LIST OF FIGURES (Continued)

Figure		Page
3.26	FTIR/ATR spectra of bare gold and P2ABA thin film	105
3.27	FTIR/ATR spectra of P2ABA thin film after the reaction with 1 mM adrenaline at an open circuit potential	105

ABBREVIATIONS AND SYMBOLS

Å	Angstrom
AA	Ascorbic acid
AFM	Atomic force microscopy
*a*mol	Attomol (10^{-18} mol)
ATR	Attenuated Total Internal Reflection
A-IgG	Anti-human Immunoglobulin G (Feb specific)
BLM	Bilayer lipid membrane
°C	Celsius degree
CA	Catecholamine
CP	Conjugated polymer
CPE	Carbon paste electrode
CV	Cyclic voltammetry
CTAB	Cation surfactant cetyltrimethyl ammonium bromide
DA	Dopamine
EC-SPR	Electrochemical-surface plasmon resonance
EC-QCM	Electrochemical quartz crystal microbalance
E_g	Energy gap
EA-HCl	Ethanolamine hydrochloride

EDC	1-ethyl-3-(3-dimethylaminopropyl)-carbodiimide Hydrochloride
e.g.	Exempli gratia (for example)
FETs	Field effect transistors
FTIR/ATR	Fourier transforms infrared spectroscopy attenuated total reflectance
*f*mol	A billion of a millionth (10^{-15}) of a mole (femtomole)
HOMO	Highest occupied molecular orbital
hr.	Hour
ICP	Intrinsically conductive polymer
IgG	Immunoglobulin G
ITO	Indium-Tin Oxide
k_f	First order rate constant
LbL	Layer by layer
LUMO	Lowest occupied molecular orbital
µm	Micrometer
mL	Milliliter
mV/ sec	Millivolt/second
min	Minute
M	Molarity
nM	Nanomolar

NHS	*N*-hydroxysuccinimide
OLEDs	Light-emitting diodes
PANI	Polyaniline
P3HT	Poly(3-hexylthiophene-2,5diyl)
PBS	Phosphate buffer saline
P2ABA	Poly(2-aminobenzylamine)
P2ABA/SWNTs	Poly(2-aminobenzylamine)/single wall carbon nanotube
P2ABA/ZnO nanoparticles	Poly(2-aminobenzylamine)/ZnO nanoparticles
PEDOT	Poly(3,4-ethylenedioxythiophene)
pM	Picomolar
PPy	Polypyrrole
PPy/PPa	Poly(pyrrole-co-pyrrolepropylic acid)
PT	Polythiophene
QCM-D	Quartz crystal microbalance with dissipation
ROMP	Ring-opening metathesis polymerization
sec	Second
SAMs	Self-assembled monolayers
SPR	Surface plasmon resonance
UA	Uric acid
UV-vis	Ultraviolet-visible
V	Volts

XPS	X-ray photoelectron spectroscopy
λ	Wavelength

CHAPTER 1

INTRODUCTION

There are five parts in this chapter consisting of the background of conducting polymers (CPs), cyclic voltammetry (CV), surface plasmon resonance spectroscopy (SPR) technique, some biomolecules (such as catecholamine (CA), uric acid (UA) and ascorbic acid (AA)) and literature review.

1.1 Conducting polymers [1–10]

Conducting polymers (CPs) are the exciting new class of electronic materials so called the intrinsically conductive polymer (ICPs) or electroactive polymer. The CPs have both electrical and optical properties plus a high conductivity, which can be changed by simple oxidation or reduction [1]. In 1967, a postgraduated student of Shirakawa at Tokyo Institute of Technology synthesized the polyacetylene using Ziegler-Natta catalysts, and a silvery thin film was produced by mistake. When this material under investigation the properties were found to be similar to that of semiconductor. Polyacetylene was doped by oxidation with halogen (iodine) referred to as p-doping or/and reduction with alkaline metal (sodium) as n-doping. In 1977, MacDiarmid et al. reported the large increase in conductivity of polyacetylene after doping with iodine that the first of ICPs was recognized, and the team received the Nobel Prize in Chemistry in 2000 [2]. The CPs have the potential of combining the high conductivity of pure metals with the processability and good corrosion stability

when contract with solution or/and in the dry state. Furthermore, they have many field applications, depending on the specific ionic and electronic resistances, such as polymer battery [3], electrochromic displays [4], light emitting diodes [5], and biosensor [6–9]. The CPs such as polypyrrole, polythiophene, polyaniline and their derivatives are used for biosensor application. Polyaniline (PANI) has been extensively studied polymer due to its high electrical conductivity, environmental stability and ease synthesize [10, 11]. Chemical structures of some of the most common conjugated polymers are shown in Table 1.1 [1, 12]. Conjugated polymers derive their semiconducting properties by having delocalized π-electron bonding along the polymer chain [13, 14].

Table 1.1 Chemical structures of some of the most common conjugated polymers [1, 12].

Name structure	Structure
Polyacetylene	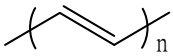
Polypyrrole	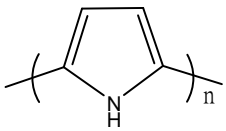
Polythiophene	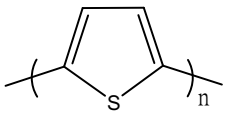
Polyaniline	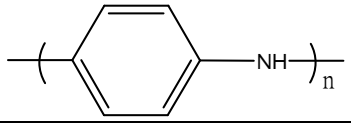
Poly(phenylenevinylene)	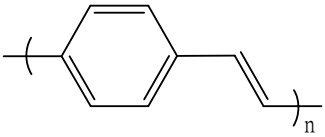

The extensive delocalization of the π-electron is well known to be responsible for the array of remarkable characteristic that these polymers tend to exhibit. These characteristic of polymer has been exploited for application in thin film technology field.

1.1.1 Conduction mechanisms [15–20]

To explain the mechanism of conductivity in CPs, a band theory has been used as shown in Figure 1.1. According to band theory [15, 16], the electrical properties of direct gap conductive materials are determined by their electronic structures, and the electrons move within discrete energy states called bands. By analogy, the bonding and antibonding π-orbitals of the sp^2 hybridized π-electron materials (e.g. polyenes) generate energy bands, which are fully occupied (π-band) and empty (π*-band). The highest occupied band is called the valence band, and the lowest unoccupied band is the conduction band. The energy difference between them is called the band gap. Electrons must have certain energy to occupy a given band and need extra energy to move from the valence band to the conduction band. Moreover, the bands should be partially filled in order to be electrically conducting, as neither empty nor full bands can carry electricity.

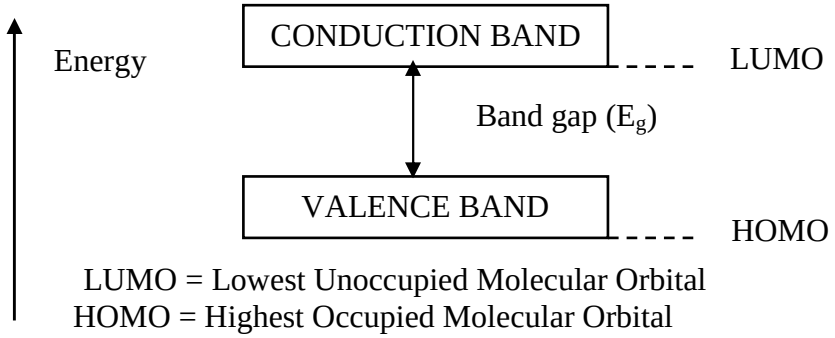

Figure 1.1 Band structure in an electronically conducting polymer [15, 16].

Electronically conducting polymers are extensively conjugated molecules that they possess a spatially delocalized band-like electronic structure [17]. These bands stem from the splitting of interacting molecular orbitals of the constituent monomer units in a manner reminiscent of the band structure of solid-state semiconductors [18]. It is generally agreed that the mechanism of conductivity in these polymers is based on the motion of charged defects with in the conjugated framework. The charge carriers, either positive p-type or negative n-type, are the products of oxidizing or reducing the polymer respectively. The following overview describes these processes in the context of p-type carriers although the concepts are equally applicable to n-type carriers. Oxidation of the polymer initially generates a radical cation with both spin and charge. Borrowing from solid state physics terminology, these species are referred to as a polaron and comprises both the hole site and the structural distortion which accompanies it. The cation and radical form a bound species, since any increase in the distance between them would necessitate the creation of additional higher energy quinoid units. Theoretical treatments have demonstrated that two nearby polarons combine to form the lower energy bipolaron [19, 20]. One bipolaron is more stable than two polarons despite the coulombic repulsion of the two ions. Since the defect is simply a boundary between two moieties of equal energy, the infinite conjugation chain on either side, it can migrate in either direction without affecting the energy of the backbone, provided that there is no significant energy barrier to the process. It is this charge carrier mobility that leads to the high conductivity of these polymers. The conductivity, σ of a conducting polymer is related to the number of charge carriers n and their mobility. Because the band gap of conjugated polymers is usually fairly large, n is very small under ambient conditions.

Consequently, conjugated polymers are insulators in their neutral state and no intrinsically conducting organic polymer is known at this time. A polymer can be made conductive by oxidation (p-doping) and/or, less frequently, reduction (n-doping) of the polymer either by chemical or electrochemical means, generating the mobile charge carriers described earlier.

1.1.2 Synthesis of conducting polymers [1, 21]

There are numerous synthetic techniques used in the synthesis of conducting polymers. CPs can be synthesized either chemically or electrochemically, with each having advantages and disadvantages as summarized in Table 1.2 [1]. Since most conjugated polymer cannot be dissolved or melted, they must be synthesized directly in desired shape and location. This necessity has frustrated many researchers since the form; most importantly the morphology of the conjugated polymer has one of the greatest influences on many of the properties, most notably the electrical conductivity of the doped polymer. Theory and experiment have placed much emphasis on justifying the formation of mobile, delocalized carriers within the polymer chains (polarons, bipolarons, solitons) [1, 21]. However, since no one polymer strand is long enough to persist over a macroscopic length, the measured conductivity of a polymer sample requires that carriers hop between polymer strands. This hopping is widely believed to limit the bulk conductivity. Synthesis of highly conductive polymer samples has become an art in some circles since small changes in synthesis, catalyst removal, or doping can dramatically affect sample morphology and result in wide variation in conductivity.

Table 1.2 Comparison of chemical and electrochemical CPs polymerization [1].

Polymerization approach	**Advantages**	**Disadvantages**
Chemical polymerization	• Larger-scale production possible • Post-covalent modification of bulk CP possible • More options to modify CP backbone covalently	• Cannot make thin films • Synthesis more complicated
Electrochemical polymerization	• Thin film synthesis possible • Ease of synthesis • Entrapment of molecules in CP • Doping is simultaneous	• Difficult to remove film from electrode surface • Post-covalent modification of bulk CP is difficult

1.1.3 Step-growth polymerization [21]

Probably the most common method of chemical synthesis of conjugated polymer is via a step-growth polymerization. Before the advent of the continuous electrochemical synthesis, this method was the only way to make a large amount of polymers such as polythiophene. These polymerizations require a high-yield reaction to proceed to a high degree of polymerization. However, in principle, any monomer that can be oxidatively polymerized electrochemically can be polymerized using a chemical oxidant (e.g. $FeCl_3$) as well. If the resulting polymer is insoluble, the end of

the polymerization may occur in the solid state. This serious limitation is avoided in the synthesis of soluble conjugated polymers. The example of this type of polymerization is the synthesis of polythiophene and its derivatives. The most commonly performed using a nickel catalyzed couplings, a polymerization based on Friedel-Crafts alkylation, coupling of the di-halide using a Ni(0) catalyst, and direct oxidation with $FeCl_3$ are employed as well [21].

1.1.4 Chain-growth polymerizations [21]

Chain-growth polymerizations are useful in the synthesis of conjugated polymers because polymer properties can often be tailored by the selection of catalyst system and because higher molecular weight polymers can be synthesized at a lower degree of conversion of monomer, a point which is particularly attractive when it is necessary to form an insoluble polymer [21]. It has already been pointed out that several conjugated “polymer” are suspected to be oligomers, particularly oxidatively coupled polyparaphenylene, and it is frustrating when the validity of a study must be questioned because it is unclear whether the material under study is really polymeric in nature. Although many would argue that molecular weight has little to do with polymer properties, this promise has little or no experimental verification. Moreover, some of these conjugated polymers are attracting interest as high strength materials, and polymer strength is certainly dependent upon molecular weight.

1.1.5 Ring-opening metathesis polymerization [19, 21]

Ring-opening polymerization can follow either a step-growth or chain growth mechanism and involves the breaking of bond in a ring to form an open-chain intermediate (Figure 1.2). Ring-opening metathesis polymerization (ROMP) involves

the use of a transition metal carbene complex to cut open a cyclic olefin molecule and “stitch” these molecules back together into a polymer chain [19]. This polymerization is of great interest for the synthesis of conjugated polymers because, among other factors, the number of double bonds in the monomer is preserved in the polymer, and because, in principle one can take the repeat unit for any conjugated polymer containing an olefin and cyclize it to form a potential new monomer. Synthetic scheme for ring-opening metathesis polymerization was reported [21]. This polymerization has been very successfully used to form several precursor polymers. However, ROMP has been applied to direct synthesis of conjugated polymers as well.

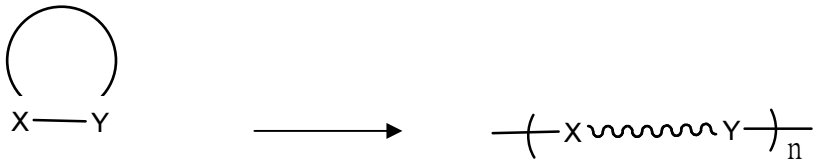

Figure 1.2 General schemes for a ring-opening polymerization [19].

1.1.6 Electrochemical synthesis [19, 22]

Most conjugated polymers are synthesized by electrochemical means. Pyrrole, thiophene and their derivatives are often polymerized in this manner as are carbazoles, azulenes and pyrenes. Typically, this oxidation is accomplished by placing in the monomer and electrolyte in a suitable solvent such as acetronitrile and oxidizing at a mind potential. A polymer film grows at the anode in a reaction. In principle, any trace species that can react with the propagating radical cation can terminate one end of the polymer. Any polymer chain that does not re-oxidize is effectively terminated as well. The kinetics of this polymerization was expected to be complex. Among other factors, the reaction occurs in a heterogeneous environment, and the polymerization is based upon coupling of the radical cations which can occur

between the oxidized forms of any combination of monomers and polymer chains. New polymers synthesized by this procedure continue to be reported as new oxidizable conjugated units become available [19]. The monomer is electrochemically oxidized at a polymerization potential giving rise to free radicals. These radicals are adsorbed onto the electrode surface and undergo subsequently a wide variety of reactions leading to the polymer network. The electropolymerization should preferably occur in aqueous solution with a neutral pH in order to be incorporated into the polymer film in a suitable form. The growth of this polymer depends on its electrical character. If the polymer is electrically non-conducting, its growth is self-limited. Such films are very thin (10–100 nm). In contrast, the growth of conductive polymers is virtually unlimited. The process is governed by the electrode potential and by the reaction time, which allowing controlling the thickness of the resulting film. The polymerization occurs locally and strictly on the electrode surface. This is particularly suitable for the coating of microelectrodes and microelectrode arrays. In addition, the combination of different conducting or non-conducting polymers allows the building of multilayer structures with extremely low thickness leading to fast responding sensors with reduced interferences. The film can be generated by cycling the potential (potentiodynamically) or at a fixed potential (potentiostatically). Polypyrrole was used for the immobilization of a wide number of enzymes, mainly onto the Pt electrode. The mechanism of the polymerization process, occurring at potentials above +600 mV, is shown in Figure 1.3. The morphology of the film depends on the nature of the electrolyte, the crystallographic structure of the underlying electrode, the speed and the potential of the deposition, the presence of

anions and polyanions or surfactants, the concentration of the monomer, and the pH of the solution.

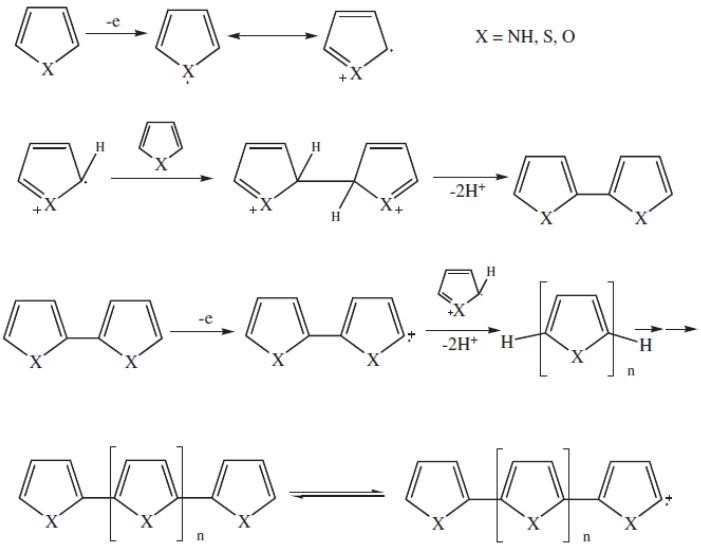

Figure 1.3 Mechanism for heterocyclic polymerization via electrochemical synthesis. X= NH, S, or O. This pathway is initiated by the oxidation of a monomer at the working electrode to give a cation species, which can react with a neutral monomer species or radical cation oligomeric species to generate the polymer [22].

1.1.7 Polyaniline [23–30]

The primary structure of polyaniline (PANI) consists of benzenoid rings with an imine (sp^2 hybridized state) and quinoid rings with an amine (sp^3 hybridized state) as shown in Figure 1.4.

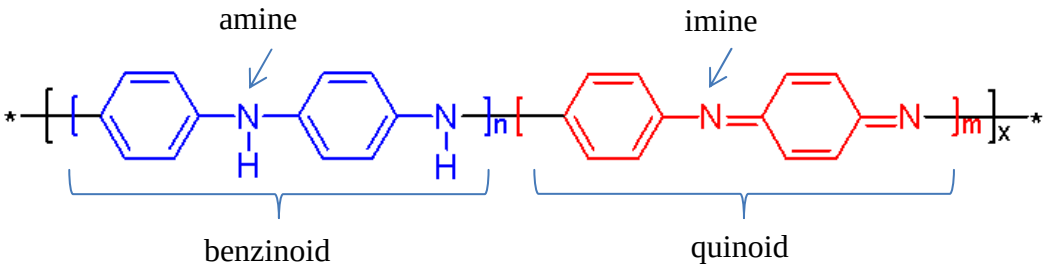

Figure 1.4 Main PANI structure n + m = 1, x = degree of polymerization [23].

Polyaniline (PANI) is one of CPs has been known and studied extensively since the 1980s [23]. PANI and their derivatives has received considerable attention due to the electrochemical and optical properties with its many attractive properties such as specific binding site, low cost, easily synthesized, environmental stability and potential application in biosensor [24]. The properties of PANI film depend on the oxidation and the protonation state of the film. PANI film was deprotonation and loss in electroactivity at pH higher than 4 [9]. PANI has three main stable oxidation states range from fully reduce leucoemeraldine (n = 1, m = 0) is found to be insulating and yellow color. The half-oxidized is called emeraldine (n = m = 0.5). The most common green protonate emeraldine salt has conductivity on a semiconductor and convert to a non-conducting blue emeraldine base when treated with ammonium hydroxide solution [25] as shown in Figure 1.5.

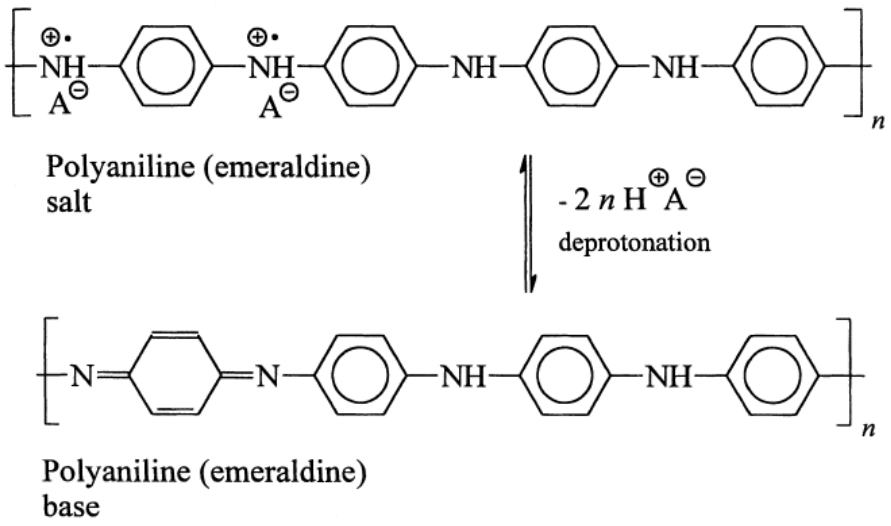

Figure 1.5 PANI (emeraldine) salt in the alkaline medium convert to PANI (emeraldine) base. A^- is an alkali ion [25].

The fully oxidized pernigraniline (n = 0, m = 1) is insulating and violet color. The color change of each three oxidation state of PANI can be used in sensor and electrochromic devices [26]. The doping in polymer to conductive form is an oxidation (p-type doping, withdraw electron from polymer chain) or reduction (n-type doping, add electron into polymer chain) process, rather than atom replacement in inorganic semiconductors. In the case of PANI oxidation, the halogen molecule attracts an electron from the PANI and PANI become positive charged. The CPs does not have only π-conjugated chain but also containing counter-ions caused by doping. The insulating π-conjugated polymers can be converted to conducting polymers by a chemical or electrochemical doping and which can be consequently returned to insulate state by de-doping. This suggests that not only de-doping can take place in CPs, but also reversible doping/de-doping process, which is different from inorganic semiconductor where de-doping can't take place [27]. The electronic properties of PANI and their derivatives were opened a large window for the biosensor applications.

Conducting polymers (CPs) have numerous (bio)analytical and technological applications. CPs are easily synthesized and deposited onto the conductive surface of a given substrate from monomer solutions by electrochemical polymerization with precise electrochemical control of their formation rate and thickness. Coating electrodes with CPs under mild conditions opens up enormous possibilities for the immobilization of biomolecules and bioaffinity or biorecognizing reagents, improve of their electrocatalytic properties, rapid electron transfer and direct communication to produce a range of analytical signals and new analytical applications [1, 28–30].

1.1.8 Electrochemical set up [31–34]

An electrochemical cell must consist of at least two electrodes and one electrolyte. An electrode may be considered to be an interface at which the mechanism of charge transfer changes between electronic (movement of electrons) and ionic movement of ions. An electrolyte is a medium through which charge transfer can take place by the movement of ions. An electrochemical cell is containing a working electrode, a counter electrode, and a reference electrode is shown in Figure 1.6. In all electrochemical experiments, the reactions of interest occur at the surface of the working electrode. Therefore, in controlling the potential drop across the interface between the surface of the working electrode and the solution (i.e., the interfacial potential) is the prime interest. However, it is impossible to control or measure this interfacial potential without placing another electrode in the solution. Thus, two interfacial potentials must be considered, neither of which can be measured independently. Hence, one requirement for this counter electrode is that its interfacial potential remains constant, so that any changes in the cell potential produce identical changes in the working electrode interfacial potential. An electrode whose potential does not vary with current is referred to an ideal non-polarizable electrode, and is characterized by a vertical region on a current vs potential plot. However, there is no electrode that behaves in this way (although some approach ideal non-polarizable behavior at low currents). Consequently, the interfacial potential of the counter electrode in the two-electrode system discussed above varies as current is passed through the cell. This problem is overcome by using a three-electrode system, in which the functions of the counter electrode are divided between the reference and auxiliary electrodes; that is, the potential between the working and reference

electrodes is controlled and the current passes between the working and auxiliary electrodes. The current passing through the reference electrode is further diminished by using a high-input-impedance operational amplifier for the reference electrode input. A current may flow between the working and counter electrodes, while the potential of the working electrode is measured against the reference electrode. This setup can be used in basic research to investigate the kinetics and mechanism of the electrode reaction occurring on the working electrode surface, or in electroanalytical applications.

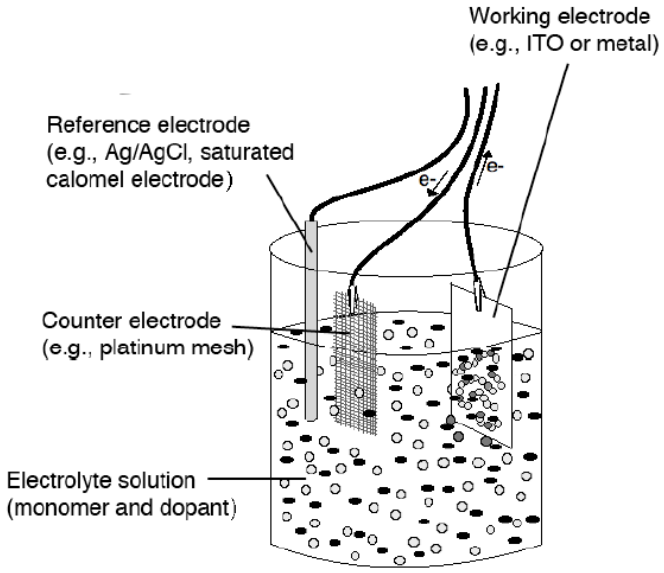

Figure 1.6 Electropolymerization setup[22].

1.1.8.1 Working electrodes or indicator electrodes [32–34]

This is the electrode at which the electrochemical phenomena being investigated takes place. There are a number of noble metal electrodes currently available for voltammetric studies. The frequently use electrodes are platinum, gold and silver followed occasionally by palladium, rhodium and iridium. Various polycrystalline forms including sheets, rods and wires are commercially available in high purity and

the materials are readily machined into useful shapes. All of the noble metals have an over potential for hydrogen evolution. The noble metal electrodes adsorb hydrogen on their surfaces although gold does so to a lesser extent. Palladium adsorbs hydrogen into the bulk metal in appreciable quantities and is not recommended for use as a cathode in protic solvents. As an inert electrode material, carbon is useful for both oxidation and reduction reaction either aqueous or non-aqueous solutions. Only graphitic forms of carbon are therefore useful as electrode materials. Ordinary spectroscopic grade of graphite rods can be used for work in which the surface area of the electrode does not need to be well defined. Other types of carbon electrode include the glassy carbon electrode and the carbon paste electrode.

1.1.8.2 Counter or auxiliary electrode [32–34]

This electrode which serves as a source or sink for electrons so that current can be passed from the external circuit through the cell. In general, neither its true potential nor current is ever measured or known. That is used only to make an electrical connection to the electrolyte so that a current can be applied to the working electrode. The processes occurring on the counter electrode are not important; it is usually made of inert materials (noble metals or carbon/graphite) to avoid its dissolution. This is the case for cells used for research or for electroanalytical purposes. Of course, for many practically used cells, the processes occurring on both electrodes can be very important and also called “auxiliary” electrode.

1.1.8.3 Reference electrodes [32–34]

This is the electrode whose potential is constant enough that it can be taken as the reference standard against the potentials of the other electrodes present in the cell can

be determined. The ideal reference electrode should possess the following properties:

• it should be reversible and obey the Nernst equation with respect to some species in the electrolyte

• its potential should be stable with time

• its potential should return to the equilibrium potential after small currents are passed through the electrode

• if it is an electrode like the Ag/AgCl reference electrode, the solid phase must not be appreciably soluble in the electrolyte

• it should show low hysteresis with temperature cycling

1.1.8.4 Silver/silver chloride reference electrode [32–34]

The redox process for this electrode is

$$AgCl + e^- \rightleftharpoons Ag + Cl^- \qquad 1.1$$

This electrode consists of a silver wire, coated with silver chloride, which is immersed in a solution containing chloride ions. This electrode uses an aqueous solution containing 3 M sodium chloride; a porous frit is used for the junction between the reference electrode solution and the sample solution. The potential E for any electrode is determined by the Nernst equation, which relates E to the standard potential E^0 and the activities of the redox components (the standard potential is the potential of the electrode at unit activity under standard conditions).

1.1.8.5 Saturated calomel reference electrode [32–34]

The redox process for this electrode is

$$Hg_2Cl_2 + 2e^- \rightleftharpoons 2Hg + 2Cl^- \qquad 1.2$$

The saturated calomel electrode (SCE) is an H-cell. One arm contains mercury covered by a layer of mercury (II) chloride (calomel). This is in contact with a saturated solution of potassium chloride; a porous frit is again used for the junction between the reference electrode solution and the sample solution at the end of the other arm. Once assembled, the electrode should be stored with porous frit and immersed in a saturated solution of potassium chloride to maintain the chloride concentration in the reference electrode.

1.1.8.6 Pseudo-reference electrode [32–34]

Pseudo-reference electrodes are simply metal wires (e.g., platinum or silver) immersed in the sample solution. Although such electrodes do provide a constant potential, the reference potential is unknown, and is dependent on the composition of the sample solution. Consequently, redox potentials measured using a pseudo reference electrode should be quoted relative to redox potential of the internal reference compound. One advantage of pseudo-reference electrodes is its low impedance.

1.1.8.7 Silver/silver ion electrode

The redox process for this electrode is

$$Ag^{+} + e^{-} \rightleftharpoons Ag \qquad 1.3$$

This electrode is less stable than the aqueous electrodes discussed above (due to diffusion of silver ions out of the electrode and the photo reactivity of these ions), and must be prepared frequently. Bioanalytical System, Inc. (BASi) provides a non-aqueous reference electrode kit, which requires assembly by the user. The BASi non aqueous reference electrode consists of a silver wire immersed in a solution of silver

nitrate or perchlorate (0.001 M to 0.01 M) and electrolyte (e.g., 0.1 M tetrabutylammonium perchlorate, (TBAP) in the desired organic solvent. Suitable organic solvents include acetonitrile, dimethylsulfoxide, methanol, ethanol and tetrahydrofuran. Silver ions are reduced by dimethylformamide and are insoluble in methylene chloride; these solvents are therefore not suitable for this reference electrode (acetonitrile can be used as the reference electrode solvent when one of these other two solvents is used for the sample solution). The potential for the silver/silver ion reference electrode depends on the solvent, the silver ion concentration the nature and concentration of the electrolyte. It is also changed by the introduction of salt bridges, which are used to decrease the contamination of the sample solution by the effect of silver ions.

1.1.8.8 Electrolyte solutions [31, 32]

The medium is required for electrochemical experiment is electrolyte solutions which must be able to conduct the current. This can be achieved by using either a molten salt or an electrolyte solution. An electrolyte solution is made by adding an ionic salt to an appropriate solvent. The salt must be fully dissociated in the solvent in order to generate a conducting (i.e., ionic) solution. The electrolyte solution must also be able to dissolve the analyte, an electrochemically inert over a wide potential range (i.e., no current due to electrolyte solution oxidation/reduction), and must be pure (e.g., the presence of water decreases the size of the potential range). It is chemically inert, so that it will not react with any reactive species generated in the experiment (e.g., acetonitrile is nucleophilic, which can react with electrogenerated cations). If the temperature is to be varied, the electrolyte solution must have an appropriate solubility range. Electrolyte solutions can be aqueous or non-aqueous. A wide range

of salts can be used for aqueous electrolyte solutions. Since the redox potentials of some compounds are pH sensitive, buffered solutions should be used for these compounds. Suitable non-aqueous solvents include acetonitrile, dimethylformamide, dimethyl sulfoxide, tetrahydrofuran, methylene chloride, and propylene carbonate. Salts for non-aqueous electrolyte solutions typically consist of a large cation (e.g., tetra-alkylammonium cations), and large anions (e.g., hexafluorophosphate, tetrafluoroborate, and perchlorate) to ensure a full dissociation. Perchlorate salts should be handled with care, since they are potentially explosive.

1.2 Cyclic voltammetry (CV) [35–38]

Cyclic voltammetry (CV) is an electrolytic method that uses microelectrodes and an unstirred solution so that the measured current is limited by analyte diffusion at the electrode surface. The electrode potential is ramped linearly to a more negative potential, and then ramped in reverse back to the starting voltage. The forward scan produces a current peak for any analyses that can be reduced through the range of the potential scan. The current will increase as the potential reaches the reduction potential of the analyst, but then falls off as the concentration of the analyte is depleted close to the electrode surface. As the applied potential is reversed, it will reach a potential that will re-oxidize the product formed in the first reduction reaction, and produce a current of reverse polarity from the forward scan. This oxidation peak will usually have a similar shape to the reduction peak. The peak current, i_p, is described by the Randles-Sevcik equation:

$$i_p = (2.69 \times 10^5)\, n^{3/2}\, A\, C\, D^{1/2}\, v^{1/2} \qquad 1.4$$

where n is the number of moles of electrons transferred in the reaction

A is the surface area of the electrode

C is the analyte concentration (in mole/cm^3)

D is the diffusion coefficient

v is the scan rate of the applied potential

The potential difference between the reduction and oxidation peaks is theoretically 59 mV for a reversible reaction. In practice, the difference is typically 70–100 mV. Larger differences, or non-symmetric reduction and oxidation peaks are an indication of a nonreversible reaction.

1.2.1 Cyclic voltammetry primer [35, 36]

A simple potential wave form that is often used in electrochemical experiment is the linear wave form i.e., the potential is continuously changed as a linear function of time. The rate of change of potential with time is referred to as the scan rate (v). The simplest technique that uses this wave form is linear sweep voltammetry. The potential range is scanned in one direction, starting at the initial potential and finishing at the final potential. A more commonly used variation of the technique is cyclic voltammetry, in which the direction of the potential is reversed at the end of the first scan. Thus, the waveform is usually of the form of an isosceles triangle. This has the advantage that the product of the electron transfer reaction that occurred in the forward scan can be probed again in the reverse scan. In addition, it is a powerful tool for the determination of formal redox potentials, detection of chemical reactions that precede or follow the electrochemical reaction and evaluation of electron transfer kinetics [35]. In this example it is assumed that only the reduced form of the species is initially present. Thus, a positive potential scan is chosen for the first half cycle during which an anodic current is observed. The reason by, the solution is quiescent; the product generated during the forward scan is available at the surface of the electrode

for the reverse scan resulting in a cathodic current. Complex wave form composed of two isosceles triangles. The voltage is first held at the initial potential where no electrolysis occurs and hence no faradaic current flows. As the voltage is scanned in the positive direction, so the reduced compound is oxidized at the electrode surface. At a particular set value, the scan direction is reversed and the material that was oxidized in the outward excursion is then reduced. Once the voltage is returned to the initial value, the experiment can be terminated. In this example however a further voltage excursion takes place to more negative (more reducing) values. This may be useful in probing for other species present in the sample or for investigating any electroactive products formed as a result of the first voltage excursion. The situation is very different when the redox reaction is not reversible, when chemical reactions are coupled to the redox process or when adsorption of either reactants or products occurs. In fact, it is these "non-ideal" situations which are usually of greatest chemical interest and for which the diagnostic properties of cyclic voltammetry are particularly suited. An example wave form that can be used in cyclic voltammetry is shown in Figure 1.7.

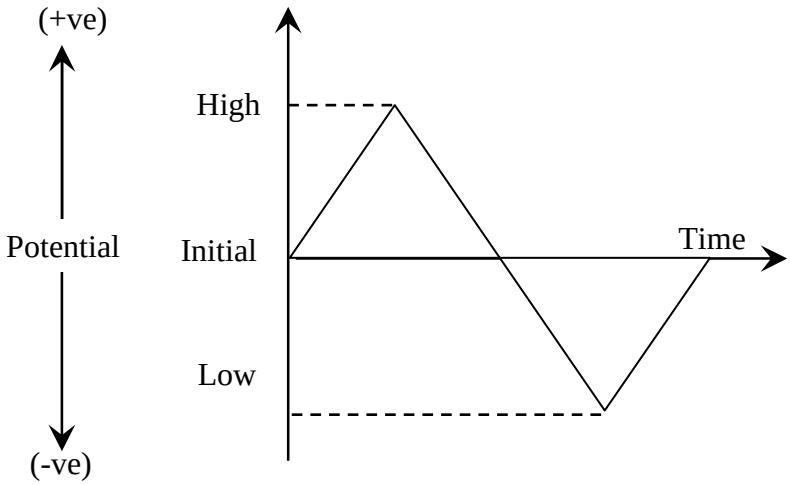

Figure 1.7 Normal wave form of cyclic voltammetry [35].

The basic shape of the current response for a cyclic voltammetry experiment is shown in Figure 1.8 [36]. At the start of the experiment, the bulk solution contains only the reduced form (R) of the redox couple (I) so that at potentials lower than the redox potential, i.e. the initial potential, there is no net conversion of R into the oxidized form (O) at point A. As the redox potential is approached, there is a net anodic current which increases exponentially with potential. As R is converted into O, concentration gradients are set up for both R and O, and diffusion occurs down these concentration gradients. At the anodic peak (point B), the redox potential is sufficiently positive that any R that reaches the electrode surface is instantaneously oxidized to O. Therefore, the current now depends upon the rate of mass transfer to the electrode surface and so the time dependence is quartet resulting in an asymmetric peak shape.

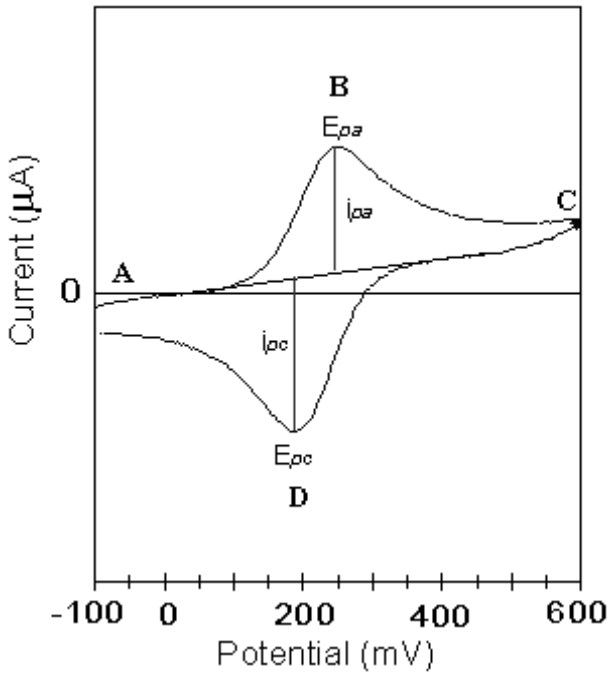

Figure 1.8 The basic shape of the current response for a cyclic voltammetry [36].

Upon reversal of the scan (point C), the current continues to decay with a quartet until the potential nears the redox potential. At this point, a net reduction of O to R occurs which causes a cathodic current which eventually produces a peak shaped response (point D).

The situation is very different when the redox reaction is not reversible, when chemical reactions are coupled to the redox process or when adsorption of either reactants or products occurs. In fact, it is these "non-ideal" situations which are usually of greatest chemical interest and for which the diagnostic properties of cyclic voltammetry are particularly suited.

1.2.2 Mechanistic complications [35, 36]

1.2.2.1 Nernstian (reversible) behavior

If a redox system remains in equilibrium throughout the potential scan, the electrochemical reaction is said to be reversible. In other words, equilibrium requires that the surface concentrations of oxidation and reduction are maintained at the values required by the Nernst Equation. Under these conditions, the following parameters characterize the cyclic voltammogram of the redox process.

• The peak potential separation (E_{pa} - E_{pc}) is equal to 57/n mV for all scan rates where n is the number of electron equivalents transferred during the redox process.

• The peak width is equal to 28.5/n mV for all scan rates.

• The peak current ratio (i_{pa}/i_{pc}) is equal to 1 for all scan rates.

• The peak current function increases linearly as a function of the square root of v.

The system under investigation is a simple one electron reversible couple so under the conditions of the experiment, the above parameters are observed. Cyclic

voltammograms for ferrocene carboxylic acid in an aqueous pH 7.0 phosphate buffer electrolyte as shown in Figure 1.9.

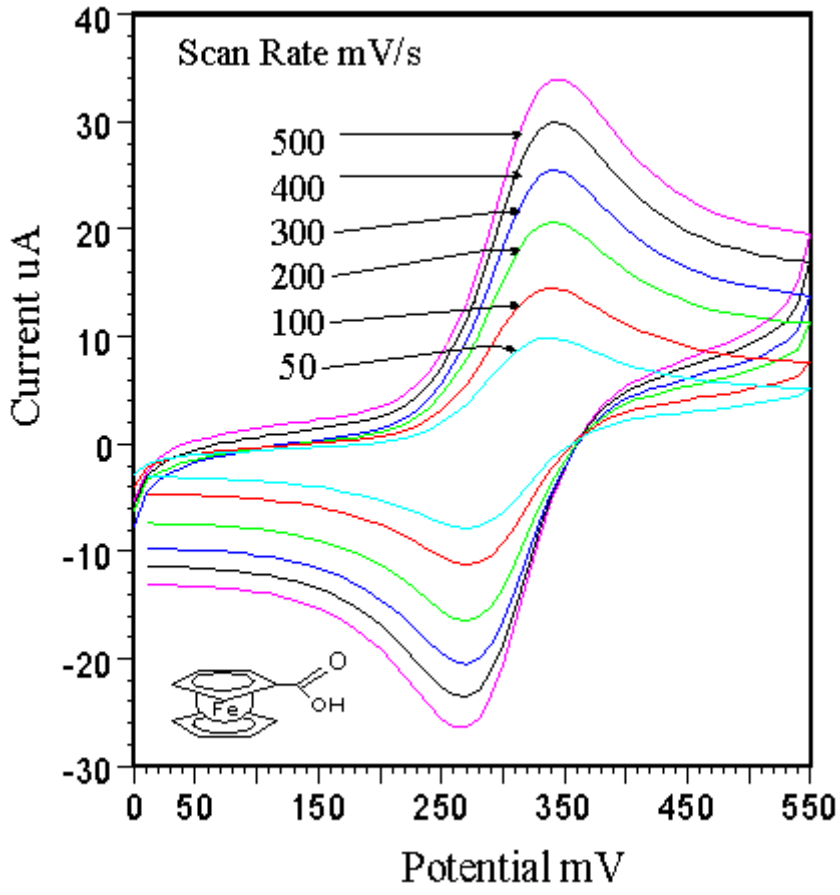

Figure 1.9 Cyclic voltammograms for ferrocene carboxylic acid at different scan rate [36].

As the voltage becomes increasingly more positive (oxidizing) value is reached where ferrocene carboxylic acid (reduced form) is converted to the oxidized ferricinium species. This results in the appearance of the anodic peak. Assuming that the reaction kinetics are very fast compared to the scan rate, the equilibrium involving the concentrations of reduced and oxidized species at the electrode surface will adjust rapidly according to the Nernst equation;

$$E = E^{o'} + (RT/nF) \ln C_O / C_R \qquad 1.5$$

where C_O and C_R represent the surface concentration of oxidized and reduced species, respectively. If the system is diffusion controlled (the normal situation for cyclic voltammetry) then Fick's law of diffusion holds for both O and R. Under these conditions, the peak current (i_p) is followed by the Randles-Sevcik equation:

$$i_p = 2.69 \times 10^5 \, n^{3/2} \, A \, D_O^{1/2} \, v^{1/2} \, C_O \qquad 1.6$$

where A is the electrode area (cm^2), n is the number of electrons transferred, D_O is the diffusion coefficient, C_O is the concentration ($mol.cm^{-3}$) and v is the scan rate (volt/s).

The basic shape of cyclic voltammograms of EC mechanism with different first-order rate constant (k_f) and heterogeneous electron transfer rate (k_{het}) are shown in Figure 1.10.

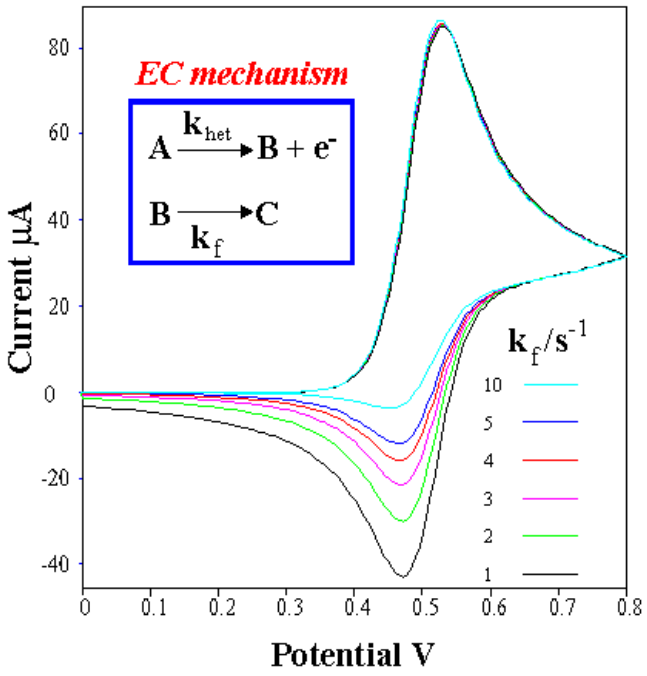

Figure 1.10 The basic shape of cyclic voltammograms of EC mechanism with different first-order rate constant (k_f) [36].

1.2.2.2 The Electrochemical Chemical (EC) mechanism [35, 36]

The shape of a voltammogram can be significantly altered if there is a coupled chemical reaction either before or after occurred in the electrochemical process. Further complications attributed to the chemical nature of the reaction, the degree of reversibility, the rate and equilibrium constants of the process can all play a part in the final shape of the voltammogram and on the information that can be obtained from a set of experiments. In general terms, coupled mechanistic schemes are described by the letters E (electrochemical) and C (chemical). The order in which they are written denotes the order in which the processes occur. Thus an EC mechanism describes a process in which an electrochemical step is followed by a chemical step which is then followed by an electrochemical step. A chemical step is a step where no electron-transfer to or from the electrode takes place. Such a step does not by itself produce a charge flow into or out of the electrode and thus is not directly observable by an external measuring circuit. It may however influence charge flow because of other steps in the mechanism which can be detected indirectly. The chemical step is not directly influenced by the electrode potential. An electrochemical step on the other hand involves electron flow to and from the electrode and as such produces a flow of charge that can be monitored by the external measuring circuit is shown in Figure 1.11.

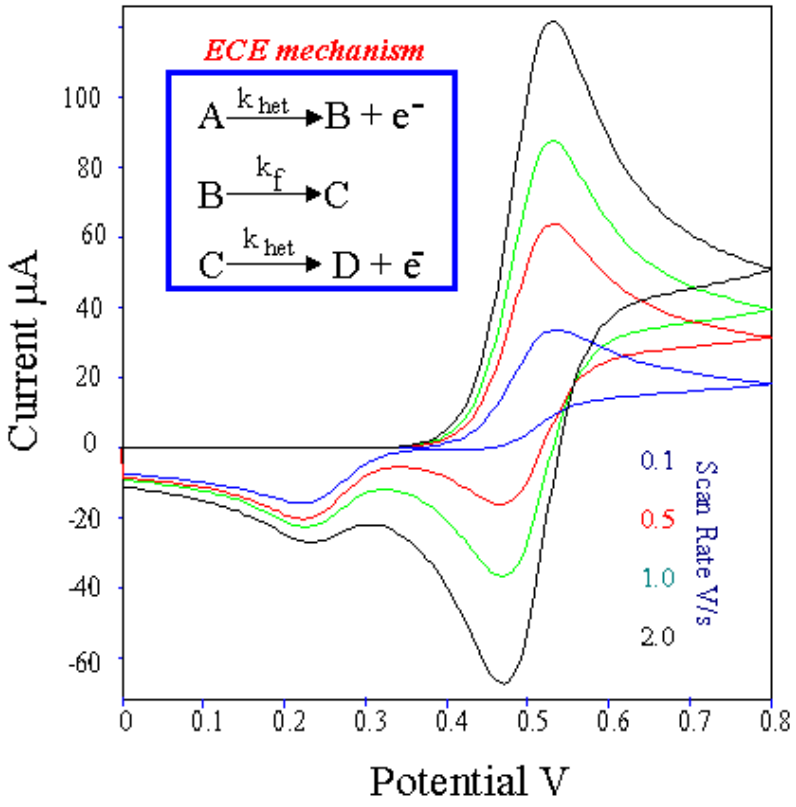

Figure 1.11 The basic shape of cyclic voltammograms of EC mechanism with different scan rates [36].

1.2.2.3 Dealing with an EC mechanism [36]

The following experimental parameters were used to obtain the simulated voltammograms shown; electrode area = 0.1 cm^2, k_{het} = 1 cm s^{-1}, v = 1 volt s^{-1}, E^o = 0.5 V and $D_O = D_R = 1 \times 10^{-5}$ cm s^{-1}. Consider the following generalized mechanistic scheme, this shows a typical EC mechanism. In the first step (E), a reduced species is oxidized at the surface of an electrode. The product of the reaction O is unstable and once formed, reacts chemically (C) for example with itself, neighboring molecules or with the solvent to give a new species A which is either electro-inactive or simply not electroactive within the potential window of interest. An example of this type of mechanism is the electrochemical oxidation of ascorbic acid (vitamin C) and its

subsequent reaction with water (the solvent) to yield electrochemically inactive dehydroascorbic acid. The electrochemical reaction is characterized by the heterogeneous rate constant k_{het} which we can assume to be very fast. The chemical reaction is characterized by a homogeneous first order rate constant k_f for which the equilibrium constant K is equal to;

$$K = [A]_o / [O]_o \qquad 1.7$$

where the concentrations of A and O are surface concentrations. The resultant voltammograms for such a process would be similar to those depicted above. Close inspection of the diagram reveals that the forward scan (the oxidation of R to O) is unaffected but the reverse scan (O to R) is altered. An important parameter in determining the shape of the voltammogram is the dimensionless ratio k_f/s^{-1}. Because the homogeneous step has a finite rate constant associated with it, there will be a limiting sweep rate (s^{-1}) which is fast enough to have completed the reverse scan before any conversion of O to A has taken place. Under these conditions, the voltammogram will not be altered in any way and the ratio of the two peak currents will be unity. This feature can be best understood by looking at the simulated voltammograms. In this case, the voltammograms for an EC reaction are recorded at increasing scan rates (1 to 10 Vs^{-1}). It is evident, that as the scan rate is increased, the contribution from the homogeneous reaction becomes less pronounced and the voltammogram approaches the shape of that for a normal, uncomplicated situation. The following experimental parameters were used to obtain the simulated voltammograms shown; electrode area = 0.1 cm^2, k_{het} = 1 cm s^{-1}, E^o = 0.5 V, $D_O = D_R$

= 1 x 10^{-5} cm s^{-1} and k_f = 10 s^{-1}. The basic shape of cyclic voltammograms of EC mechanism with different scan rates is shown in Figure 1.12.

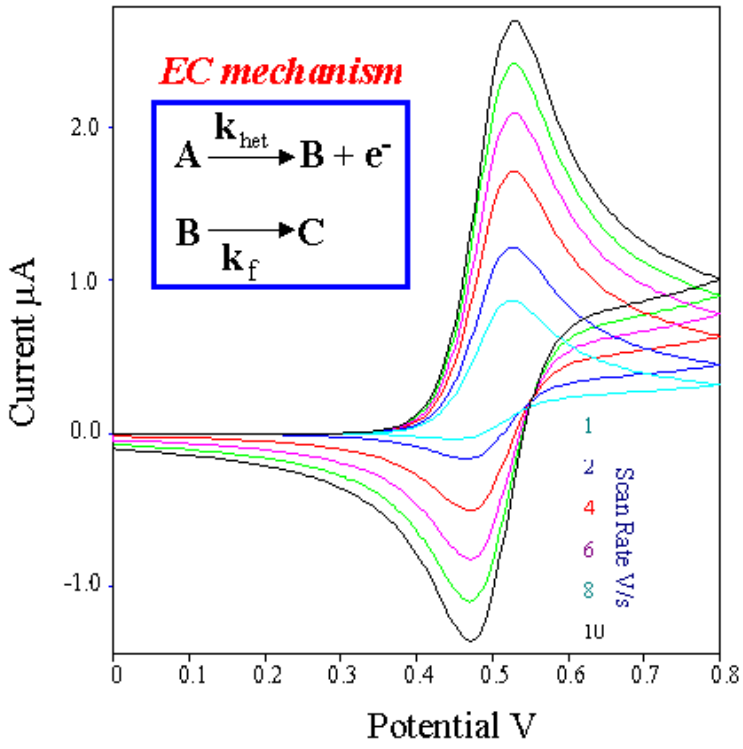

Figure 1.12 The basic shape of cyclic voltammograms of EC mechanism with different scan rates [36].

1.3 Surface Plasmon Resonance Spectroscopy (SPR) [39–41]

1.3.1 Theoretical background

SPR is a technique which associated with the total internal reflection of light (evanescent wave) at the boundary between two media of different optical properties described by their different dielectric function, ε_i [39]. The example of this observation is the boundary between a glass prism and water. A plane wave from a laser light source (wavelength λ) or incoming light impinging upon the interface from glass side, i.e. from material with higher refractive index, will be totally (internally)

reflected if the angle of incidence exceeds a critical value, θ_c. This can be observed by recording the reflectivity, R (the ratio between reflected and incoming intensity) with a diode detector as a function of the angle of incidence, θ. In typical experiment, at angles of incidence smaller than θ_c, most of incoming light is transmitted and therefore the reflectivity is low. When the angle of incidence approaches θ_c, the reflectivity reaches unity. The evanescent wave is an electromagnetic field which the electric field perpendicular to the interface (E_Z) does not fall to zero abruptly but decays exponentially with a decay length, l. This decay length is a function of the angle of incidence. On the other hand, the component along the propagation direction (E_X) had the usual oscillatory character of an electromagnetic mode. The evanescent wave is formed at the angle greater than critical angle. When the interface between a metal and a dielectric material is considered, the term “plasmon surface polaritons (PSP) or surface plasmons” for short was described [39–41]. The coupling of the collective plasma oscillations (called “plasmon”) of the nearly free electron gas in a metal to an electromagnetic field has been shown to produce the surface plasmon. This surface plasmon propagates at the metal/dielectric material with the coupling angle which can be excited with photons when the energy and momentum matching conditions between photons and surface plasmons has reached [39–41].

1.3.2 The architecture of experimental setup

Three different coupling schemes had been proposed among which are grating, edge, and prism [40]. The different schemes by using prism have been widely used for many applications. In principle, there are two concepts for this experimental setup: Otto-configuration and Kretschmann configuration. The latter one is the most widely used and convenient configuration because the resulting plasmon can be observed

directly through the metal. In the Otto-configuration, photons are not coupled directly to the metal/dielectric interface, but via the evanescent tail of light totally internally reflected at the base of a high-index prism ($\varepsilon_p > \varepsilon_d$). By choosing the appropriate angle of incidence, resonant coupling between evanescent photons and surface plasmons can be obtained. This resonant coupling is observed by monitoring the laser light, which is reflected by the base of prism, as a function of the incident angle. However, since the major technical drawback of this configuration is the need to obtain the metal surface closes enough to the prism base, typically ~ 200 nm. This means even a few dust particles can be the spacers preventing the efficient coupling. As this drawback, the Otto-configuration has not gained any practical importance despite its potential importance for the optical analysis of polymer coated bulk metal samples. On the other hand, the experimentally easier and hence the most wide spread configuration, Kretschmann configuration, has the similar scheme for exciting surface plasmons to Otto-configuration. In Kretschmann configuration, photons in the prism couple through a very thin metal layer (typically ~ 45–50 nm thick), which is deposited directly onto the base of the prism or onto a glass slide, to surface plasmons at the other side in contact with the dielectric medium. In qualitative, the same consideration for energy and momentum matching are applied as discussed in Otto configuration. Quantitatively, however, the finite thickness of the metal layer causes some modification of the dispersion behavior at surface plasmons. By solving Maxwell's and/or Fresnel's equations for the layer architecture of glass/Ag-layer/ dielectric, the angular dependence of the reflectivity can be described.

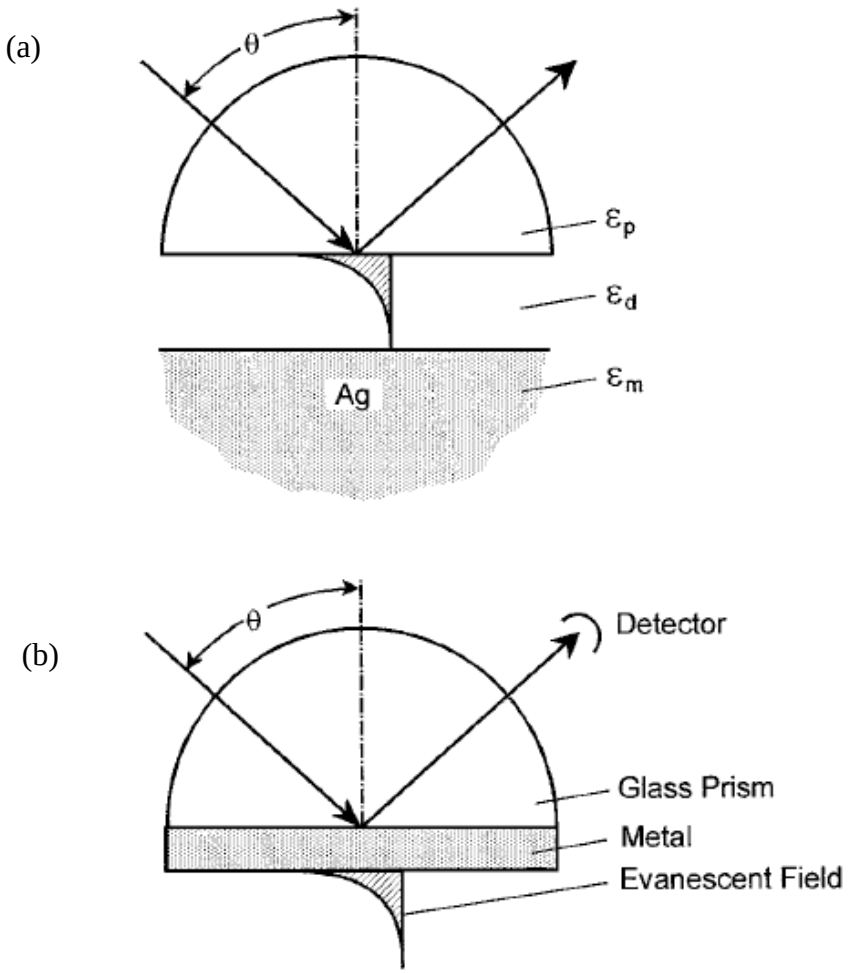

Figure 1.13 Two concept for experimental setup of surface plasmon resonance spectroscopy (a) The Otto-configuration (b) Kretschman configuration with attenuated total internal reflection (ATR) construction [39].

1.3.3 SPR for investigation of the adsorption processes

SPR has been shown to be a technique which has high sensitivity for characterization of ultrathin film, interfaces, and kinetic processes at the nanometer scale [39, 42, 43]. The experimental SPR system for characterization of ultrathin films which relatively simple. A laser beam of wavelength λ incidents at angle θ on the noble metal coated base of the prism, which is covered with the thin film of interest

material, is reflected. The intensity of the reflected light is then monitored with a detector as function of θ. The curve labeled was taken in air on a bare Au-film evaporated-deposited onto the prism base. The deposition of an ultrathin organic layer of interest molecules which can be prepared by spontaneous self-assembly process, Langmuir-Blodgett (LB) technique, layer by layer (LbL) deposition method or even simple technique; spin-coating, from solution to Au-surface results in a shift of the curve for PSP running along this modified interface and hence in a shift of the resonance angle (from θ to θ^1). The example for using of SPR to in situ investigation of the self-assembly polymer solution adsorption process was studied by Knoll group [42].

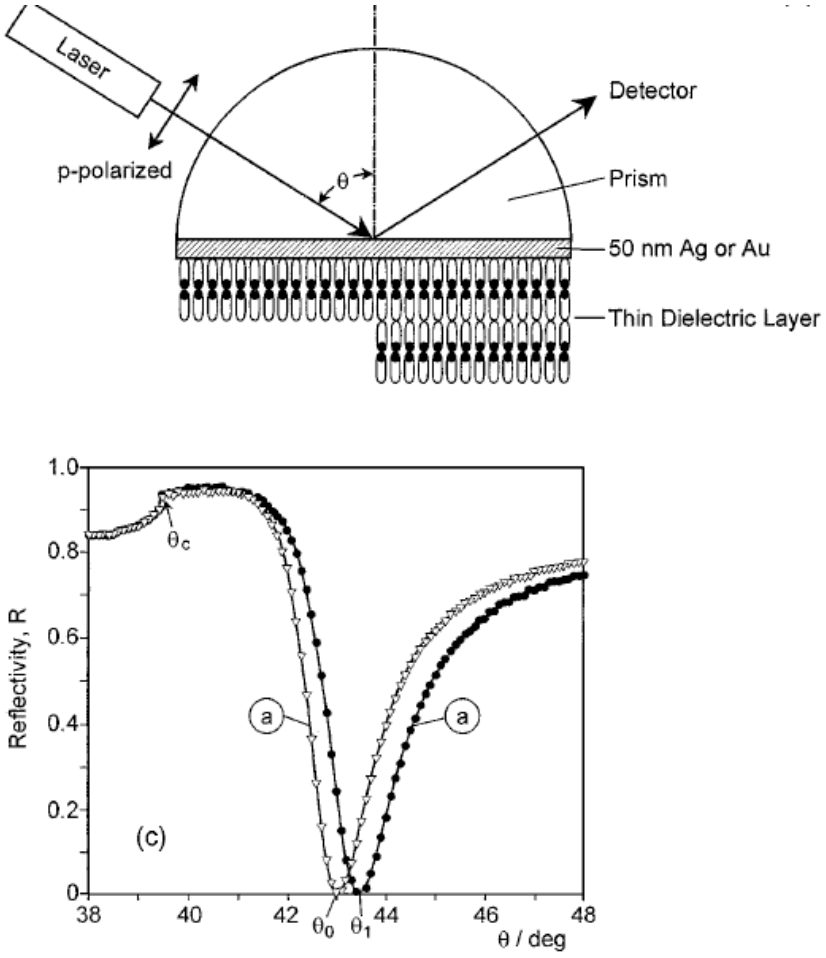

Figure 1.14 Schematic of the experimental system for SPR reflectivity curve obtained from a bare Au-film and self-assembled monolayer [39].

The experimental setup in this study is Kretchmann configuration with ATR condition. The monolayers of each interest materials were stepwisely deposited by LB process onto the high refractive index glass/Au/octadecyl-thiol layer. A sequence of reflectivity data taken after consecutive depositions showed the linear increases of the multilayer thickness after analysis with Fresnel equation [42]. In addition, the other information, which can be studied by using SPR, is the kinetic information on the interfacial of the multilayer. The kinetic information on any changes of the interfacial

architecture is the time-dependant process which can be obtained by monitoring the reflectivity at a fixed angle of observation, θ^{obs}. At t = 0, the solution is injected and the adsorption followed in real time as a change in reflectivity. The adsorption process for each layer is complete after several minutes, thus giving the important information for the subsequence of the alternating multilayers preparation.

1.3.4 Electrochemical-Surface Plasmon Resonance Spectroscopy (EC-SPR) [23, 39–44]

The combination of SPR, particularly in the Kretschmann configuration, with electrochemical measurements has become a powerful technique for simultaneous characterization and manipulation of an electrode/electrolyte interfaces [23, 39–43]. This combination has been known as Electrochemical-Surface Plasmon Resonance Spectroscopy (EC-SPR). A schematic diagram for EC-SPR set up is shown in Figure 1.15.

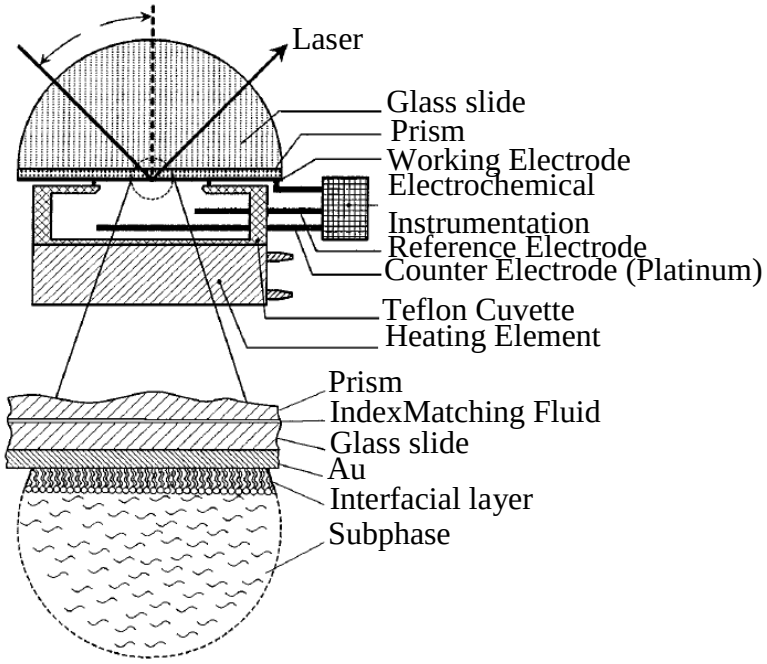

Figure 1.15 Schematic diagram showing the experimental set up of EC-SPR [39].

The gold substrate which carries the optical surface mode is simultaneously used as the working electrode in electrochemical experiments. One advantage of EC-SPR is that the electrochemical and optical properties can be obtained simultaneously during film forming on the nanometer thickness scale [23, 39]. Recently, EC-SPR was applied for characterization of a number of conducting polymer films including polyaniline [41, 43] and poly(3,4-ethylenedioxythiophene) [42]. The time dependent processes could be induced by a potential sweep which the setup allows simultaneously record the reflectivity and the flow of charges through the electrical circuit, e.g. a classical cyclic voltammogram. In addition, the EC-SPR technique had also been applied to many applications including biosensor development [9, 44].

1.4 Biomolecules (such as catecholamine, uric acid and ascorbic acid) [45–50]

1.4.1 Catecholamine

A catecholamine (CA) is an organic compound that has a catechol (benzene with two hydroxyl side groups) and a side-chainamine [45] as shown in Figure 1.16. A catechol is a 1,2-dihydroxybenzene group. Catecholamines derive from the amino acid tyrosine [46]. Catecholamines are water-soluble and are 50%–bound to plasma proteins, so they circulate in the blood stream. In the human body, the most abundant catecholamines are epinephrine (adrenaline), norepinephrine (noradrenaline) and dopamine, all of which are produced from phenylalanine and tyrosine. Release of the hormones epinephrine and norepinephrine from the adrenal medulla of the adrenal glands is part of the fight-or-flight response [49].

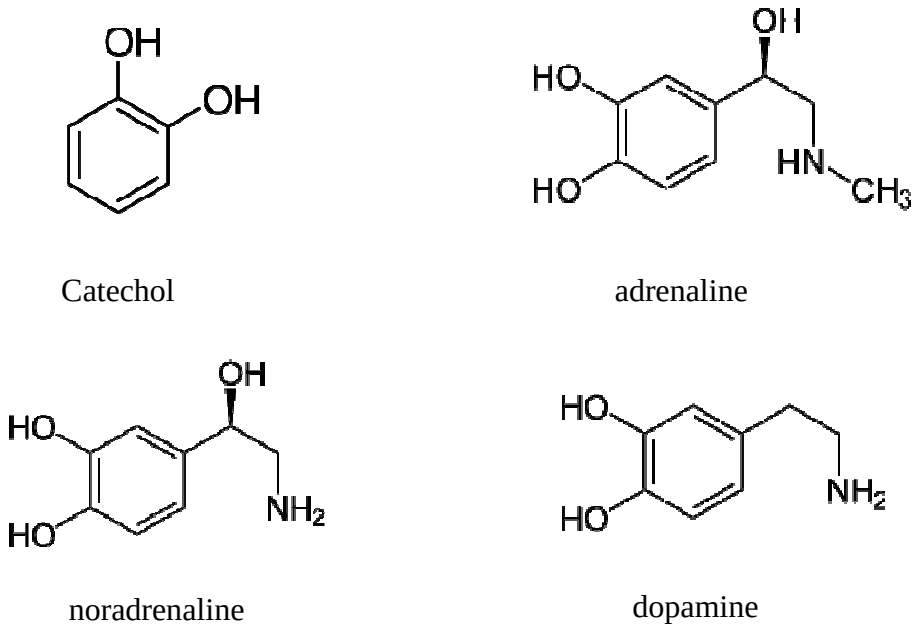

Figure 1.16 Chemical structures of catechol and catecholamines [45].

Tyrosine is created from phenylalanine by hydroxylation via the enzyme phenylalanine hydroxylase as shown in Figure 1.17. Tyrosine is also ingested directly from dietary protein. It is then sent to catecholamine-secreting neurons. Here, several reactions serially convert tyrosine to L-DOPA, to dopamine, to norepinephrine, and eventually to epinephrine [48]. Various stimulant drugs are catecholamine analogues.

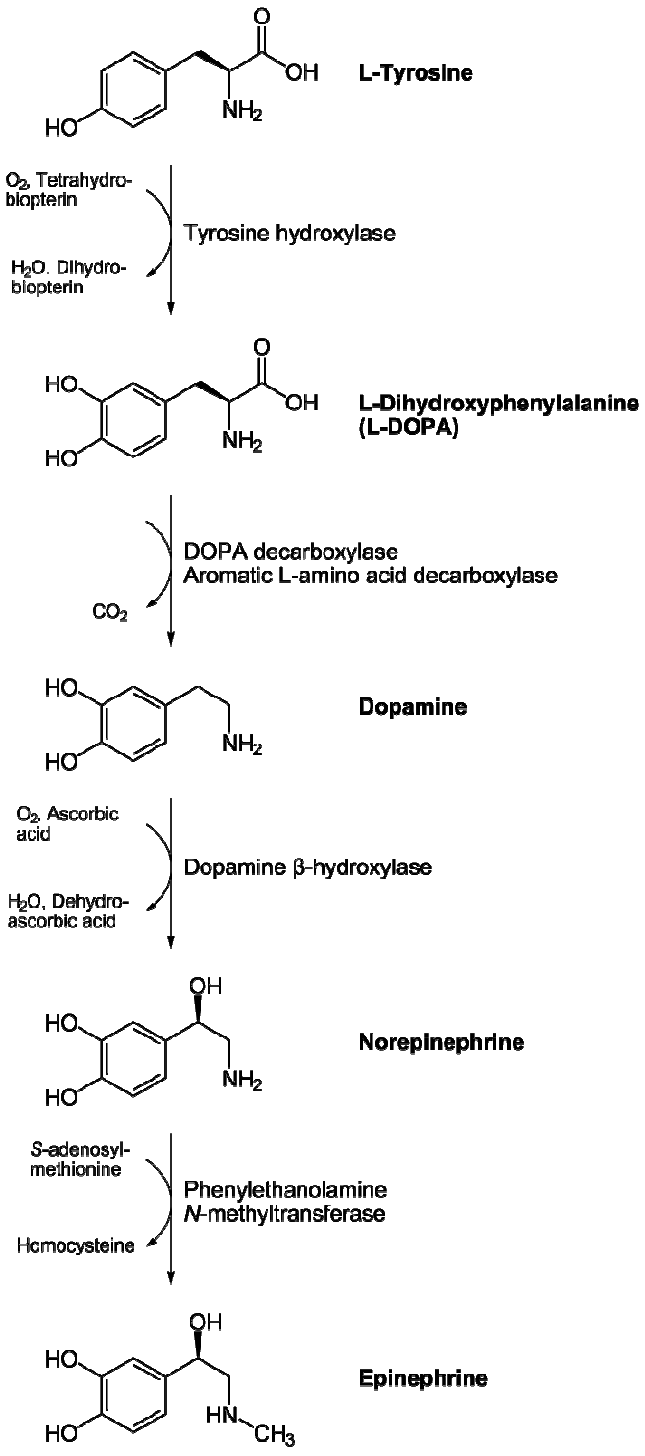

Figure 1.17 Synthesis of catecholamines (adrenaline, noradrenaline, dopamine) from tyrosine [48].

Two catecholamines, norepinephrine and dopamine, act as neuromodulators in the central nervous system and as hormones in the blood circulation. The catecholamine norepinephrine is a neuromodulator of the peripheral sympathetic nervous system but is also present in the blood (mostly through "spillover" from the synapses of the sympathetic system). High catecholamine levels in blood are associated with stress, which can be induced from psychological reactions or environmental stressors such as elevated sound levels, intense light, or low blood sugar levels. Extremely high levels of catecholamines (also known as catecholamine toxicity) can occur in central nervous system trauma due to stimulation and/or damage of nuclei in the brain stem, in particular those nuclei affecting the sympathetic nervous system. In emergency medicine, this occurrence is widely known as catecholamine dump. Extremely high levels of catecholamine can also be caused by neuroendocrine tumors in the adrenal medulla, a treatable condition known as pheochromocytoma. High levels of catecholamines can also be caused by monoamine oxidase A (MAO-A) deficiency. MAO-A is one of the enzymes responsible for degradation of these neurotransmitters, thus its deficiency increases the bioavailability of them considerably. It occurs in the absence of pheochromocytoma, neuroendocrine tumors, and carcinoid syndrome, but it looks similar to carcinoid syndrome such as facial flushing and aggression [49, 50].

Catecholamines cause general physiological changes that prepare the body for physical activity (fight or flight response). Some typical effects are increasing in heart rate, blood pressure, blood glucose levels, and a general reaction of the sympathetic nervous system. Some drugs, like tolcapone, raise the levels of all catecholamines.

1.4.2 Adrenaline [51–53]

Adrenaline is a hormone produced by the adrenal glands during high stress or exciting situations. This powerful hormone is part of the human body's acute stress response system, also called the "fight or flight" response. It works by stimulating the heart rate, contracting blood vessels, and dilating air passages, all of which work to increase blood flow to the muscles and oxygen to the lungs. Additionally, it is used as a medical treatment for some potentially life-threatening conditions including anaphylactic shock. In the US, the medical community largely refers to this hormone as epinephrine, although the two terms may be used interchangeably [51].

The adrenal glands are found directly above the kidneys in the human body, and are roughly 3 inches (7.62 cm) in length. Adrenaline is one of several hormones produced by these glands. Along with norepinephrine and dopamine, it is a catecholamine, which is a group of hormones released in response to stress. These three hormones react with various body tissues, preparing the body to react physically to the stress causing situation.

The term "fight or flight" is often used to characterize the body's reaction to very stressful situations [52]. It is an evolutionary adaptation that allows the body to react to danger quickly. Dilated air passages, for example, allow the body to get more oxygen into the lungs quickly, increasing physical performance for short bursts of time. The blood vessels contract in most of the body, which redirects the blood toward the heart, lungs, and major muscle groups to help fuel there action.

When a person encounters a potentially dangerous situation, the hypothalamus in the brain signals the adrenal glands to release adrenaline and other hormones directly into the blood stream. The body's systems react to these hormones within seconds,

giving the person a nearly instant physical boost. Strength and speed both increase, while the body's ability to feel pain decreases. This hormonal surge is often referred to as an "adrenaline rush".

In addition to a noticeable increase in strength and performance, this hormone typically causes heightened awareness and increased respiration. The person may also feel lightheaded, dizzy, and experience changes in vision. These effects can last up to an hour, depending on the situation. When there is stress but no actual danger, a person can be left feeling restless and irritable. This is partly because adrenaline causes the body to release glucose, raising blood sugar, and giving the body energy that has no outlet. Many people find it beneficial to "work off" the adrenaline rush after a particularly stressful situation. In the past, people handled this naturally through fighting or other physical exertion, but in the modern world, high-stress situations often arise that involve little physical activity. Exercise can use up this extra energy.

Though adrenaline can play a key role in the body's survival, it can also cause detrimental effects over time. Prolonged and heightened levels of the hormone can put enormous pressure on the heart muscle and can, in some cases, cause heart failure. Additionally, it may cause the hippocampus to shrink. High levels of adrenaline in the blood can lead to insomnia and jittery nerves, and are often an indicator of chronic stress.

First synthesized in 1904, adrenaline is a common treatment for anaphylaxis, also known as anaphylactic shock [53]. It can be quickly administered to people showing signs of severe allergic reactions, and some people with known severe allergies carry epinephrine auto-injectors in case of an emergency. For these individuals, dosage

should be assigned by a licensed medical professional in advance, and instructions should be given on how and where it should be administered.

Adrenaline is also one of the main drugs used to treat low cardiac output the amount of blood the heart pumps and cardiac arrest. It can stimulate the muscle and increases the person's heart rate. In addition, by concentrating blood in the vital organs, including the heart, lungs, and brain, it helps increase the chances that the person will recover more fully.

1.4.3 Uric acid [54–58]

Uric acid (UA) is a heterocyclic compound of carbon, nitrogen, oxygen, and hydrogen with the formula $C_5H_4N_4O_3$ as Figure 1.18. It forms ions and salts known as urates and acid urates such as ammonium acid urate. UA is a product of the metabolic breakdown of purine nucleotides. High blood concentrations of UA can lead to a type of arthritis known as gout. The chemical is associated with other medical conditions including diabetes and the formation of ammonium acid urate kidney stones.

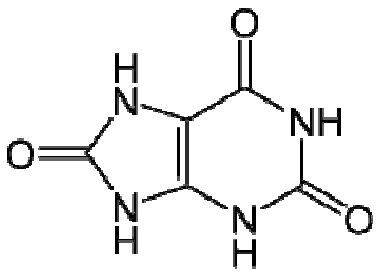

Figure 1.18 Chemical structure of uric acid.

In human blood plasma, the reference range of UA is between 3.6 mg/dL (~214 µmol/L) and 8.3 mg/dL (~494 µmol/L) (1 mg/dL = 59.48 µmol/L), and 2.3-6.6 mg/dL for woman (137–393 µmol/L) [54]. This range is considered normal by the

American Medical Association Manual of Style [55]. UA concentrations in blood plasma above and below the normal range are known, respectively, as hyperuricemia and hypouricemia. Similarly, UA concentrations in urine above and below normal are known as hyperuricosuria and hypouricosuria. Such abnormal concentrations of UA are not medical conditions, but are associated with a variety of medical conditions.

Excess serum accumulation of UA in the blood can lead to a type of arthritis known as gout. This painful condition is the result of needle-like crystals of UA precipitating in joints, capillaries, skin, and other tissues. Kidney stones can also form through the process of formation and deposition of sodium urate microcrystals. A study found that men who drank two or more sugar-sweetened beverages a day have an 85% higher chance of developing gout than those who drank such beverages infrequently. Gout can occur where serum UA levels are as low as 6 mg/dL (~357 µmol/L), but an individual can have serum values as high as 9.6 mg/dL (~565 µmol/L) and not have gout [56].

Saturation levels of UA in blood may result in one form of kidney stones when the urate crystallizes in the kidney. These UA stones are radiolucent and so do not appear on an abdominal plain X-ray, and thus their presence must be diagnosed by ultrasound for this reason. Very large stones may be detected on X-ray by their displacement of the surrounding kidney tissues. UA stones, which form in the absence of secondary causes such as chronic diarrhea, vigorous exercise, dehydration, and animal protein loading, are felt to be secondary to obesity and insulin resistance seen in metabolic syndrome. Increased dietary acid leads to increased endogenous acid production in the liver and muscles, which in turn leads to an increased acid load to the kidneys. This load is handled more poorly because of renal fat infiltration and

insulin resistance, which are felt to impair ammonia excretion (a buffer). The urine is therefore quite acidic, and UA becomes insoluble, crystallizes and stones form. In addition, naturally present promoter and inhibitor factors may be affected. This explains the high prevalence of uric stones and unusually acidic urine seen in patients with type 2 diabetes. UA crystals can also promote the formation of calcium oxalate stones, acting as "seed crystals" (heterogeneous nucleation) [57].

UA has been successfully used in the treatment and prevention of the animal (murine) model of MS. A 2006 study found elevation of serum UA values in multiple sclerosis patients, by oral supplementation with inosine, resulted in lower relapse rates, and no adverse effects [58].

1.4.4 Ascorbic acid [59, 60]

Ascorbic acid (AA) is a naturally occurring organic compound with antioxidant properties. It is a white solid, but impure samples can appear yellowish. It dissolves well in water to give mildly acidic solutions. AA is one form ("vitamer") of vitamin C. It was originally called L-hexuronic acid, but when it was found to have vitamin C activity in animals ("vitamin C" being defined as a vitamin activity, not then a specific substance), the suggestion was made to rename L-hexuronic acid. The new name for L-hexuronic acid is derived from *a-* (meaning "no") and scorbutus (scurvy), the disease caused by a deficiency of vitamin C. Because it is derived from glucose, many animals are able to produce it, but humans require it as part of their nutrition. Other vertebrates lacking the ability to produce AA include other primates, guinea pigs, teleost fishes, bats, and birds, all of which require it as a dietary micronutrient (that is, a vitamin) [59].

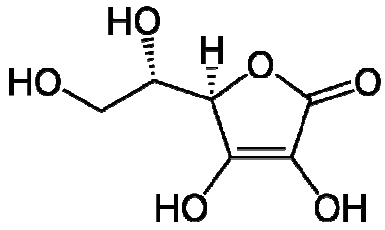

Figure 1.19 Chemical structure of ascorbic acid.

Chemically, there exists a D-ascorbic acid which does not occur in nature. It may be synthesized artificially. It has identical antioxidant properties to L-ascorbic acid (as shown in Figure 1.19), yet has far less vitamin C activity (although not quite zero) [60]. This fact is taken as evidence that the antioxidant properties of AA are only a small part of its effective vitamin activity. Specifically, L-ascorbate is known to participate in many specific enzyme reactions which require the correct primer (L-ascorbate and not D-ascorbate).

As a mild reducing agent, AA degrades upon exposure to air, converting the oxygen to water. The redox reaction is accelerated by the presence of metal ions and light. It can be oxidized by one electron to a radical state or doubly oxidized to the stable form called dehydroascorbic acid.

Ascorbate usually acts as an antioxidant. It typically reacts with oxidants of the reactive oxygen species, such as the hydroxyl radical formed from hydrogen peroxide. Such radicals are damaging to animals and plants at the molecular level due to their possible interaction with nucleic acids, proteins, and lipids. Sometimes these radicals initiate chain reactions. Ascorbate can terminate these chain radical reactions by electron transfer. AA is special because it can transfer a single electron, owing to the

stability of its own radical ion called "semi-dehydroascorbate", dehydroascorbate as shown in Figure 1.20. The net reaction is:

$$RO^{\bullet} + C_6H_7O_6^{-} \rightarrow ROH + C_6H_6O_6^{\bullet -} \qquad 1.8$$

The oxidized forms of ascorbate are relatively unreactive, and do not cause cellular damage. However, being a good electron donor, excess ascorbate in the presence of free metal ions can not only promote but also initiate free radical reactions, thus making it a potentially dangerous pro-oxidative compound in certain metabolic contexts.

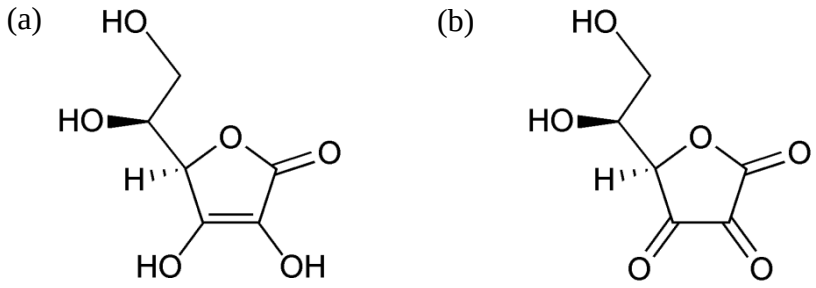

Figure 1.20 Chemical structure of (a) ascorbic acid (reduced form of Vitamin C) and (b) dehydroascorbic acid (oxidized form of Vitamin C).

Dehydroascorbic acid (DHA) is the oxidized form of AA. Both DHA and AA are important compounds in various dietary components. DHA has stronger antiviral effect and different mechanism of action than ascorbic acid.

1.5 Literature review

Conducting polymers (CPs) have received considerable attention because of their electronic conducting properties and unique chemical and biochemical properties. CPs are materials discovered just over 20 years ago which have aroused considerable

interest on account of their electronic conducting properties and unique chemical and bio-chemical properties [1, 28–30].

In 1990, adrenaline is the active moieties of ibopamine, a cardiovascular prodrug used in congestive heart failure were reported by Musso *et al* [61]. This catecholic compound shows dopaminergic and adrenergic properties. Moreover the drug seems to affect plasma catecholamine levels in patients with heart failure. They reported a method developed for the simultaneous determination of epinine and catecholamine plasma levels. Free epinine and catecholamines were extracted from human venous plasma via an alumina adsorption procedure. The extracts underwent an ion-pair reversed-phase HPLC separation with three-electrode coulometry. Quantitation was made by an internal standard method. Coefficients of variation were < 9%. The validity was assessed as the peak height-picograms correlation (r >0.997). The detection limits were ≤ 5 pg of each catechol after extraction.

In 1992, the highly sensitive detection of catecholamine has been achieved by using an interdigitated array microelectrode as an electrochemical detector in a microbore high-performance liquid chromatography (HPLC) system were reported by Takahashi *et al* [62]. The current responses for catecholamine are measured for interdigitated array electrodes with different gaps between their adjacent band electrodes. An interdigitated array electrode with a narrow gap produces a high current density and reduces the influence of the auxiliary electrode position on the current response. The current response measured for an interdigitated array electrode incorporated in the microbore HPLC system is about four times greater than that

measured for a combination of the same interdigitated array electrode and an ordinary sized column due to current enhancement by redox cycling in the slower stream.

In 1996, liquid chromatographic (LC) method with 2-phenylcinonotrile (PGN) and benzylamine (BA) were successfully applied to the determination of CA in human urine was reported by Notha *et al* [63]. The PGN and BA reagent were the suitable reagents in terms of selectivity and sensitivity with catecholamines under mild conditions in the presence of ammonium molybdate and sodium periodate for PGN and potassium hexanoferrate (III) for BA to give fluorescent derivatives. The derivatives of adrenaline, noradrenaline and dopamine could be separated within 13 min by reversed phase liquid chromatography with isocratic elution and measured fluorimetrically as described above. The detection limit (S/N = 3) were in the range 5.2–11 *f*mol for PGN and 1.6–100 *f*mol for BA in a 50 µL injection volume.

In 1998, a contributions summarize the use of plasmon surface polaritons and guided optical waves for the characterization of interfaces and thin organic films were as reported by Knoll *et al*. [39]. The interfacial “light” can be employed to monitor thin coatings at a solid/air or solid/liquid interface. Examples were given for a very sensitive thickness determination of samples ranging from self-assembled monolayer, to multilayer assemblies prepared by the Langmuir/Blodgett/Kuhn technique or by the alternate polyelectrolyte deposition. These were complemented by the demonstration of the potential of the technique to also monitor time dependent processes in a kinetic mode.

In 2000, a highly sensitive method for the determination of human blood plasma catecholamines (adrenaline, noradrenaline and dopamine) is descripted which employs liquid chromatography with chemiluminescence detection were reported by Ragab *et al* [64]. Solid-phase extraction using cation exchange cation exchange cartridges was used for selective and quantitative isolation of the catecholamines and isoproterenol from 20 µL of human plasma containing 0.1 pmol mL^{-1} isoproterenol. The amines and isoproterenol, derivertized with 1,2-bis(3-chlorophenyl)ethylene diamine, were separated on a reversed-phase liquid chromatography column with isocratic elution using a mixture of imidazole buffer (120 mM, pH 5.8), methanol, acetronotrile (13 : 4 : 18, v/v/v). The eluate was detected by a post-column chemiluminescence reaction system using bis[4-nitro-2-(3,6,9-trioxadecyloxycarbonyl)phenyl]oxalate and hydrogen peroxide. The detection limits were 42.6, 14.2 and 35.5 *f*mol mL^{-1} (120, 40 and 100 *a*mol in a 100 µL injection volume), respectively.

In 2001, electrochemical oxidation/reduction and the transition in the conductivity of polyaniline (PANI) film on gold electrode surface were reported by Kang *et al*. [65]. Based on the amplification response of SPR to the redox transformation of PANI film, a direct result of the enzymatic reaction between horseradish peroxidase (HRP) and PANI in the presence of H_2O_2 was presented. The novel PANI-mediated HRP sensor has been fabricated of SPR biosensor because the other oxidoreductases can all be used as immobilization enzyme to transform PANI film. The SPR biosensor posed a number of potential advantages. First, a larger SPR signal could be obtained in the SPR measurement than in the direct binding assay of SPR. Second, the SPR measurement did not require electrochemical instrument to operate.

In 2003, CPs were reported by Vidal *et al*. [28] with numerous (bio)analytical and technological applications. CPs are easily synthesized and deposited onto the conductive surface of a given substrate from monomer solutions by electrochemical polymerization with precise electrochemical control of their formation rate and thickness. Coating electrodes with CPs under mild conditions opens up enormous possibilities for the immobilization of biomolecules and bioaffinity or biorecognizing reagents, improve of their electrocatalytic properties, rapid electron transfer and direct communication to produce a range of analytical signals and new analytical applications. CPs still has many unexplored possibilities, and so a lot of future research into the development of new CP-based biosensors can be expected.

In 2003, combination of SPR and surface plasmon enhanced photoluminescence spectroscopy (SPPL) with electrochemical techniques for the detection of photoluminescence in poly(3,4-ethylenedioxythiophene) (PEDOT) ultrathin films were reported by Baba and Knoll [66]. The photoluminescence from PEDOT was detected when the polymer was dedoped under the influence of the corresponding applied potential. The photoluminescence intensity was controlled by the potential and was dependent on the angular position in an SPR reflectivity experiment. The SPR characterization of the PEDOT film was consistent with the PEDOT bulk electrochromic properties obtained from UV-vis-NIR spectra. A mechanistic model of the photoluminescence from PEDOT was obtained by taking into consideration the reflectivity and the SPPL data, which could be observed simultaneous by their system.

In 2003, MWNTs film-coated glassy carbon electrode (GCE) exhibited a marked enhancement effect on the current response of dopamine (DA) and serotonin (5–HT)

and lowers oxidation over potentials were reported by Wu *et al*. [67]. The results confirmed that the Nafion–MWNTs modified disk form CFME possesses the obvious advantage of easy preparation in a rapid and simple procedure, effective electrocatalytic properties, and very low detection limits for DA, even in the presence of a 100 to 1000–fold excess of AA. The combination of the good electrical properties of MWNTs with the negatively charged polymer of Nafion on the carbon fiber micro electrode surface has realized an efficient electrochemical microsensor capable of maintaining reproducibility and stability. The resulting technique can be used to monitor DA concentrations at nM levels in micro-volume samples.

In 2003, poly(acridine red) modified glassy carbon electrode was used for the detection of dopamine in the presence of AA in a pH 7.4 phosphate buffer solutions (PBS) by cyclic voltammetry and differential pulse voltammetry were reported by Zhang *et al*. [68]. The electrode was disposed by cyclic sweeping from –1.0 to +2.5 V at 100 mV s^{-1} for 10 circles in pH 7.4 PBS containing 1.0×10^{-4}mol dm^{-3}acridine red solution. The poly(acridine red) film modified electrode could promote DA oxidation. Peak current of DA was proportional to the concentration over the range of 1.0×10^{-7} ~ 1.0×10^{-4} mol dm^{-3} with a detection limit (S/N = 3) of 1.0×10^{-9} mol dm^{-3}. AA had hardly interference with the determination of dopamine. The proposed method exhibited good recovery and reproducibility.

In 2003, gold nanoparticles immobilized on an amine-terminated self-assembled monolayer (SAM) on a polycrystalline gold electrode were successfully used for the selective determination of dopamine in the presence of ascorbate were reported by Raj *et al* [69]. The voltammetric peaks of dopamine were separated from ascorbate. The

oxidation potential of ascorbate is shifted to less positive potential due to the high catalytic activity of gold nanoparticle. The reversibility of the electrode reaction of dopamine is significantly improved at the gold nanoparticle-immobilized electrode, which results in a large increase in the square-wave voltammetric peak current with a detection limit of 0.13 μM. The coexistence of a large excess of ascorbate does not interfere with the voltammetric sensing of dopamine. The gold nanoparticle-immobilized electrode shows sensitivity, good selectivity and antifouling properties.

In 2003, electronic polymers in aqueous media may offer bioelectronic detection of biospecific interactions were reported by Peter *et al* [70]. They reported a fluorometric DNA hybridization detection method based on non-covalent coupling of DNA to a water-soluble zwitterionic polythiophene derivative. Introduction of a single-stranded oligonucleotide will induce a planar polymer and aggregation of the polymer chains, detected as a decrease of the intensity and a red-shift of the fluorescence. On addition of a complementary oligonucleotide, the intensity of the emitted light is increased and blue-shifted. The detection limit of this method is at present ~10^{-11} moles. The method is highly sequence specific, and a single-nucleotide mismatch can be detected within five minutes without using any denaturation steps. The interaction with DNA and the optical phenomena persists when the polymer is deposited and patterned on a surface. This offers a novel way to create DNA chips without using covalent attachment of the receptor or labelling of the analyte.

In 2004, polymers have gained tremendous recognition in the field of artificial sensor with the goal of mimicking natural sense organs [29]. Better selectivity and rapid measurements have been achieved by replacing classical sensor materials with

polymers involving nanotechnology and exploiting either the intrinsic or extrinsic functions of polymers. Semiconductors, semiconducting metal oxides, solid electrolytes, ionic membranes, and organic semiconductors have been the classical materials for sensor devices. Polymers with sensing behavior were reported by Adhikari and Majumdar through modification of the polymer by functionalization.

In 2004, the electropolymerization and doping/dedoping properties of polyaniline ultrathin films on Au electrode surfaces were investigated by Baba *et al*. [23] using EC-SPR and the electrochemical quartz crystal microbalance (EC-QCM). Surface plasmons are excited by reflecting p-polarized laser light off the Au-coated base of the prism. The excitation sources employed were two different He–Ne lasers: λ = 632.8 and 1152 nm. Kinetic measurements were performed in order to monitor the formation of the PANI film and the oxidation/reduction and doping/dedoping properties of the deposited PANI thin film via reflectivity changes as a function of time. The real and imaginary parts of the dielectric constant of the PANI thin film at several doping levels was determined quantitative by taking into consideration the thickness values obtained from the EC-QCM measurement. The combination of these two techniques provides a powerful method for probing the electrical, optical, and dielectric properties of conjugated ultrathin polymer films.

In 2005, The neurotransmitters dopamine, L-DOPA, adrenaline, and nor-adrenaline mediate the generation and growth of gold nanoparticles (Au-NPs) were reported by Baron *et al* [71]. The plasmon absorbance of the Au-NPs allows the quantitative colorimetric detection of the neurotransmitters. Neurotransmitters dopamine, L-DOPA, and noradrenaline are sensed with a detection limit of 2.5×10^{-6}

M, whereas the detection limit for analyzing adrenaline corresponds to 2 x 10^{-5} M. The neurotransmitter-mediated growth of the Au-NPs is also used to probe the activity of tyrosinase. The later biocatalyst oxidizes tyrosine to L-DOPA that mediates the growth of the Au-NPs. The analysis of tyrosinase activity is important for detecting melanoma cells and Parkinson disease.

In 2005, a sensitive method for the detection of catecholamine based on the fluorescence quenching of CdSe nanoparticles was developed by Ma *et al* [72]. The sodium citrate-protected CdSe nanoparticles were synthesized in water solution. The fluorescence quenching of CdSe nanoparticles by dopamine, uric acid, ascorbic acid and catechol were studied; the results showed that all of this four kinds of compound could quench the fluorescence of nanoparticles, and the quenching constant were 6.3 x 10^4, 2.57 x 10^3, 2.14 x 10^3 and 1.168 x 10^3, respectively. The order of sensitivity for the biosensor was: dopamine>latic acid>ascorbic acid>catechol. This method shows good selectivity for dopamine, the detection limit reaches 5.8 x 10^{-8} M.

In 2006, electroactive polymers such as polypyrrole (PPy) were used as coating for electrodes or neural probes and as scaffolds to induce tissue regeneration by Lee *et al* [30]. Acid functionalized PPy substituted at the N–position, poly(1-(2-carboxyethyl)pyrrole) (PPyCOOH), was demonstrated as a bioactive platform for surface modification and cell attachment. PPyCOOH films were prepared by electrochemical polymerization of 1-(2-carboxyethyl)pyrrole monomer that was synthesized from 1-(2-cyanoethyl)pyrrole. Human umbilical vascular endothelial cells (HUVECs) cultured on PPyCOOH films surface-modified with the cell adhesive Arg–Gly–Asp (RGD) motif demonstrated improved attachment and spreading. Thus,

PPyCOOH could be useful in developing PPy composites that contain a variety of biological molecules as bioactive conducting platforms for specific biomedical purposes.

In 2006, SPR technique was reported by Damos *et al*. [73] to monitor the electropolymerization and doping/dedoping processes of thin polypyrrole films on flat gold surfaces. The changes in the electrochemical and optical properties of the thin polypyrrole films upon applying potential sweeps produced a significant change in the SPR angle position due to changes in the real and imaginary parts of the complex dielectric constant during doping/dedoping processes, the doping and dedoping processes in the polypyrrole film can act directly on optical properties while the EC-SPR technique can give the same information indirectly.

In 2007, the specific information of CPs was provided on their modification for use in applications such as biosensors, tissue engineering, and neural probes were reported by Guimard *et al*. [1]. This was especially true in biomedicine, where many applications benefit from the presence of conductive materials, whether for biosensing or for control over cell proliferation and differentiation.

In 2007, most of the current techniques for detection of dopamine exploit its ease of oxidation were reported by Ali *et al* [74]. However, the oxidative approaches suffer from a common problem. The products of dopamine oxidation can react with ascorbic acid present in samples and regenerate dopamine again, which severely limits the accuracy of detection. In this reported a nonoxidative approach to electrochemically detect dopamine with high sensitivity and selectivity. This approach takes advantage of the high performance of the newly developed poly(anilineboronic acid)/carbon

nanotube composite and the excellent permselectivity of the ion-exchange polymer Nafion. The binding of dopamine to the boronic acid groups of the polymer with large affinity affects the electrochemical properties of the polyaniline backbone, which act as the transduction mechanism of this nonoxidative dopamine sensor. The unique reduction capability and high conductivity of single-stranded DNA functionalized, single-walled carbon nanotubes greatly improved the electrochemical activity of the polymer in physiological buffer, and the large surface area of the carbon nanotubes largely increased the density of the boronic acid receptors. The high sensitivity along with the improved selectivity of this sensing approach is a significant step forward toward molecular diagnosis of Parkinson's disease.

In 2008, EC-SPR measurement used for in situ monitoring the formation of polypyrrolepropylic acid (PPA) film was report by Dong *et al*. [75]. Further precise control of the film thickness for tailor the film for an optimized architecture of an immunosensor was performed.0.3 M PPA monomer in 0.1 M phosphate buffer saline (PBS) solution was used for electropolymerization of PPA film on gold surface, which was conducted by cyclic voltammetry in a range from −0.3 to 0.75 V versus SCE. Specifically, 150 μL above mentioned solutions were added into the cuvette and the SPR baseline was recorded for several minutes until the SPR angle became stable. The calibration curves of EC-SPR measurement exhibited a similar dependence on the bulk concentration of antigen. An approximate linear relationship could be obtained by plotting the data in semi-logarithmic reference frame compared with EC-SPR showed higher sensitivity with prolonged time.

In 2008, SPR was employed to study protein immobilization on poly(pyrrole-co-pyrrolepropylic acid) (PPy/PPa) for immunosensing applications by Hu *et al*. [76]. SPR was employed to in situ monitor the electropolymerization process and to control thickness of the PPy/PPa copolymer film. Goat IgG as a model protein was covalently immobilized on the carboxyl containing film through ethyl(dimethylaminopropyl) carbodiimide/N-hydroxysuccinimide (EDC/NHS) as the coupling reagents. The effect of pyrrolepropylic acid (Pa) proportion in the deposition solution on the protein immobilization capability was systemically investigated. The immobilization efficiency was demonstrated by a label-free SPR immunosensor.

In the same year of 2008, SPR method was employed bilayer lipid membrane (BLM) based on immobilizing horseradish peroxidase (HRP) in the BLMs supported by the redox polyaniline (PANI) film to detect enzymatic reaction by Wang *et al*. [77]. SPR kinetic curve in situ monitoring the redox transformation of PANI film resulted from the reaction between HRP and PANI. The enzymatic reaction of HRP with H_2O_2 was successfully analyzed by electrochemical SPR spectroscopy. The results showed that this BLM supported on PANI film could not only preserve the bioactivity of HRP immobilized in the membrane, but also provide a channel for the transfer of electrons between HRP and PANI on electrode surface. These characteristics enabled the development of SPR biosensor for sensitively detecting H_2O_2. The SPR sensor surface was complete regenerated by electrochemical reducing the oxidized PANI to its reduced state.

In 2008, selective DA determinations using porous-carbon-modified glassy carbon electrodes (GCE) in the presence of AA were reported by Song *et al*. [78]. The

effects of structure textures and surface functional groups of the porous carbons on the electrochemical behavior of DA was analyzed based on both cyclic voltammetry (CV) and differential pulse voltammetry (DPV) measurements. The differential pulse voltammetry of DA on the modified GCE was determined in the presence of 400–fold excess of AA, and the linear determination ranges of 0.05–0.99, 0.20–1.96, and 0.6–12.60 μM with the lowest detected concentrations of 4.5×10^{-3}, 4.4×10^{-2}, and 0.33 μM respectively were obtained on the mesoporous carbon, mesoporous carbon with carboxylic and amino groups modified electrodes.

In 2008, carbon fiber microelectrode (CFME) modified by Nafion and single-walled carbon nanotubes (SWNTs) was reported by Jeong and Jeon [79] using voltammetric methods for determination of DA in the presence of AA in phosphate buffer saline (PBS) solution at pH 7.4. The SWNTs have high surface area, good electrical properties and Nafion is a negatively charged polymer and surfactant, therefore composite of SWNTs and Nafion in the electrode film should promote the selectivity and sensitivity of DA detection in the presence of the interfering AA molecule. Voltammetric techniques separated the anodic peaks of DA and AA, the interference from AA was effectively excluded from DA determination. Dopamine can be determined without any interference from AA at the modified microelectrode, thereby increasing the sensitivity, selectivity, and reproducibility and stability. The result of this technique can be used to monitor DA concentrations at nM levels in micro-volume samples.

In 2008, Screen-printed electrodes modified with carbon paste that consisted of graphite powder dispersed in ionic liquids were used for the electrochemical

determination of dopamine, adrenaline and dobutamine in aqueous solution was reported by D. V. Chernshov *et al* [80]. The ionic liquids plays a dual role in modifying composition, acting both as a binder and chemical modifier (ion-exchanger); ion-exchange analyte pre-concentration increases analytical signal and improve the sensitivity. The calibration graphs are linear in concentration range 3.9 x 10^{-6} to 1.0 x 10^{-4} M (dopamine), 2.9 x 10^{-7} to 1.0 x 10^{-4} M (adrenaline) and 1.7 x 10^{-7} to 1.0 x 10^{-4} M (dobutamine); detection limits are (1.2±0.1) x 10^{-6}, (1.3±0.1) x 10^{-7} and (5.3±0.1) x 10^{-8} M, respectively. Using an additive of Co (III) tetrakis-(tert-butyl)-phthalocyanine leads to the increase of signal, lowering detection limit and improves the selectivity of catecholamine determination in presence of ascorbic acid.

In 2008, a novel conductive composite film containing multi-walled carbon nanotubes (MWNTs) with poly(methylene blue) has been synthesized on glassy carbon electrode, gold and indium tin oxide electrodes by potentisostatic methods were reported by Yogeswaran and Chen [81]. The presence of MWNTs in the composite film enhance the surface coverage concentration (Γ) of poly(methylene blue), increased the electron transfer rate constant (Ks) by 43.53% and decreased the degradation of poly(methylene blue) during the cycling. The composite film exhibits a promising higher electrocatalytic activity towards the oxidation of ascorbic acid (AA), adrenaline and dopamine (DA) present in pH 7.4 aqueous solution. The presence of poly(methylene blue) in the composite film enhances the functional properties and overall increase in the sensitivity of the composite film modified electrodes. Both, the cyclic voltammetry and square wave voltammetry have been used for the measurement of electroanalytical properties of analytes by means of composite film modified electrodes. In cyclic voltammetry, well-separated voltammetric peaks have

been obtained at the composite film modified glassy carbon electrodes for AA-adrenaline and AA-DA mixture with a peak separation of 144.36 and 164.00 mV, respectively. The detection limit in the presence of 10 mM AA are 96 µM of adrenaline and 8.53 µM of DA at a signal to noise ratio of 3, which covered the concentration ratio found in physiological condition. Similar sensitivity values have been observed in cyclic voltammetry and semi-derivative square wave voltammetry. Furthermore, the electrochemical quartz crystal microbalance and scanning electron microscopy have been used to reveal the enhancements in functional properties and surface morphology of the composite film.

In 2009, the attenuated total reflection (ATR) and emission light properties utilizing surface plasmon (SP) excitations were measured for the electrochemical change of poly(3-hexylthiophene-2,5diyl) (P3HT) thin films in situ was reported by Kato *et al*. [82]. The SP emission light could detect the SP excited by molecular luminescence of P3HT. SPs were excited at the metal dielectric interface, upon total internal reflection of polarized light from a He–Ne laser with the wavelength of 632.8 nm. The optical/electrochemical process at the Au thin film was detected by monitoring the reflectivity as a function of the incident angle. The SP emission light was obtained by the irradiation of Ar^+ laser beam with the wavelength of 488.0 nm. The P3HT thin film was luminous upon the light irradiation, and excited SP emission light was measured. The SP emission light also decreased by decrease of the molecular luminescence of P3HT by the doping. For the dedoped-state P3HT thin films, the SP emission light also increased with increase of the molecular luminescence. The ATR and SP emission light properties were remarkable changed with the doping and dedoping. The reversible change of the SP emission light was

observed by the doping and the dedoping. The SP emission light excited by molecular luminescence can be controlled by the control of doping-dedoping state.

In 2009, cation surfactant cetyltrimethyl ammonium bromide (CTAB) modified carbon paste electrode (CPE) was reported by Shankar *et al*. [83] for simultaneous determination of AA, DA and UA. The CPE was prepared as fallows, 70% graphite powder and 30% silicone oil were mixed by hand in an agate mortar to produce a homogeneous paste. The paste was then packed into the cavity of a homemade CPE and smoothed on a weighing paper. CTAB modified CPE (CTABMCPE) was prepared by immobilizing the CTAB solution on to the surface of bare CPE. CTABMCPE strongly enhanced both anodic and cathodic peak current of DA. The increase in the concentration of DA resulted in greater the enhancement of electrochemical oxidation at certain stage. Electrochemical process was found to be adsorption controlled and the results also indicated that the problem of the overlapped voltammetric responses of DA with AA and UA, due to their co-existence in real biological matrixes could be effectively overcome by the use of CTABMCPE the modified electrode which has a good selectivity, sensitivity and reproducibility.

In 2010, electrochemical system was fabricated using layer by layer (LbL) technique on graphite electrode, by positively charged poly(diallyldimetheylammonium chloride) (PDDA) and negatively charged MWCNTs wrapped with poly styrene sulfonate (PSS) through electrostastatic interaction, for the simultaneous determination of AA, DA and UA were reported by Manjunatha *et al*. [84]. Solubility of MWNTs in water was increased by using linear

polymer PSS. The PSS wrapped MWCNTs modified electrodes were characterized by electrochemical impedance spectroscopy (EIS), cyclic voltammetry (CV) and differential pulse voltammetry (DPV) and chronoamperometric techniques. The modified electrode exhibits superior electrocatalytic activity towards AA, DA and UA than the bare graphite electrode. No electrode fouling was observed during all the experiments and good stability and reproducibility was obtained for simultaneous determination of AA, DA and UA.

In 2010, poly(3-aminobenzylamine) (P3ABA) prepared by electropolymerization of 3–aminobenzylamine on gold-coated glass electrode, which specific reaction of benzylamine within the P3ABA structure with adrenaline was reported by Baba *et al*. [6]. Adrenaline was detected in real time by EC-SPR spectroscopy, which provides simultaneous monitoring of both optical and current response upon injection of adrenaline into P3ABA film. Furthermore, UV-vis spectroscopy and XPS were studied the reaction of adrenaline with the PABA film. UV-vis spectra at 320 nm increased and 410 nm diminished after injection of adrenaline were changed, which suggest that the chemical structure of the PABA film had changed as a result of the reaction with adrenaline. The $–NH_3^+$ bonds decreased from 49.0 to 20.3%, –N= bonds were measured from 7.2 to 22.1% and the increased in the –NH– bond from 20.9 to 49.1% in XPS results, which suggested that the reaction of adrenaline into PABA film included specific the reaction from benzylamine site and physical adsorption. The EC-SPR reflectivity response of UA and AA showed interference smaller than the reflectivity change in adrenaline because of non-specific reaction with PABA thin film. The number of changes in both current and SPR reflectivity on the injection of

adrenaline exhibited the linear relation to the concentration and the detection limit was 100 pM.

In 2010, a glassy carbon electrode modified with single wall carbon nanotubes (SWNTs/GC) for electrochemical determination of dopamine was reported by Chuekachang *et al*. [85] using cyclic voltammetry (CV) and differential pulse voltammetry (DPV). The electrode was coated with 10 µL of the black suspension of SWNT (1 mg/mL) in N,N-dimetheylformamide (DMF) and heated under an infrared lamp to remove the solvent. The SWNTs/GC 10 µL was used to test the linearity of anodic oxidation of dopamine by DPV. The peak current increased linearly with concentration of dopamine in the range of 2.5–25 ppm (R^2 = 0.9766). For the life time of the SWNTs/GC, the cut-off criterion of the DPV was detected in the reduction of current by 50 %. The lifetime of the modified SWNTs depended on the oxidation of dopamine because of fouling of the electrode surface due to the adsorption of oxidation products, 34 repetition cycles was obtained. The detection limit of the dopamine as obtained from the oxidation current in DPV was 0.021 ppm (S/N = 3) with minimum current for the detection of dopamine of 0.033 µA. The reproducibility of electrocatalytical studies was better within 90% (10% RSD). The relative standard deviation (RSD) of 8.42% for 100 ppm dopamine (n = 20) showed excellent reproducibility.

In 2011, poly(pyrrole-3-carboxylic acid) film constructed by electro-polymerization of pyrrole-3-carboxylic acid monomer on gold-coated glass electrode for the detection of human immunoglobulin G was reported by Janmanee *et al*. [8]. In this research study the kinetic property and electroactivity property of the PP3C thin

film by EC-SPR. The carboxylic acid surface of the PP3C film was activated for the immobilization of anti-human IgG, which have more space inside the polymer chain for the binding of anti-human IgG and human IgG. UV-vis spectroscopy was performed to characterize the PP3C thin film at a difference applied constant potentials. Furthermore, AFM was performed to characterize the mechanism of improved sensitivity of immobilized human IgG.

Therefore, this study aims to fabricate poly(2-aminobenzylamine) (P2ABA) thin film by EC-SPR spectroscopy for the detection of some biomolecules such as adrenaline, AA and UA. The P2ABA thin film will be employed to detect adrenaline because P2ABA thin film has a good electrical conductivity, environmental stability, ease to synthesis and stable at neutral solution. Furthermore, P2ABA has a benzylamine group in the structure which specifically reacts with adrenaline. P2ABA thin film formation on the gold-coated glass substrate will be evaluated by EC-SPR spectroscopy. The interaction between the adrenaline and the benzylamine within P2ABA structure on the gold-coated glass substrate will be detected in real time by a change in SPR reflectivity signal. Furthermore, the reaction of P2ABA thin film with adrenaline will be studied by UV-vis absorption spectroscopy, AFM, FT-IR/ATR and QCM-D techniques compared to the response interference detection of UA and AA. The QCM-D techniques will be employed to study the molecular interaction and adsorption between P2ABA thin film and adrenaline.

1.6 Research Objectives

1.61 To fabricate P2ABA thin film by electrochemical-surface plasmon resonance (EC-SPR) spectroscopy technique

1.62 To characterize and study the properties of P2ABA thin film using EC-SPR spectroscopy, UV-vis absorption spectroscopy, FTIR/ATR, AFM and QCM-D techniques

1.63 To detect some biomolecules such as adrenaline, UA and AA using P2ABA thin film

1.7 Usefulness of the Research (Theory and/or Applied)

P2ABA thin film fabricated by EC-SPR will be obtained for the detection of some biomolecules (such as adrenaline, UA and AA).

1.8 Research plan, methodology and scope

1.8.1 Literature review

1.8.2 Fabrication of P2ABA thin films by EC-SPR spectroscopy technique

1.8.3 Characterize and study the properties of P2ABA thin films by using EC-SPR spectroscopy, UV-vis absorption spectroscopy, FT-IR/ATR, AFM and QCM-D techniques

1.8.4 Detection of some biomolecules such as adrenaline, UA and AA, using P2ABA thin films

1.8.5 Discussions and conclusion

CHAPTER 2

EXPERIMENTAL

2.1 Chemicals

All chemicals were analytical reagent are shown in Table 2.1

Table 2.1 Chemical, purity, molecular formula, molecular weight and company

Chemical	**Purity**	**Molecular formula**	**Molecular weight(unit or Dalton)**	**Company**
2-Aminobenzylamine	98%	$C_7H_{10}N_2$	122.17	Tokyo Kasei Kogyo Co, Ltd
Adrenaline	99%	$C_9H_{13}NO_3$	183.21	Sigma-Aldrich
L-ascorbic acid	99%	$C_6H_8O_6$	176.12	Tokyo Kasei Kogyo Co, Ltd
Uric acid	99%	$C_5H4N_4O_3$	168.11	Sigma-Aldrich
Sulfuric acid	98%	H_2SO_4	98.08	Kanto Chemical
Phosphate buffer saline (Sigma tablets)				Sigma-Aldrich

2.2 Instruments

1. Electrochemical set- a three electrode cell driven by HZ-5000 potentiostat (Hokuto Denko Ltd., Japan)

2. SPR- a home-built SPR system using Kretschmann optical configuration

3. UV-vis spectrophotometer- a V-650 UV-VIS Spectrophotometer (JASCO International Co., Ltd., Japan)

4. Thermal evaporation- a home-built thermal evaporation sources with resistive molybdenum boats.

5. Quartz crystal microbalance with dissipation (QCM-D)-a Q-Sense D300 microbalance material analyzer (qsense, Gothenburg, Sweden)

6. Atomic force microscope (AFM)- a scanning probe microscope SPM-9600 (SHIMADZU, Japan)

7. Fourier transforms infrared spectroscopy attenuated total reflectance (FTIR/ATR)- a nicolet 6700 FI-IR spectrometer (Thermo scientific, USA)

Cyclic voltammetry and amperometry were performed using a potentiostat HZ-5000 (Hokuto Denko Ltd., Japan) interface with a conventional three electrodes cell. The reference electrode was a Ag/AgCl (3 M NaCl, BAS Inc.) aqueous electrode, a platinum wire served as counter electrode and the gold film used both excitation surface plasmon and used as working electrode. The thickness of gold film about 47 nm was chosen for optimum excitation of the surface plasmon vacuum evaporated onto a glass substrate (with an adhesion layer of 3 nm chromiumfor ensure mechanical stability of the gold film during electrochemical experiment) previously evaporated on glass substrate. The surface area of the gold electrode was 0.785 cm^2. A triangular S-LAH66 prism was also used. The Au/glass substrates were clamped

against a Teflon cell with an O-ring, providing a liquid-tight seal. The Teflon cell was then mounted onto a two-axis goniometer to enable investigation by SPR. Details of this setup can be found elsewhere [39]. Surface plasmon resonance spectroscopy (SPR) setup combines the three electrode electrochemical cell with a Kretschmann configuration for the excitation of surface plasmon [9, 25]. The excitation source is a He–Ne laser with λ = 632.8 nm as shown in Figure 2.1. Kinetic measurements were performed to monitor both the P2ABA thin film grown on gold film surface and the oxidation/reduction, doping/dedoping properties of the deposited P2ABA thin film and the some biomolecule-sensing via reflectivity changes as a function of time. Angular measurements were performed by scanning an incident angle range of deionized water before and after electropolymerization of 2ABA monomer and/or P2ABA thin film.

The biomolecules sensing were investigated via reflectivity changes (at a fixed incident angle lower than the dip angle) as a function of time. EC-SPR is a powerful technique to study the reaction of some biomolecules on P2ABA thin film and compared to the response detection of the interference.

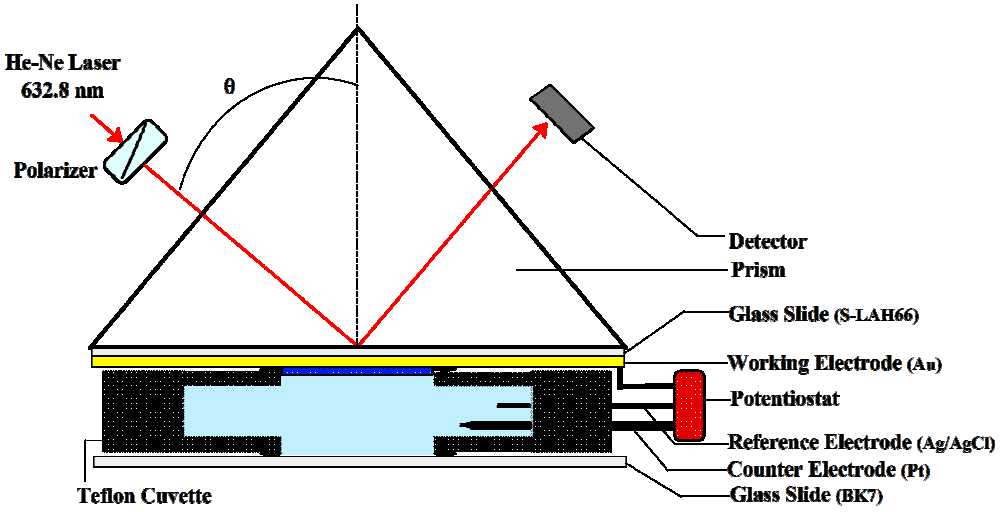

Figure 2.1 EC-SPR instrument setup**.**

2.2.1 Thermal evaporator

Evaporation is a common method of thin film deposition. The source material is evaporated in vacuum. The vacuum allows vapor particles to travel directly to the target (substrate), where they condense back to a solid state. Evaporation is used in micro-fabrication. The thermal evaporation process is shown in Figure 2.2.

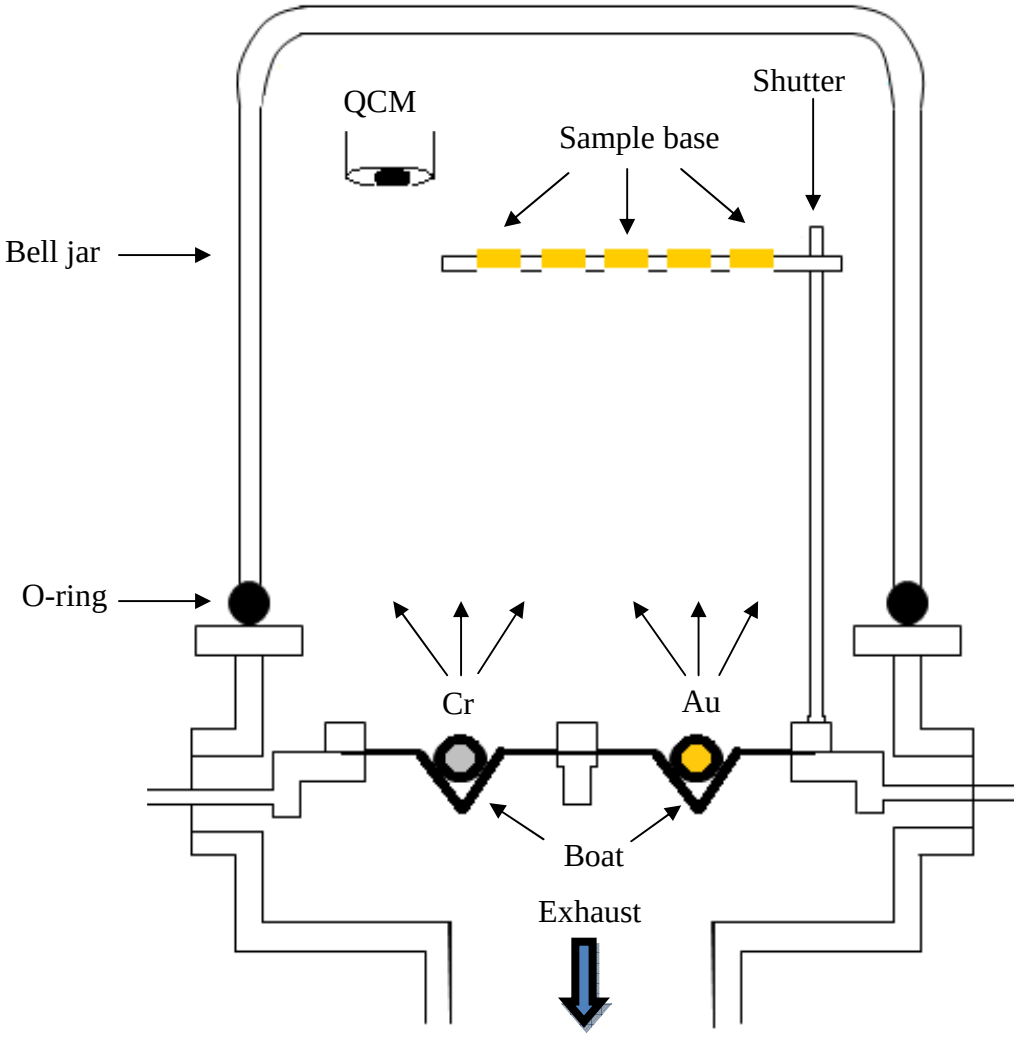

Figure 2.2 Schematic diagram showing vacuum evaporation device.

2.3 Electropolymerization of 2ABA on gold electrode

The gold-coated glass substrate and QCM electrode were washed with 0.5M sulfuric acid and deionized water before thin film formation. The P2ABA thin film was grown on the working electrode by electropolymerization of 50 mM 2ABA monomer in 0.5 M H_2SO_4 by cycling the potential between –0.2 and 0.1 V vs. Ag/AgCl for 10 cycles at a scan rate of 20 mV/s as shown in Figure 2.3. The thickness of P2ABA thin film on the gold electrode was calculated by Winspall software version 3.02 (Winspall program, MPIP, Germany). The P2ABA thin film thickness was estimated to be 10 nm. Finally, the P2ABA thin film was rinsed thoroughly with 0.5 M H_2SO_4 and deionized water respectively before use. Polyaniline and their derivative were poor solubility in various solvents and its loss of electroactivity in neutral solution [9]. The reason for the better performance of the P2ABA film may be due to the film can be electroactive in neutral solution, the electronic properties and the self-doping effect from the functional group. Electroactivity of P2ABA was confirmed from cyclic voltammetry in PBS solution, indicated that the signal can be enhanced with event potential and probe sensitive P2ABA thin film based electrochemical sensors.

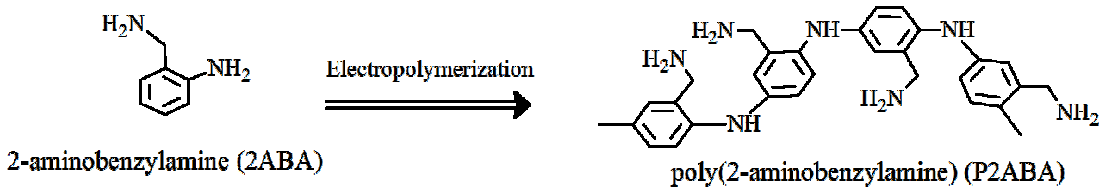

Figure 2.3 Immobilization of P2ABA thin film on gold film electrode by electropolymerization of 50 mM 2ABA monomer in 0.5 M H_2SO_4 followed by cycling the potential between –0.2 and 0.1 V vs. Ag/AgCl for 10 cycles at a scan rate 20 mV/s.

2.4 Characterization of the P2ABA thin films

2.4.1 Quartz crystal microbalance with dissipation (QCM-D) measurement

The QCM-D is a sensitive mass sensor for study molecular interaction and adsorption between P2ABA thin film and adrenaline. The interaction between the adrenaline and the benzylamine structure on the gold film surface was detected in real time by a change in the frequency. The mass changed on the quartz crystal surface was related to change in the oscillation frequency through the Sauerbrey relationship [82]. The Sauerbrey equation can be applied with the frequency change in the QCM setup. The obtained P2ABA thin film-modified gold coated QCM crystal were used to detect various concentrations of adrenaline (1–1000 μM/mL) at an open circuit potential in PBS solution. The QCM-D instrument is shown in Figure 2.4.

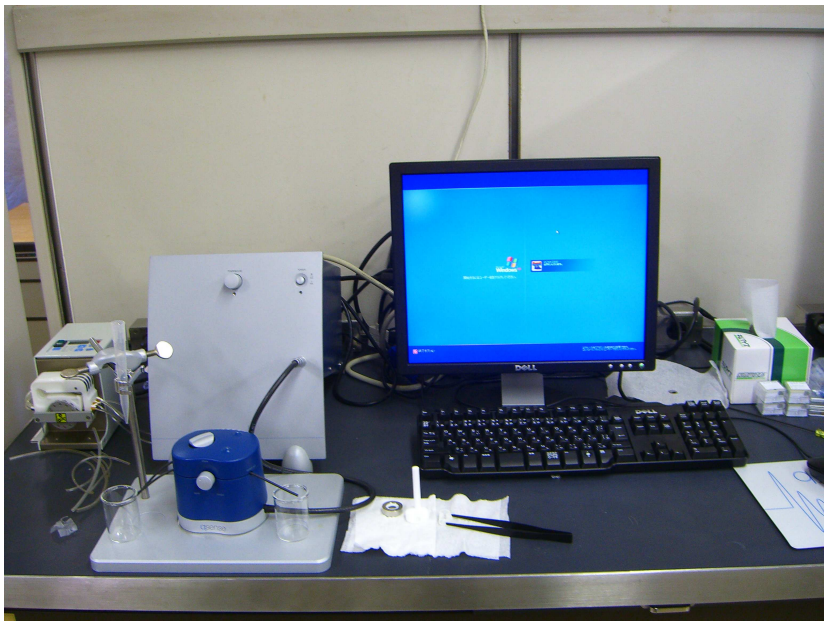

Figure 2.4 QCM-D instrument**.** (Q-Sense D300 microbalance material analyzer (qsense, Gothenburg, Sweden))

2.4.2 UV-vis absorption properties of P2ABA thin film

UV-vis absorption spectroscopy was performed using a V-650 UV-vis Spectrophotometer (JASCO International Co., Ltd., (Figure 2.5)) for studies absorption properties of P2ABA thin film before and after injection of adrenaline, uric acid (UA) and ascorbic acid (AA). An ITO-coated glass substrate was used as working electrode instead of gold thin film used in EC-SPR spectroscopy. The reaction of adrenaline, UA and AA were carried out in PBS solution for 20 min at a constant applied potential of 0.5 V, which corresponds to the oxidation potential of P2ABA film. The UV-vis spectrum of P2ABA film without the reaction with adrenaline, UA and AA were measured after applied constant potential of 0.5 V for 5 min in PBS solution to compared it with the UV-vis spectrum of P2ABA film after the reaction with adrenaline, UA and AA.

Figure 2.5 V-650 UV-vis Spectrophotometer.

2.4.3 Fourier transforms infrared spectroscopy attenuated total reflectance (FTIR/ATR)

FTIR is a technique which is used to obtain an infrared spectrum of absorption, emission, photoconductivity or Raman scattering of a solid, liquid or gas. An FTIR spectrometer simultaneously collects spectral data in a wide spectral range. This

confers a significant advantage over a dispersive spectrometer which measures intensity over a narrow range of wavelengths at a time. FTIR technique has made dispersive infrared spectrometers all but obsolete (except sometimes in the near infrared) and opened up new applications of infrared spectroscopy. FTIR/ATR instrument is shown in Figure 2.6. FTIR/ATR spectrum of P2ABA film without the reaction was measured after electropolymerized 2ABA on gold electrode and compared it with the FTIR/ATR spectrum of P2ABA film after the reaction with adrenaline.

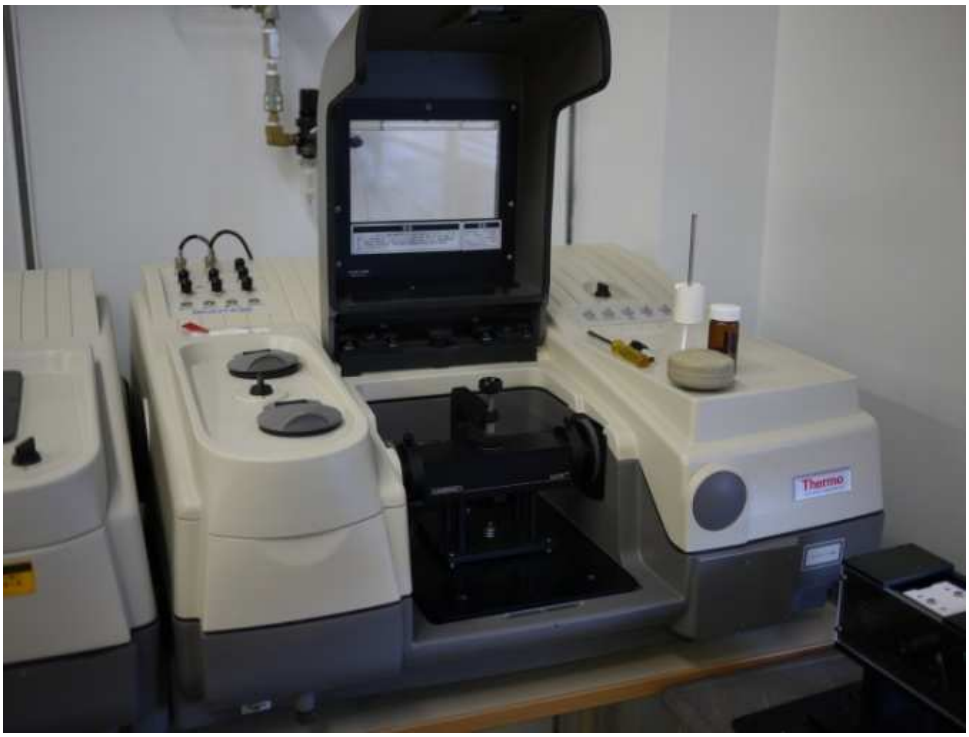

Figure 2.6 FTIR/ATR instrument.

2.4.3.1 KBr Spectra determinations

The powder mixture of the original commercial samples and spectroscopic grade KBr in the ratio of 1:50 was finely ground in an agate mortar and pestle. Pellets were prepared using a handy press. The KBr spectra were recorded in absorbance.

2.4.3.2 ATR Spectra determinations

The surface modification step on P2ABA samples were determined by ATR measurement. Each prepared substrate was put on a ZnSe prism of a sample holder, and ATR spectra were recorded in absorbance. Figure 2.7 shows ATR measurement.

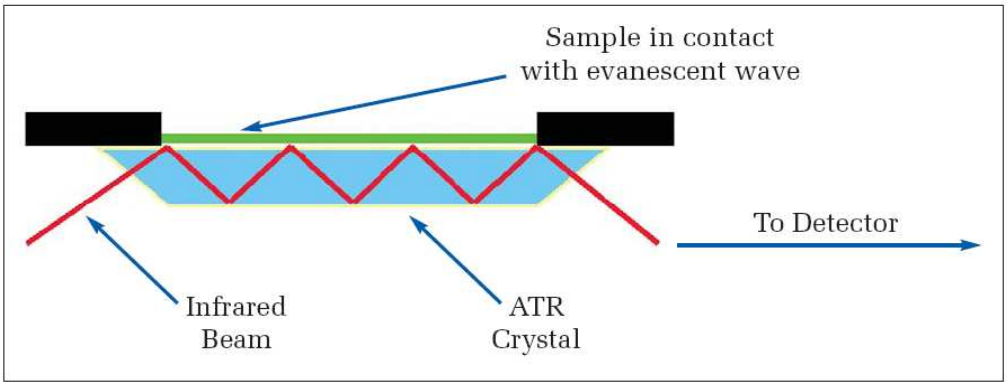

Figure 2.7 ATR measurement**.**

The advantages of FTIR/ATR spectroscopy technique are as follows:

- Faster sampling
- Improving sample-to-sample reproducibility
- Minimizing user-to-user spectral variation
- Higher quality spectral databases for more precise material verification and identification

2.4.4 Atomic Force Microscopy (AFM) Analysis

The AFM was invented by Binning et al. [86] in 1986. The AFM consists of a cantilever with a sharp tip (probe) at its end that is used to scan the specimen surface. The cantilever is typically silicon or silicon nitride with a tip radius of curvature on the order of nanometers. When the tip is brought into proximity of a sample surface, forces between the tip and the sample lead to a deflection of the cantilever

according to Hooke's law. Attractive or repulsive forces resulting from interactions between the tip and the surface will cause a positive or negative bending of the cantilever. The bending is detected by means of a laser beam, which is reflected from the back side of the cantilever as shown in Figure 2.8 [87]. The AFM is a very high resolution scanning probe microscopes, which demonstrated resolution of fractions of a nanometer, more than 1000 times better than the optical diffraction limit. AFM was used to examine the specific reaction, the surface topography of binding reaction of adrenaline to P2ABA film at a several applied constant potentials were observed.

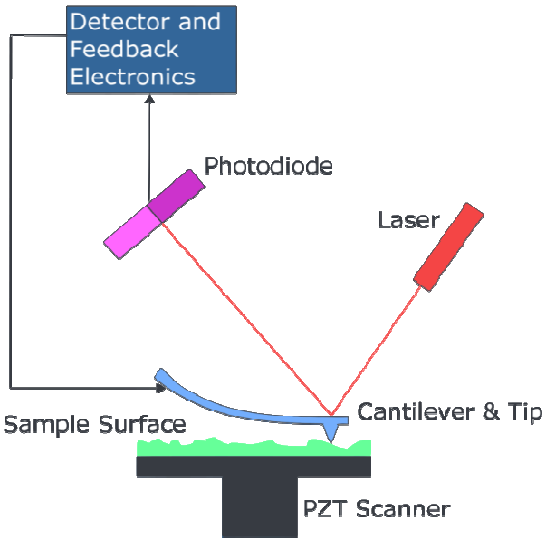

Figure 2.8 Blockdiagram of AFM [87].

2.5 Detection of adrenaline on the P2ABA thin films

The P2ABA thin film was grown on the gold surface by electropolymerization of 2-ABA monomer. Angular measurements were performed by scanning an incident angle range of deionized water before and after electropolymerization of 2-ABA monomer. The thickness of the film was calculated by Fresnel calculation (Winspall software version 3.02) by fitting the obtained SPR curves. Kinetic measurements were

performed to monitor the adrenaline-sensing via reflectivity changes (at the fixed incident angle lower than dip angle) as a function of time.

2.6 Detection of adrenaline in the presence of UA and AA

SPR reflectivity changes after injection of 1 mM adrenaline in the presence of UA and AA at a constant applied potential of –0.2 V, open circuit and 0.5 V were performed by kinetic measurements of the binding reaction. The real time detection of optical and electrochemical signals from the reaction of adrenaline, UA and AA with P2ABA thin films were reported by EC-SPR spectroscopy.

2.7 Method

All experiments were carried out at room temperature and the solutions for electrochemistry measurement were degassed for 5 min before using. A phosphate buffered saline (PBS, pH 7.4) solution was used as the supporting electrolyte for adrenaline detection. The solutions of adrenaline, UA and AA in PBS solution were freshly prepared. The real time detection of optical and electrochemical signals from the reaction of adrenaline, UA and AA with P2ABA thin films were reported by EC-SPR spectroscopy. This research, EC-SPR and QCM-D technique were employed for investigation of the specific reaction from benzylamine site in P2ABA structure with adrenaline compared with the major interference UA and AA. The QCM electrode was plasma cleaned before performing QCM-D experiment.

CHAPTER 3

RESULTS AND DISCUSSION

3.1 Fabrication of P2ABA thin film by EC-SPR

3.1.1 EC-SPR measurement for electropolymerization of 2ABA

The P2ABA thin film was grown on the working electrode by electropolymerization of 50 mM 2ABA monomer in 0.5 M H_2SO_4 by cycling the potential between –0.2 and 0.1 V vs. Ag/AgCl for 10 cycles at a scan rate of 20 mV/s. During cyclic voltammetry scan, the first oxidation peak was observed at about 0.85 V corresponds to the oxidation of 2ABA monomer to form P2ABA film as shown in Figure 3.1. The dedoping peak at about 0.4 V in the cathodic scan and doping peak at about 0.5 V in the anodic scan of the second cycle correspond to the electron transfer to formation of redox couple during the oxidation of P2ABA on electrochemical sensor. The SPR angular curves taken by scanning an incident angle range of deionized water before and after electropolymerization are shown in Figure 3.2. The SPR curve was shifted to the higher dip angle after electropolymerization indicating the P2ABA was deposited on the gold electrode [88]. The thickness of the film was calculated by Fresnel calculation (Winspall software version 3.02) and by curve fitting to obtained SPR curves. The thickness of deposited P2ABA film was estimated to be 10 nm.

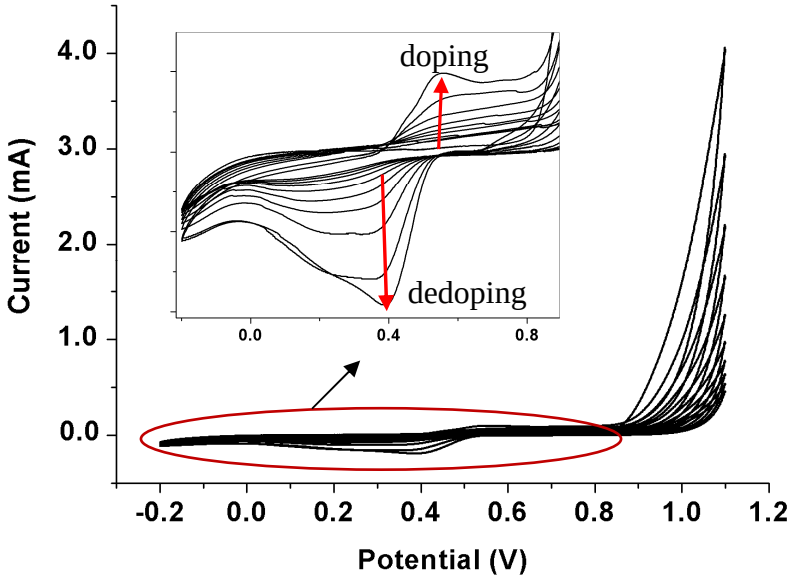

Figure 3.1 Cyclic voltammograms of 50 mM 2ABA monomer on gold electrode by cycling the potential between –0.2 and 0.1 V vs. Ag/AgCl for 10 cycles at a scan rate of 20 mV/s to form P2ABA film.

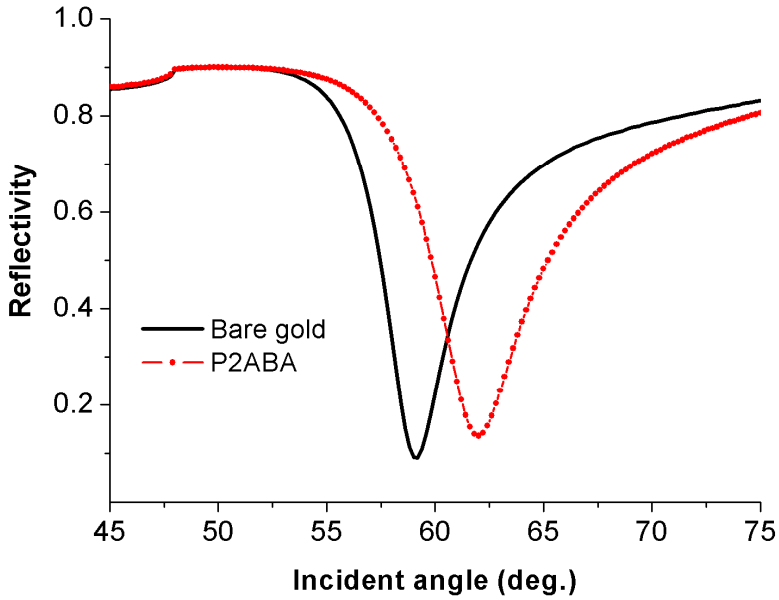

Figure 3.2 Angular-reflectivity curves before and after electropolymerization of P2ABA thin film on gold-coated high reflective index glass substrate.

3.1.2 Electrochemical behavior of P2ABA thin film

After electropolymerlization, the P2ABA thin film was rinsed thoroughly with 0.5 M H_2SO_4 and deionized water just before use. Since polyaniline and derivative were poor solubility in various solvents and its loss of electroactivity in neutral solution. Electroactivity of P2ABA was confirmed from cyclic voltammetry in PBS solution, which indicating that the signal can be enhanced with every potential, as shown in Figure 3.3**.**

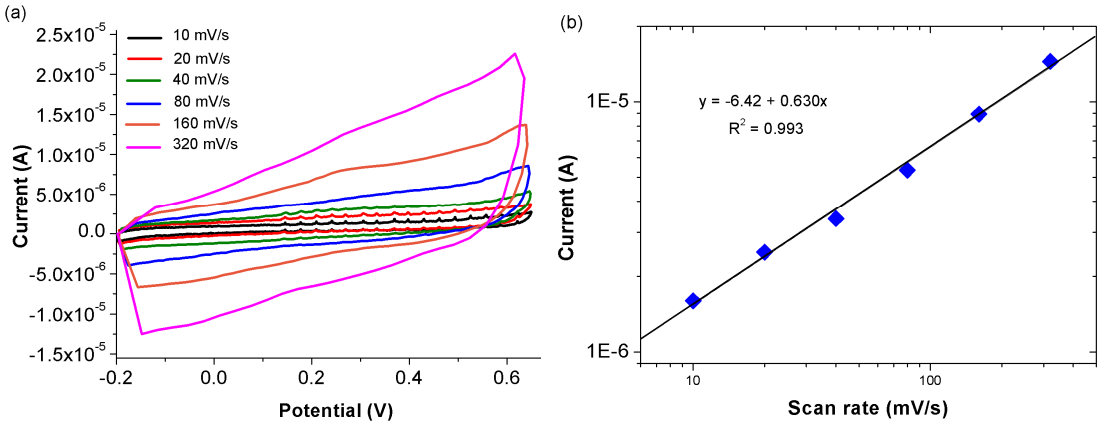

Figure 3.3 (a) CV of P2ABA film at a different scan rates in PBS solution and (b) the plots of anodic peak currents with scan rate.

The CV traces of P2ABA in neutral PBS solution show high oxidation and reduction with increasing the number of scan rate. The reason for the better performance of the P2ABA film may be due to the film can be electroactive in neutral solution [9, 23, 41, 74], the electronic properties and the self–doping effect from the

functional group. The peak currents increase linearly with the scan rate, indicating that electrode reaction was controlled by the diffusion.

The properties of the P2ABA film for study the electrochemical sensor was measured by using EC-SPR measurement. The angular curves of P2ABA thin film were monitored in neutral PBS solution at a different applied potentials of –0.2, open circuit, 0.2, 0.3 and 0.5 V, respectively.

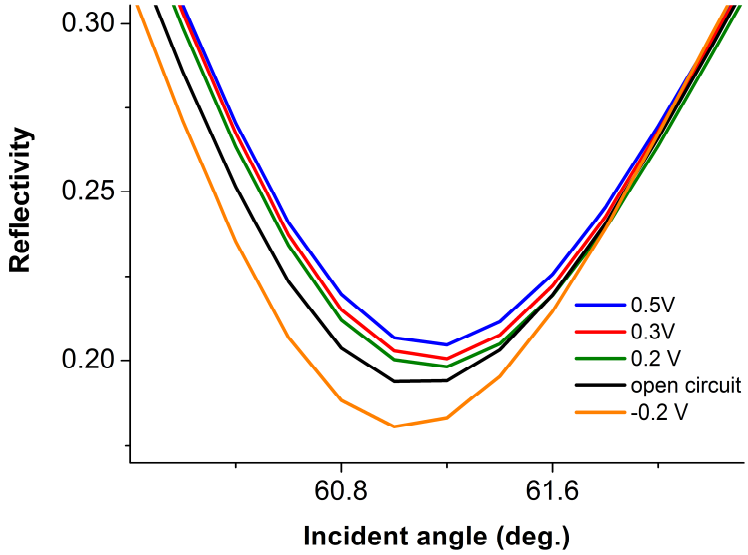

Figure 3.4 SPR angular curves of P2ABA film in PBS solution at several constant applied potentials.

Figure 3.4 shows the SPR angular curves of P2ABA film in neutral PBS solution at several constant applied potentials. The dip angle increases and shifts to higher dip angle with increasing the constant applied potential, indicating the change of the thickness or in dielectric constant. The topography of P2ABA was changed because the P2ABA film might swell due to the doping effect by applying the potential. Another reason is that the film can be electroactive in neutral solution due

to the kind of self-doping is common in PANI derivatives containing sulfuric group in the structure [29, 30]. P2ABA has amino functional group in the structure, which expected to attract negative charge ions in H_2SO_4 during electropolymerization process. Therefore, the negative charge ions are present within P2ABA film. As a result, the P2ABA film becomes doped-state in PBS solution.

3.1.3 Study of an active surface P2ABA film

Figure 3.5 shows SPR reflectivity response upon injection of 1 mM adrenaline into P2ABA film at constant applied potentials of –0.2 V and 0.5 V. The adrenaline–P2ABA electrode was performed by CV with potential range from –0.2 V to 0.8 V at scan rate of 20 mV/s after resting under open circuit for 3 min. The SPR reflectivity after CV at a constant applied potential of –0.2 V was observed to be higher than that of 0.5V because the P2ABA from dedoped state became doped-state has more active specific site for adrenaline.

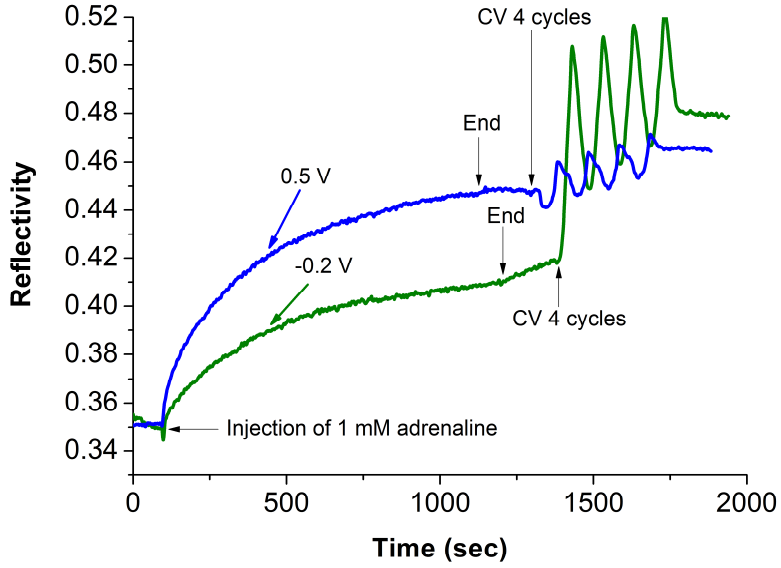

Figure 3.5 SPR reflectivity response upon injection of 1 mM adrenaline into P2ABA film at constant applied potentials of –0.2 V and 0.5 V.

Figure 3.6 shows CV with potential range from –0.2 V to 0.8 V recorded for a solution of 1 mM adrenaline after applied constant potentials of –0.2 V (a) and 0.5 V (b). The electrochemical behaviour during CV experiment at pH 7.4 supposes an oxidation of catechol group (protonated adrenaline) in adrenaline structure giving rise to adrenochrome, as shown in Figure 3.7. The shifts of CV at a constant applied potential of –0.2 V was observed to be higher than 0.5 V corresponds to the SPR reflectivity result to form flurescent derivative.

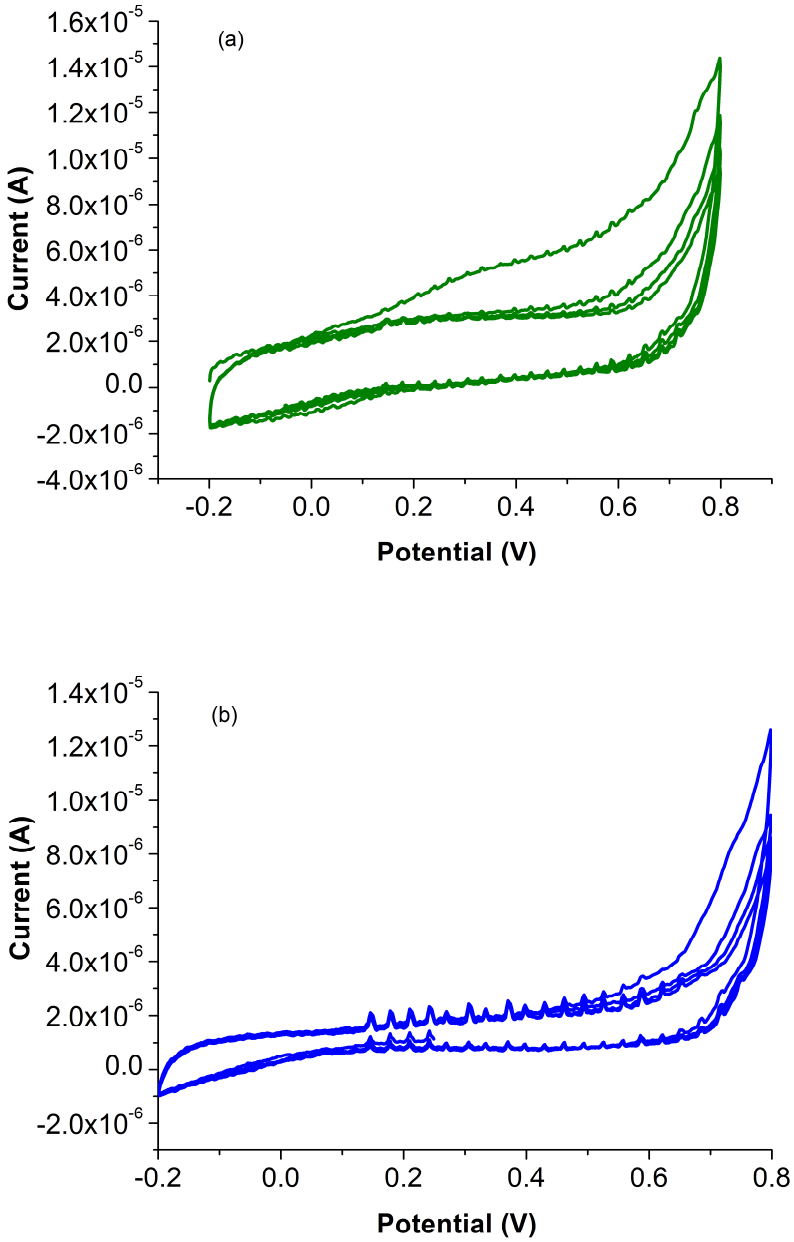

Figure 3.6 CV traces after completing detection adrenaline at constant applied potentials of (a) –0.2 V and (b) 0.5 V.

3.1.4 Detection of adrenaline on the P2ABA thin film

Polyaniline (PANI) film was deprotonation and loss in electroactivity at pH higher than 4 [24]. Electroactivity of P2ABA was studied in PBS supporting

electrolyte solution (pH 7.4) by cyclic voltammetry, which indicated that the electrochemical signal can be enhanced event of specific reaction with adrenaline [23, 89]. The reaction of adrenaline with the P2ABA film was shown in Figure 3.7.

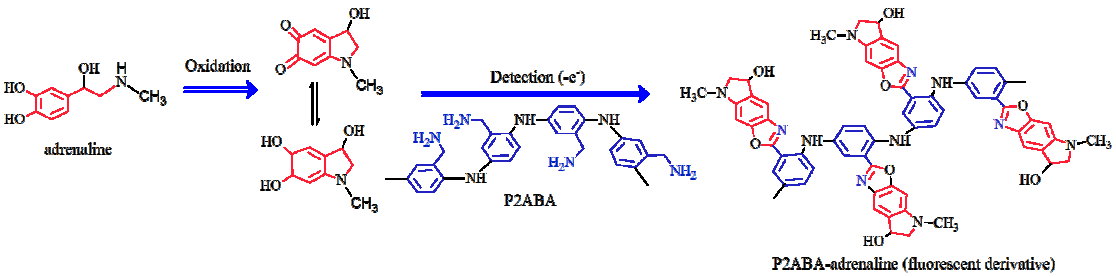

Figure 3.7 The specific reaction of adrenaline to P2ABA film.

The SPR responses of P2ABA and PANI thin film on the detection of adrenaline as observed in the reflectivity change at a constant potential of 0.5 V and an open circuit are shown in Figure 3.8 (a) and (b), respectively. The reflectivity changes in PANI thin film was observed smaller than the reflectivity changes in P2ABA thin films because P2ABA have benzylamine group in the structure, which shows specific adsorption and physical adsorption.

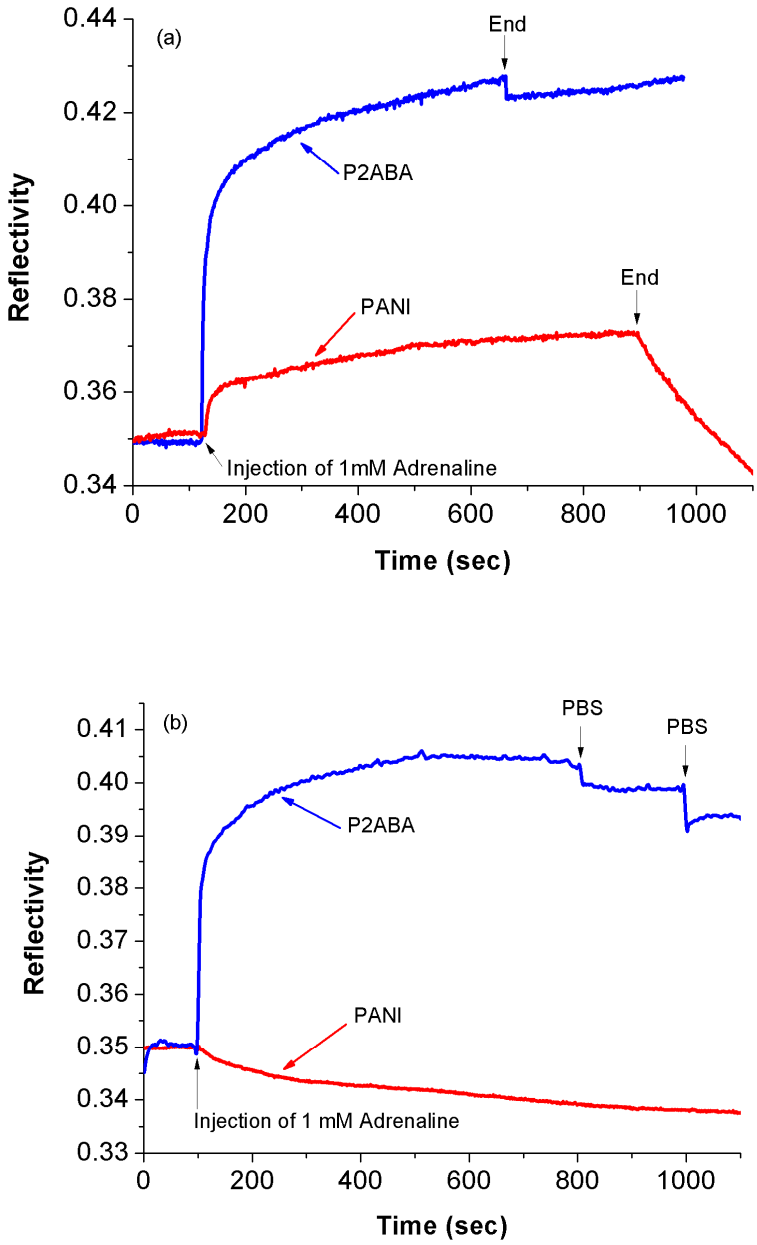

Figure 3.8 SPR reflectivity responses upon injection of 1 mM adrenaline into P2ABA and PANI thin film at (a) constant potentials of 0.5 V and (b) an open circuit potential.

The current response upon injection of 1 mM adrenaline in PBS solution at the doped-state of P2ABA and PANI as shown in Figure 3.9. The current response of PANI is less than that of P2ABA because the oxidation of adrenaline, since it faciliates the electron transfer with benzylamine in P2ABA structure.

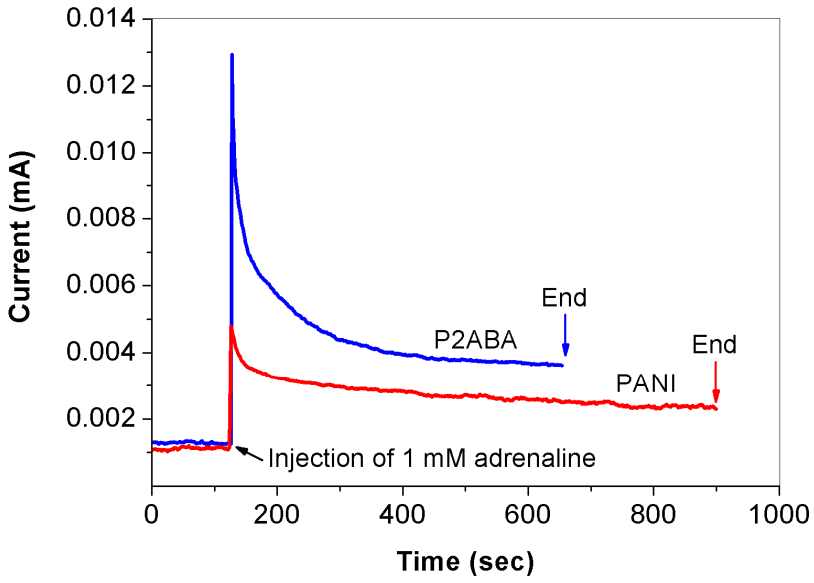

Figure 3.9 The current response upon injection of 1 mM adrenaline into P2ABA and PANI thin film at a constant applied potential of 0.5 V.

Furthermore, we studied the specific reaction at de-doped state (–0.2 V), as shown in Figure 3.10. P2ABA is a sensing film for adrenaline, due to its high binding specificity than PANI.

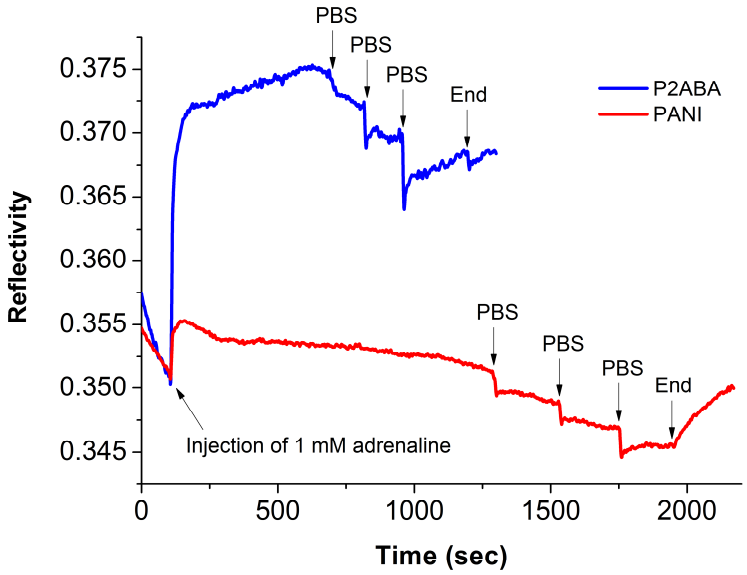

Figure 3.10 SPR reflectivity and current response upon injection of 1 mM adrenaline into P2ABA and PANI thin film at a constant applied potential of –0.2 V.

Figure 3.11 shows the SPR responses during the detection of adrenaline with comparison with UA and AA of P2ABA film at a constant applied potential of 0.5 V (doped-state of P2ABA film). The reflectivity change in adrenaline was obviously higher than those of the UA and AA. The SPR reflectivity change was observed after injection of 1 mM adrenaline at an applied potential of 0.5 V. SPR reflectivity increase rapidly and gradually increase due to the specific adsorption and physical adsorption between adrenaline with benzylamine in P2ABA structure [6, 63, 90].

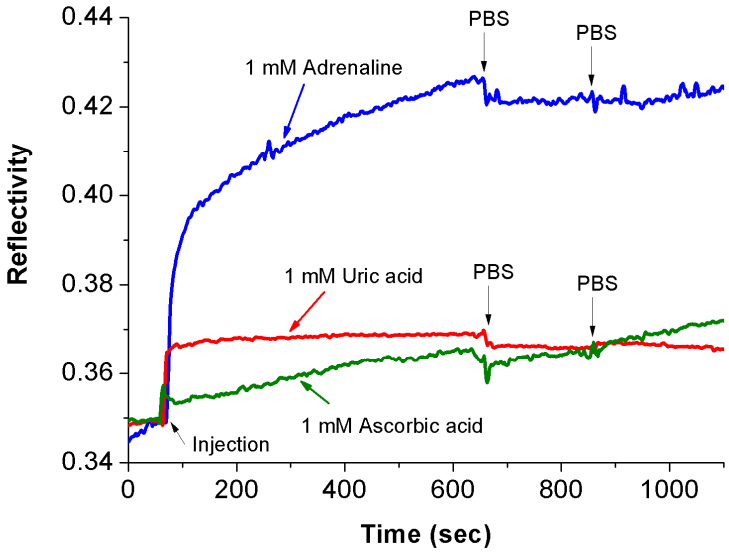

Figure 3.11 SPR reflectivity response after injection 1 mM each of adrenaline, UA and AA into P2ABA thin film at a constant applied potential of 0.5 V.

SPR response of adrenaline in the presence of UA and AA was also studied, the current and reflectivity changes in the UA and AA were observed to be smaller than that of adrenaline because UA and AA did not has a catechol group in the structure to react with benzylamine to form fluorescence derivative structure [63, 90, 91]. Furthermore, the experiment at –0.2 V and open circuit (dedoped and neutral state range of P2ABA in PBS solution) were found that the selectivity of adrenaline detection over UA and AA were increased. Figure 3.12 (a) shows the reflectivity changes after injection of 1 mM adrenaline in the UA and AA at –0.2 V. Figure 3.12 (b) shows the good efficiency of P2ABA thin film during the measurement 1 mM each of adrenaline, AA and UA in PBS solution at an open circuit. Since adrenaline easily oxidizes to react with benzylamine site and offered the electron to P2ABA, the P2ABA becomes the dedoped state [6, 23]. Moreover, the P2ABA film has an amino-

functionalized group, which can attract the negative ion from adrenaline [6]. Adrenaline cannot be oxidized with P2ABA at −0.2 V. Therefore, the reflectivity change is much less than that at 0.5 V, indicating that only a small amount of adrenaline can react with P2ABA at −0.2 V (Figure 3.13). It should be noted that the injected adrenaline is a mixture of both oxidized and non-oxidized forms. Because there is virtually no change upon PBS rinsing after the adsorption of adrenalin, it again supports the notion that the adsorption is due to a specific chemical reaction. Therefore, EC-SPR response of adrenaline in the presence of UA and AA at –0.2 V and an open circuit was observed in terms of better selectivity than that of 0.5 V.

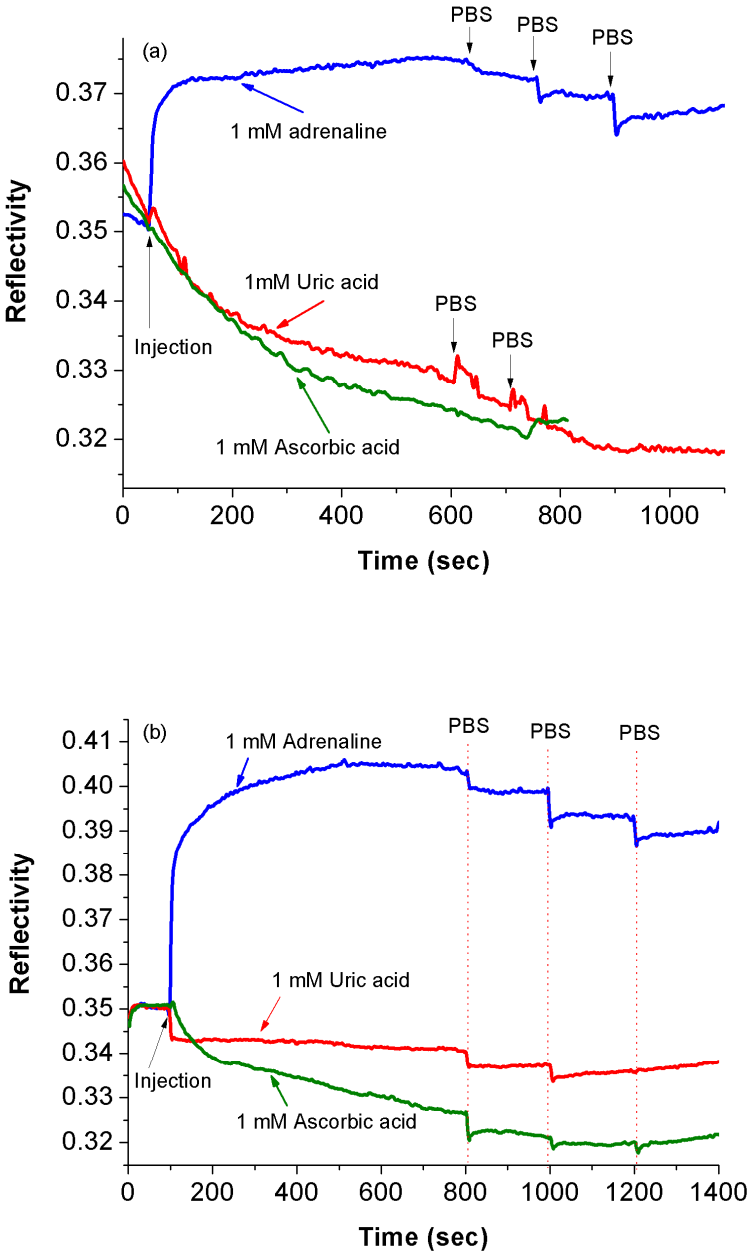

Figure 3.12 The SPR reflectivity result of P2ABA film after reaction with 1 mM each of adrenaline, UA and AA at constant applied potentials of (a) –0.2 V and (b) an open circuit potential.

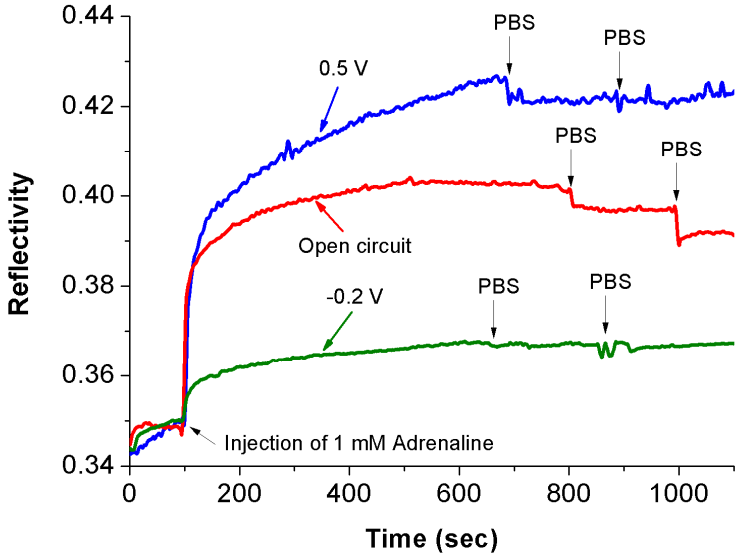

Figure 3.13 SPR reflectivity responses upon injection of 1 mM adrenaline into P2ABA thin film at −0.2, open circuit potential, and 0.5 V.

3.1.5 Detection limit

Figure 3.14 shows SPR reflectivity response upon injection of 1 mM to 10 pM adrenaline into P2ABA thin film at an open circuit potential. The detection limit in an experiment was determined to be 10 pM from SPR response detection at an open circuit.

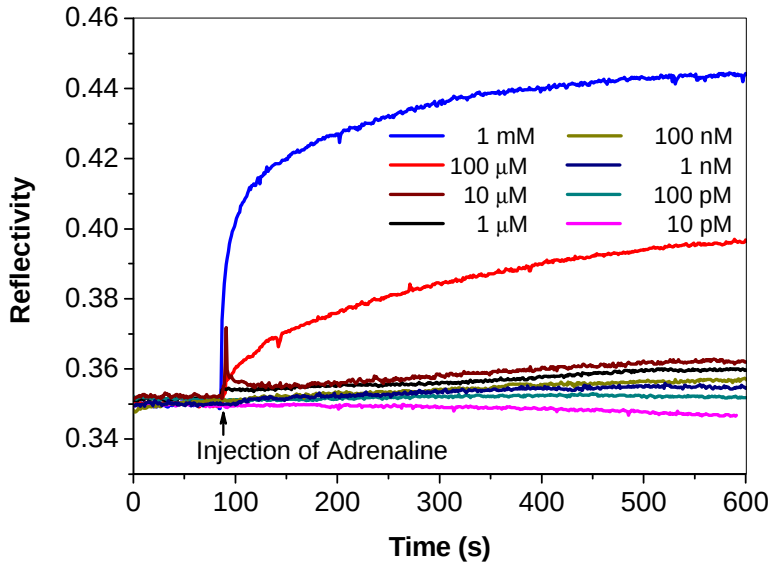

Figure 3.14 SPR reflectivity response upon injection of 1 mM to 10 pM adrenaline into P2ABA thin film at an open circuit.

Figure 3.15 shows plots of the changes in reflectivity as a function of adrenaline concentration was observed at open circuit potential. In these plots, the relationship is linear. The Langmuir-Freundlich model instead of a simple Langmuir model was used for fitting the kinetic curves [92, 93], as the binding reaction of benzylamine with adrenaline occurs not only at the surface but also inside the P2ABA film. This hypothesis confirm by QCM-D technique will be described located below.

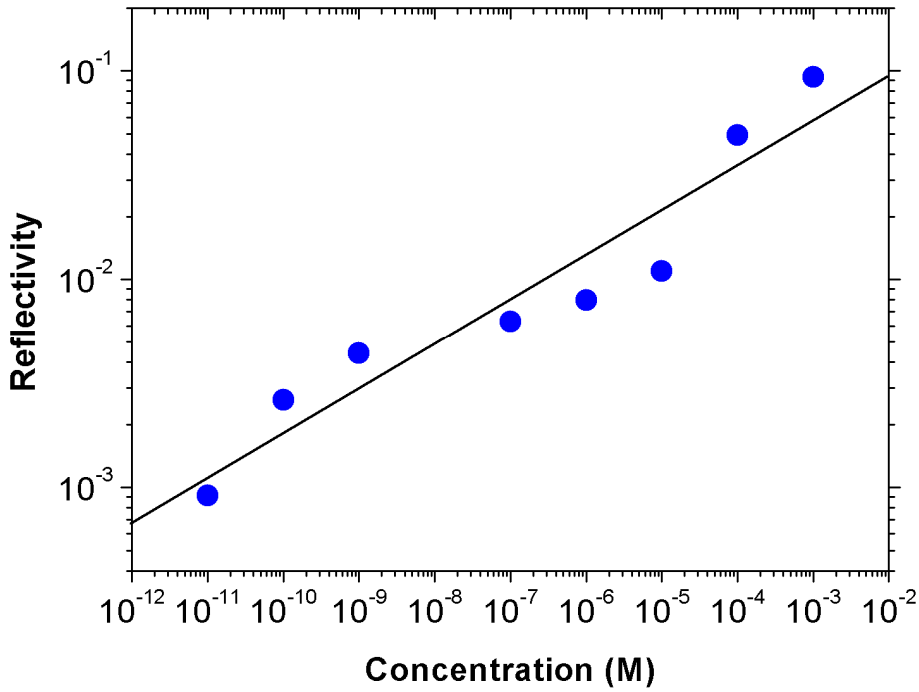

Figure 3.15 Calibrated double-logarithmic plots of the change of the reflectivity as a function of adrenaline concentration.

3.1.6 Efficiency of P2ABA thin film

Figure 3.16 shows the efficiency of P2ABA thin film during the measurement of 1 mM adrenaline, AA and UA in PBS solution at an open circuit. The reflectivity of PBS solution was at baseline followed by injection of 1 mM adrenaline, AA and UA. Adrenaline was carried out by P2ABA in PBS solution for 20 min and cleaned with PBS solution for 3 times for remove adrenaline and generate the SPR baseline before injection AA, and UA respectively. The results show high sensitivity and selectivity of P2ABA at an open circuit potential.

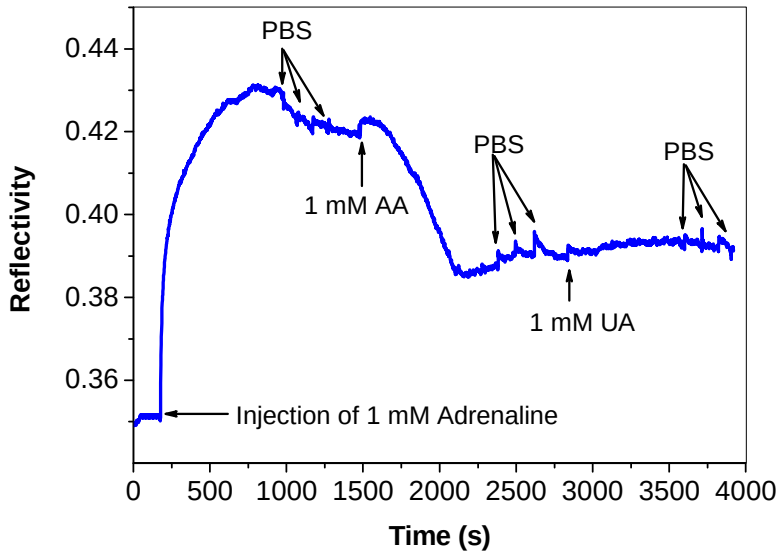

Figure 3.16 Simultaneous observation of SPR reflectivity response upon injection of 1 mM adrenaline, AA and UA into P2ABA thin film at an open circuit potential.

3.1.7 SPR reflectivity change of P2ABA film before and after detection of adrenaline, UA and AA

SPR reflectivity change of P2ABA film before and after detection of adrenaline, UA and AA were carried out by the calculation from the change of dip angle, as shown in Figures 3.17 - 3.19. The reflectivity change of UA and AA were smaller than the reflectivity change of adrenaline, indicating that the specific reaction between benzylamine in P2ABA film with adrenaline.

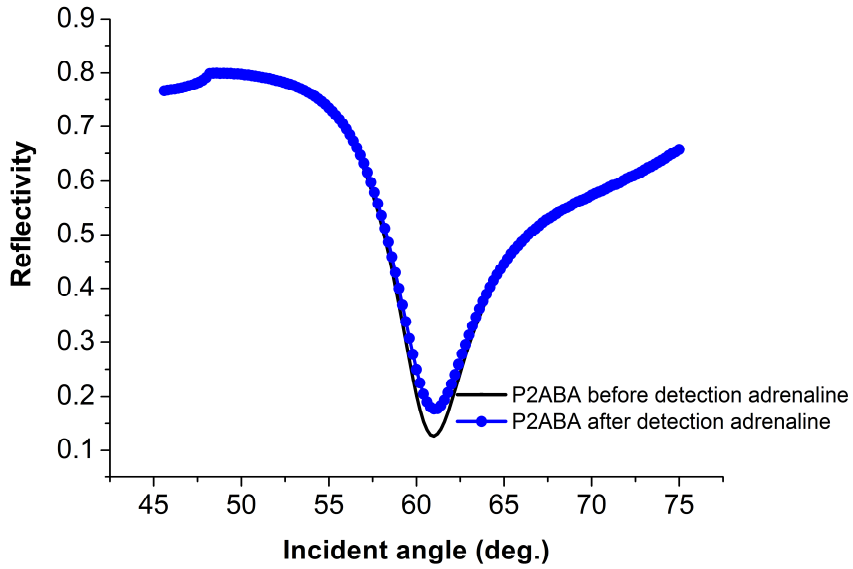

Figure 3.17 SPR reflectivity of P2ABA film before and after injection of 1mM adrenaline at a constant applied potential of 0.5V.

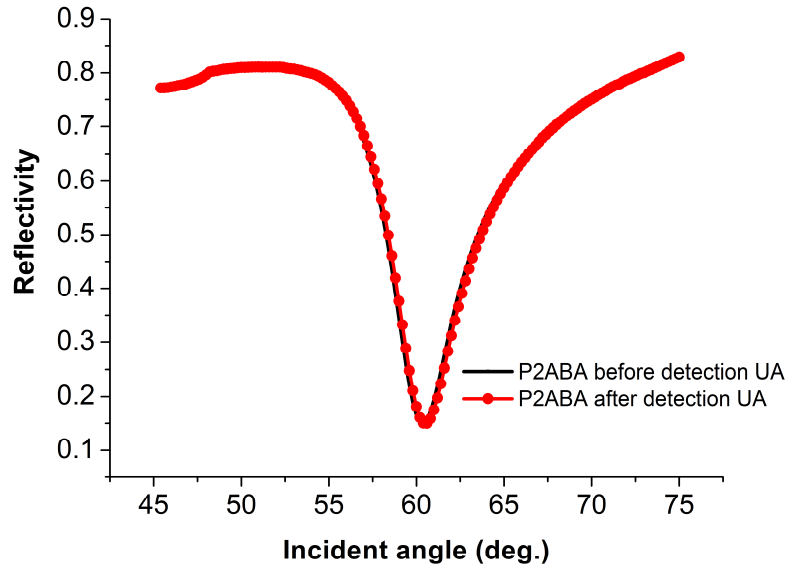

Figure 3.18 SPR reflectivity of P2ABA film before and after injection of 1mM UA at a constant applied potential of 0.5V.

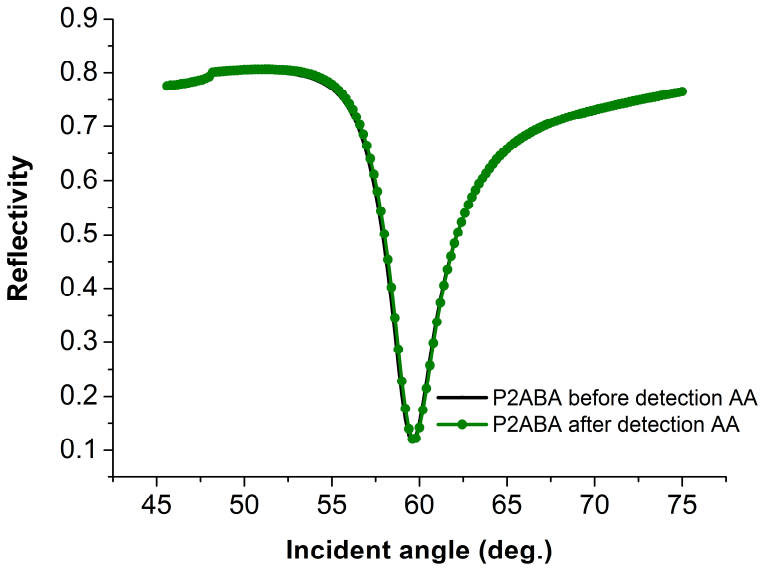

Figure 3.19 SPR reflectivity of P2ABA film before and after injection of 1mM AA at a constant applied potential of 0.5V.

Figure 3.20 shows the plot of SPR reflectivity change of P2ABA film in PBS solution after the injection of 1mM adrenaline at constant applied potentials of –0.2 V, open circuit, 0.2 V, 0.3 V and 0.5V, respectively. The plot of SPR reflectivity change, the relation was also linear to the constant applied potential. This result indicates that the specific reaction that can be occurred at any potentials.

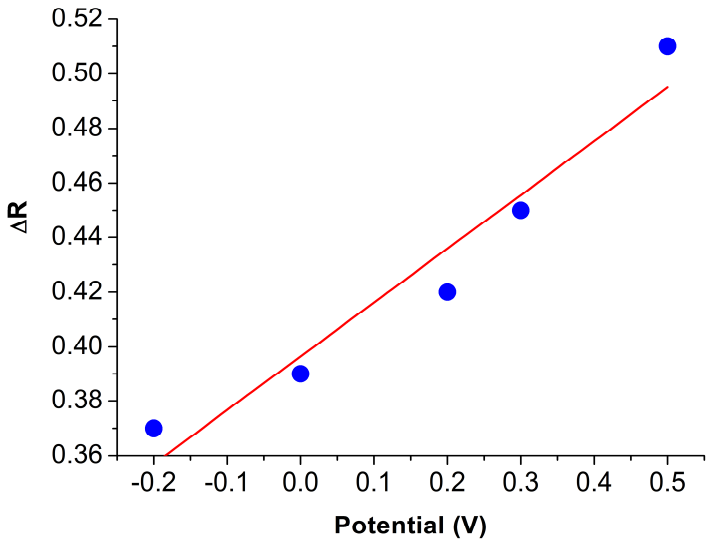

Figure 3.20 The plot of SPR reflectivity change of P2ABA film in PBS solution after the injection of 1mM adrenaline at constant applied potentials of –0.2, open circuit, 0.2, 0.3 and 0.5V.

3.2 Characterization of P2ABA thin films

3.2.1 QCM-D measurement

To study the reaction of adrenaline with the P2ABA thin film, QCM-D of P2ABA thin films was studied at an open circuit. Figure 3.21 shows the frequency and dissipation change of 15 MHz quartz crystal microbalance upon injection of 1 mM, 100 µM, 10 µM, and 1 µM adrenaline, the frequency rapidly decreased when injection of adrenaline and gradually decreased, which suggested that the specific reaction from benzylamine site in P2ABA with adrenaline was a physical adsorption.

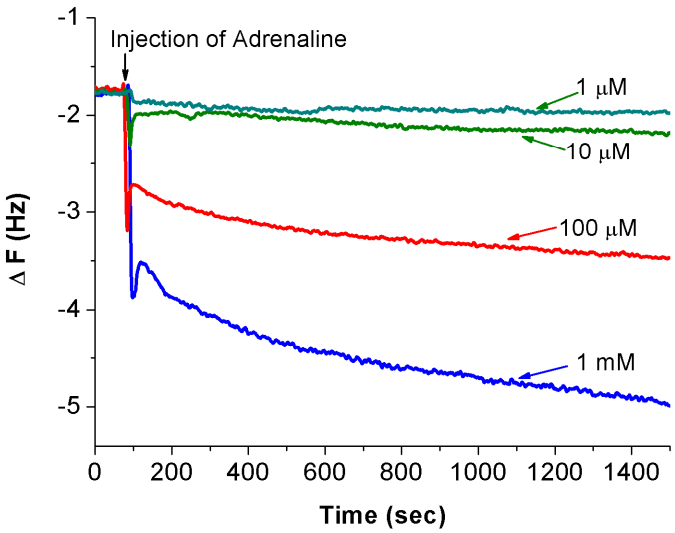

Figure 3.21 QCM-D response upon injection of 1 mM, 100 µM, 10 µM, and 1 µM adrenaline into P2ABA thin film at an open circuit potential.

The mass change was calculated by Sauerbrey equation [94]:

$$\Delta m = -C\Delta f \qquad 3.1$$

where Δm is = mass change, C is = 17.7 ng $cm^{-2}s^{-1}$ and Δf is = frequency change (n is over tone number = 1) . The mass change of 93.0, 53.0, 28.7 and 10.5 ng cm^{-2} can be obtained for 1 mM, 100 µM, 10 µM, and 1 µM adrenaline, respectively. The experimental detection limit was determined to be 100 pM at an open circuit potential. The mass changes after injection of UA (mass change 10 ng cm^2) and AA (mass not change) were observed to be smaller than the mass change in adrenaline due to non-specific reaction with P2ABA thin film [6] as shown in Figure 3.22 and support the SPR result at an open circuit potential. Figure 3.23 shows plots of the changes in frequency as a function of adrenaline concentration, as obtained from Figure 3.21. In these plots the relationship was linear indicating that the binding reaction of

benzylamine with adrenaline occurs not only at the surface but also inside the P2ABA film. The experimental detection limit was determined to be 100 pM.

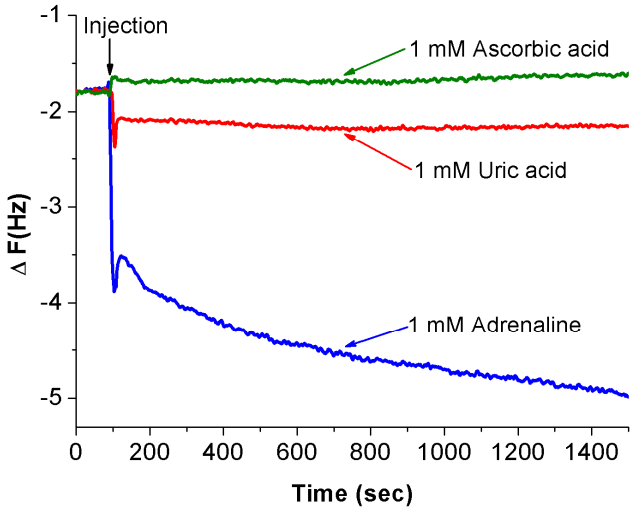

Figure 3.22 QCM-D response upon injection of 1 mM adrenaline into P2ABA thin film compared with UA and AA at an open circuit potential**.**

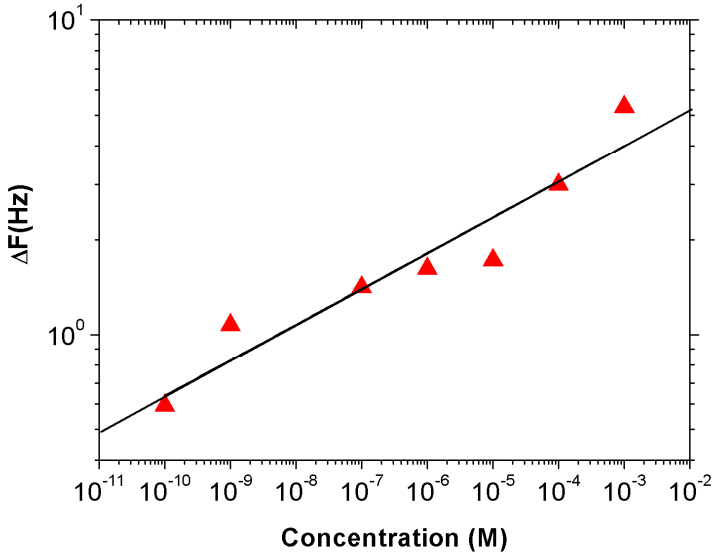

Figure 3.23 Plots the change of the QCM frequency as a function of concentration.

3.2.2 UV-vis absorption properties of P2ABA thin film before and after adsorption of adrenaline

UV-vis absorption spectra of each material in PBS solution and after injection of 1 mM each of adrenaline, UA and AA. The UV-vis spectrum of P2ABA thin film without the reaction with 1 mM adrenaline, UA and AA was obtained after applying the constant potential of 0.5 V for 20 min in PBS solution (pH 7.4) as shown in Figure 3.24 (a) comparing with the UV-vis spectrum of P2ABA thin film after the reaction with 1 mM adrenaline, UA and AA at 0.5 V for 20 min as shown in Figure 3.24 (b).

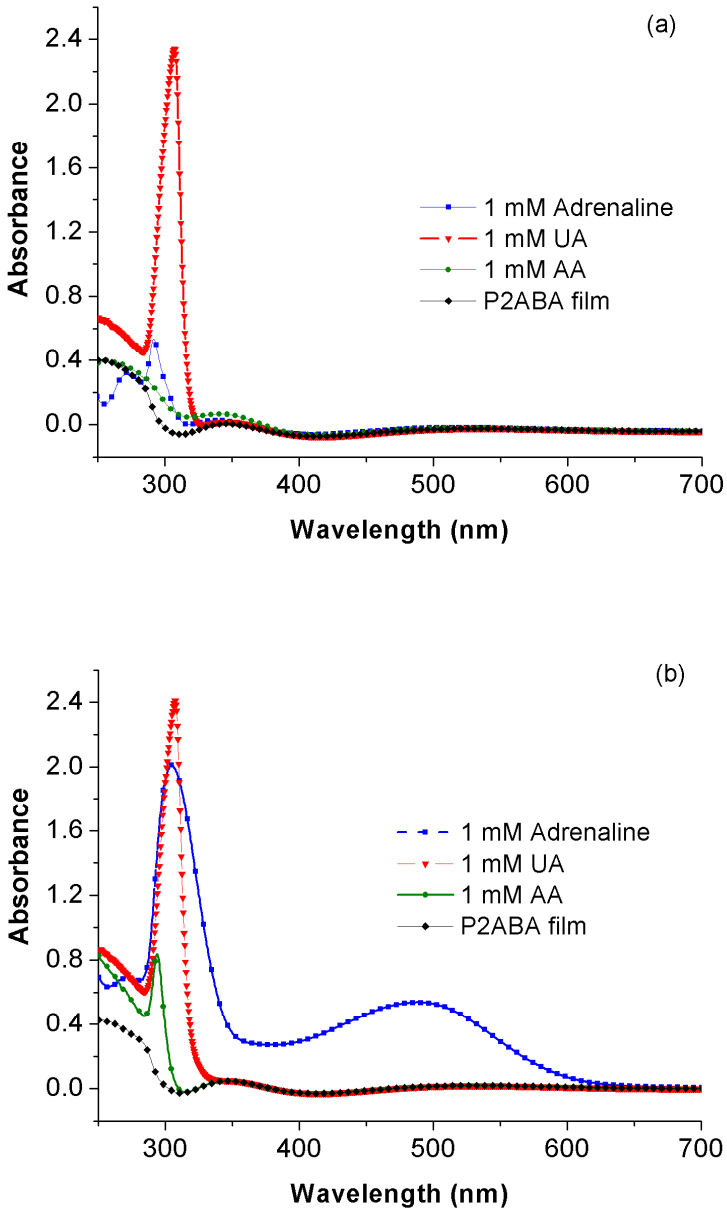

Figure 3.24 (a) UV-vis spectrum of each material in PBS solution and (b) UV-vis spectrum of P2ABA after the reaction with 1mM each of adrenaline, UA and AA at a constant applied potential of 0.5 V.

The new peak appeared at 490 nm after injection of 1mM adrenaline should be due to the specific reaction with benzylamine site in P2ABA structure. The maximum

peak at 301 nm was a main peak of adrenochrome [95]. A mechanism for this reaction to produce fluorescent derivative, it may possible due to the P2ABA thin film was remain in the doped state in the PBS solution and oxidized adrenaline by accepting the electron from adrenaline, then the P2ABA become the dedoped state [6].

3.2.3 Atomic force microscopy (AFM) analysis

The AFM is a very high-resolution scanning probe microscopes, which demonstrated resolution in fractions of a nanometer, more than 1000 times better resolution than the optical diffraction limit. AFM was used to examine the specific reaction, the surface topography of binding reaction of adrenaline to P2ABA film at a several applied constant potentials as shown in Figure 3.25. The roughness of P2ABA film (7.617 nm) for the binding reaction of adrenaline at a constant potentials of –0.2 V, open circuit and 0.5 V were 4.106, 2.111 and 1.448 nm, respectively. The roughness decreased with increasing the constant applied potential, suggesting that P2ABA-surface has a rough topography and space filling the specific reaction site. P2ABA film became smooth surface after the binding reaction with adrenaline. This result coresponds with the SPR reflectivity upon injection of 1 mM adrenaline into P2ABA film at a different applied constant potential in Figure 3.13.

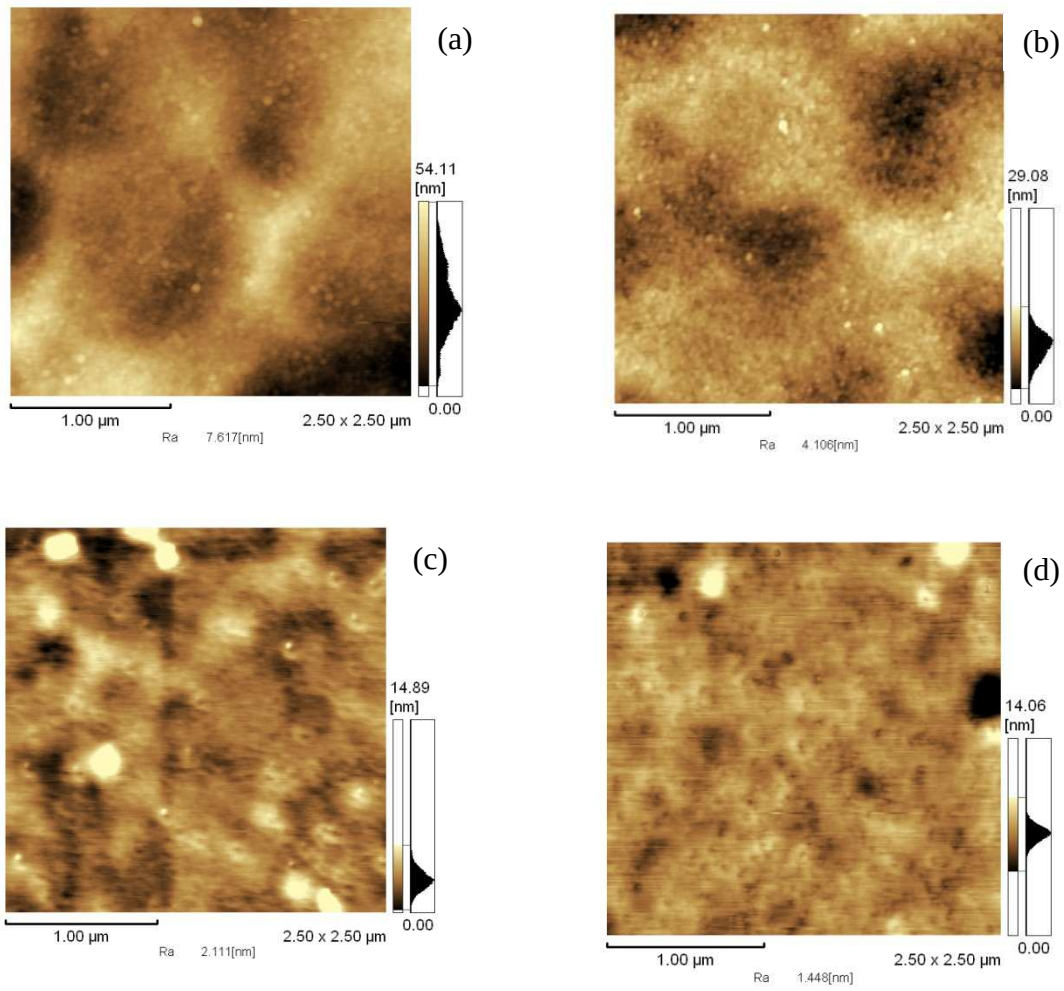

Figure 3.25 AFM images of P2ABA film (a) after binding reaction with adrenaline at constant applied potentials of (b) –0.2 V, (c) open circuit and (d) 0.5 V.

3.2.4 Fourier transforms infrared spectroscopy attenuated total reflectance (FTIR/ATR) analysis

FTIR/ATR is a technique which is used to obtain an infrared spectrum of absorption, emission, photoconductivity or Raman scattering of a solid, liquid or gas. The FTIR spectrometer simultaneously collects spectral data in a wide spectral range. This confers a significant advantage over a dispersive spectrometer, which measures intensity over a narrow range of wavelengths at a time. FTIR technique has made

dispersive infrared spectrometers all but obsolete (except sometimes in the near infrared) and opened up new applications of infrared spectroscopy. The P2ABA film was electropolymerization on the gold-coated high reflective index glass substrate to study the specific reaction. Figure 3.26 shows the FTIR/ATR spectra of bare gold and P2ABA film before the specific reaction. The board adsorption at 3300 cm^{-1} indicates the presence of –OH group. The absorption band in the 3000–2800 cm^{-1} region indicates the $–NH_2$ group. After the reaction of P2ABA with 1mM adrenaline, the adsorption at 3300 cm^{-1} and 3000–2800 cm^{-1} region disappeared. This suggests that the reaction of –OH group in adrenaline structure with the benzylamine structure in P2ABA, as shown in Figure 3.27. The adsorption spectra at 1710 cm^{-1} region disappeared after reaction with adrenaline, indicating that adrenaline was oxidized to adrenochrome and give electron to P2ABA. The C=O bond to form fluorescent derivative (see the reaction at Figure 3.3) and P2ABA became de-doped state. The detail of the specific reaction was waiting for more reference to confirm the reaction between adrenaline with P2ABA film.

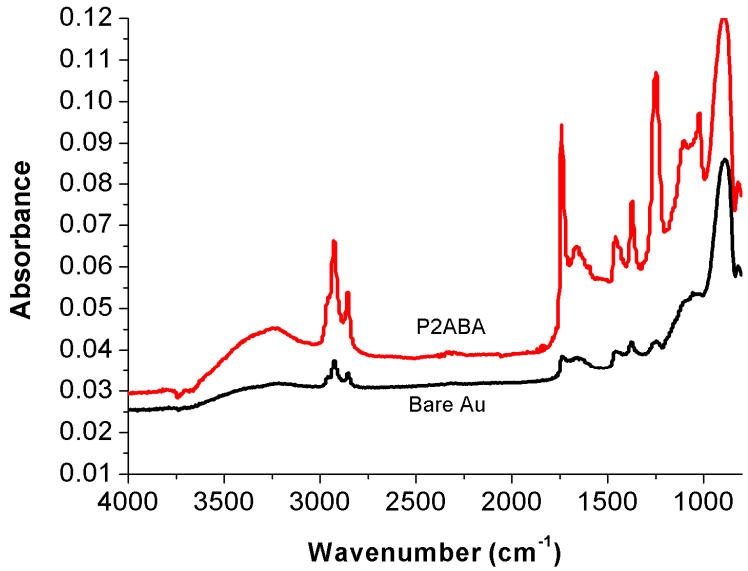

Figure 3.26 FTIR/ATR spectra of bare gold and P2ABA thin film.

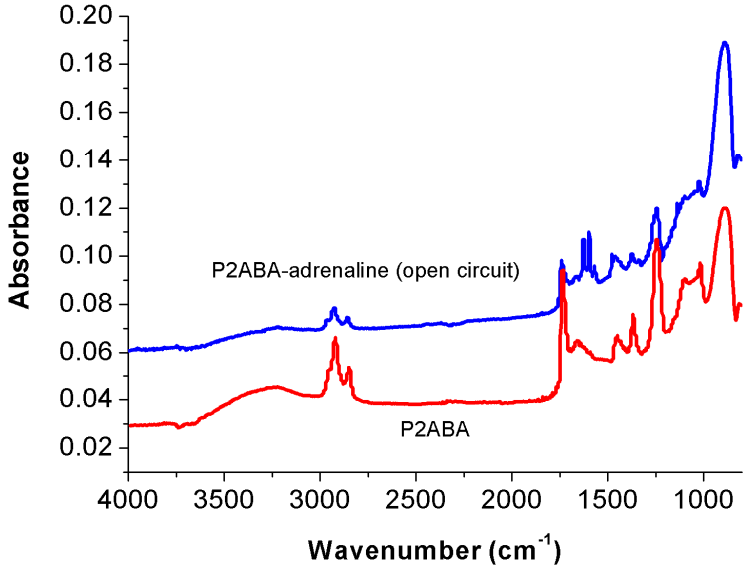

Figure 3.27 FTIR/ATR spectra of P2ABA thin film after the reaction with 1 mM adrenaline at an open circuit potential.

CHAPTER 4

CONCLUSION

Fabrication of P2ABA thin films by electrochemical-surface plasmon resonance (EC-SPR) spectroscopy technique was successfully prepared. Characterize and study the properties of P2ABA thin films were investigated by using EC-SPR, UV-vis, AFM, FT-IR/ATR and QCM-D techniques**.** Detection of some biomolecules such as adrenaline, UA and AA, using P2ABA thin films were investigated.

The P2ABA thin film was grown on the gold surface by electropolymerization of 2-ABA monomer. During cyclic voltammetry scan the first oxidation peak at about 0.85 V corresponds to the oxidation of 2-ABA monomer to form P2ABA film. The dedoping peak at about 0.4 V in the cathodic scan and doping peak at about 0.5 V in the anodic scan of the second cycle correspond to the electron transfer to formation of redox couple during the oxidation of P2ABA on electrochemical sensor. The SPR curve was shifted to the higher dip angle after electropolymerization indicating the P2ABA was deposited on the gold electrode. The thickness of the film was calculated by Fresnel calculation (Winspall software version 3.02) by fitting the obtained SPR curves. The thickness of deposited P2ABA film was estimated to be 10 nm.

For the detection of adrenaline on the P2ABA thin film, electroactivity of P2ABA was studied in PBS supporting electrolyte solution (pH 7.4) by cyclic voltammetry, which indicated that the electrochemical signal can be enhance event of specific reaction with adrenaline. The SPR reflectivity change was observed after

injection of 1 mM adrenaline at an applied potential of 0.5 V. SPR reflectivity increase rapidly and gradually increased due to the specific adsorption and physical adsorption between adrenaline with benzylamine in P2ABA structure. The detection limit of SPR reflectivity response upon injection of adrenaline into P2ABA thin film was determine to be 10 pM at an open circuit potential. EC-SPR response of adrenaline in the presence of UA and AA was also studied, the current and reflectivity changes in the UA and AA were observed to be smaller than that of adrenaline because UA and AA did not has a catechol group in the structure react with benzylamine to form fluorescence derivative structure. Furthermore, the experiment at –0.2 V and open circuit (dedoped and neutral state of P2ABA in PBS solution) were found that increase the selectivity of adrenaline detection over UA and AA. Since adrenaline easily oxidizes to react with benzylamine site and offers the electron to P2ABA, the P2ABA becomes the dedoped state. Moreover, the P2ABA film has an amino-functionalized group, which can attract the negative ion from adrenaline. Therefore, EC-SPR response of adrenaline in the presence of UA and AA at –0.2 V and an open circuit was observed in terms of selectivity than that of 0.5 V. UV-vis absorption spectra properties at applied constant potential of 0.5 V indicated that the specific reaction of adrenaline with benzylamine in P2ABA structure. The selectivity of adrenaline by detected at a constant applied potential of –0.2 V and an open circuit, which showed improvement of the selectivity because SPR reflectivity response of adrenaline separating from the SPR reflectivity responses detect of UA and AA. Furthermore, QCM-D result at an open circuit indicated that adrenaline reacted with benzylamine site in the P2ABA films and confirmed the result from EC-SPR spectroscopy.

More characterization on P2ABA were performed using UV-vis spectrophotometry. UV-vis absorption spectra of P2ABA thin films were studied before and after injection of 1mM of adrenaline, UA and AA. The new peak appeared at 490 nm after injection of 1mM adrenaline this should be because of the specific reaction with benzylamine site in P2ABA structure. The maximum peak at 301 nm was a form main peak of adrenochrome [95]. A mechanism for this reaction to produce fluorescent derivative, it may possible due to the P2ABA thin film was stilled in the doped state in the PBS solution and oxidized adrenaline by accepting the electron from adrenaline, then the P2ABA become the dedoped state [6].

FTIR/ATR is a technique which is used to obtain an infrared spectrum of absorption, emission, photoconductivity or Raman scattering of a solid, liquid or gas. An FTIR spectrometer simultaneously collects spectral data in a wide spectral range. This confers a significant advantage over a dispersive spectrometer, which measures intensity over a narrow range of wavelengths at a time. FTIR technique has made dispersive infrared spectrometers all but obsolete (except sometimes in the near infrared) and opened up new applications of infrared spectroscopy. The P2ABA film was electropolymerization on the gold-coated high reflective index glass substrate to study the specific reaction. The board adsorption at 3300 cm^{-1} indicates the presence of –OH group. The absorption band in the 3000–2800 cm^{-1} region indicates the $–NH_2$ group. After the reaction of P2ABAwith 1mM adrenaline, the adsorption at 3300 cm^{-1} and 3000–2800 cm^{-1} region disappeared. This suggests that the reaction of –OH group in adrenaline structure with the benzylamine structure in P2ABA. The adsorption spectra at 1710 cm^{-1} region disappeared after reaction with adrenaline, indicating that adrenaline was oxidized to adrenochrome and give electron to P2ABA. The C=O

bond to form fluorescent derivative (see the reaction at Figure 3.7) and P2ABA became de-doped state.

The atomic force microscopes (AFM) is a very high-resolution scanning probe microscopes, which demonstrated resolution of fractions of a nanometer, more than 1000 times better than the optical diffraction limit. AFM was used to examine the specific reaction, the surface topography of binding reaction of adrelaline to P2ABA film at a several applied constant potentials were observed as shown in Figure 3.18. The roughness of P2ABA film for the binding reaction of adrelaline at a constant potentials of –0.2V, open circuit and 0.5V were 4.106, 2.111 and 1.448 nm, respectively. The roughness decreased with increasing the constant applied potential, suggesting that P2ABA-surface has a rough topography and space filling the specific reaction site. P2ABA film became smooth surface after the binding reaction with adrenaline. The adsorption occur more readily on P2ABA surface, since applied a constant potential at the positive compared to that an open circuit potential.

CURRICULM VITAE

Name Mr. Sopis Chuekachang

Date of Birth February 12, 1976

Education Background

Ph.D. Electrical and Information Engineering, 2013, Graduate School of Science and Technology, Niigata University, Niigata, JAPAN

Thesis Topic: Electrochemically Controlled Detection of Some Bio-molecules on Poly(2-aminobenzylamine) Thin Films by Surface Plasmon Resonance Spectroscopy

Thesis Advisor: Assoc. Prof. Dr. Akira Baba

Ph.D. Chemistry, Chiang Mai University, Chiang Mai, THAILAND

Thesis Topic: Fabrication of conducting polymer-single walled carbon nanotube composites thin film by electrochemical surface Plasmon resonance (EC-SPR) spectroscopy for the detection of some biomolecules

Thesis Advisor: Assoc. Prof. Dr. Sukon Phanichphant

M.Sc. Chemistry (Analytical Chemistry), August 2005, King MongKut's Institute of Technology Ladkrabang, Bangkok, THAILAND.

Thesis Topic: Single-wall carbon nanotube modified glassy carbon electrode for electroanalytical determination of dopamine

Thesis Advisor: Assoc. Prof. Dr. Suwan Chaiyasit

B.Sc. Chemistry , March 1999, Maha Sarakham University, Maha Sarakham THAILAND

Thesis Topic: Determination of magnesium, potassium and sodium ions in soil by gravimetric titration

Thesis Advisor: Dr. Neramit Morakot

Scholarship:

1. The Center for Innovation in chemistry (PERCH-CIC) Thailand, 2009–2012
2. “Global Circus” Program of Niigata University supported by the Ministry of Education, Culture, Sports, Science and Technology, Japan, 2010–2012

Conferences

1. Sopis Chuekachang, Sukon Phanichphant, Suwan Chaiyasit, Single-wall carbon nanotube modified glassy carbon electrode for electroanalytical determination of dopamine, Poster Presentation, The 2nd German-Thai Symposium on Nanoscience and Nanotechnology, September 21–22, 2009, Chiang Mai Orchid Hotel, Chiang Mai, THAILAND

2. Sopis Chuekachang, Sukon Phanichphant, Suwan Chaiyasit, Fabrication of modified SWNTs/glassy carbon electrode for the determination of dopamine, Poster Presentation, KJF International Conference on Organic Material for Electronics and Photonics (KJF) 2010, August 22–25, 2010, Kitakyushu, Fukuoka, Japan.

3. Sopis Chuekachang, Akira Baba, Sukon Phanichphant, Saengrawee Sriwichai, Udom Sriyotha, Kazunari Shinbo, Keizo Kato, Futao Kaneko, Nobuko Fukuda, Hirobumi Ushijima, Detection of catecholamine using electropolymerized poly(2-aminobenzylamine) thin film, Oral Presentation, JSPS Hokuriku-Shinetsu Branch conference, 19–20 November 2010, Kanazawa, Japan.

4. Sopis Chuekachang, Akira Baba, Sukon Phanichphant, Saengrawee Sriwichai, Udom Sriyotha, Kazunari Shinbo, Keizo Kato, Futao Kaneko, Nobuko Fukuda, Hirobumi Ushijima, Electrochemical-surface plasmon resonance sensor for the detection of adrenaline on poly(2–aminobenzylamine) thin film, Poster Presentation, May 20–23, 2012, 14th International Meeting on Chemical Sensors-IMCS, Nürnberg/Nuremberg, Germany

5. Sopis Chuekachang, Akira Baba, Sukon Phanichphant, Saengrawee Sriwichai, Udom Sriyotha, Kazunari Shinbo, Keizo Kato, Futao Kaneko, Nobuko Fukuda, Hirobumi Ushijima, Fabrication of thin film from conducting polymer/single wall carbon nanotube composites for the detection of uric acid, Poster Presentation, August 29–September 1, 2012, KJF International Conference on Organic Materials for Electronics and Photonics, Sendai, Japan

Publications

1. Sopis Chuekachang, Sukon Phanichphant, Suwan Chaiyasit, Viruntachar Kruefu, Single-wall carbon nanotube modified glassy carbon electrode for electroanalytical determination of dopamine, Proceedings of the 2010 5th IEEE International Conference on Nano/Micro Engineered and Molecular Systems, January 20–23, 2010, Xiamen, China

2. Sopis Chuekachang, Sukon Phanichphant, Suwan Chaiyasit, Fabrication of modified SWNTs/glassy carbon electrode for the determination of dopamine, Published, *Molecular crystals and Liquid Crystals*, 16 May 2011.

3. Rapiphun Janmanee, Sopis Chuekachang, Saengrawee Sriwichai, Akira Baba, Sukon Phanichphant, Functional conducting polymer in the application of SPR biosensors, Published, May 21, 2012, *Journal of Nanotechnology*, Volume 2012.

4. Sopis Chuekachang, Akira Baba, Sukon Phanichphant, Saengrawee Sriwichai, Udom Sriyotha, Kazunari Shinbo, Keizo Kato, Futao Kaneko, Nobuko Fukuda, Hirobumi Ushijima, Electrochemical-surface plasmon resonance sensor for the detection of adrenaline on poly(2–aminobenzylamine) thin film, Published, ICMS 2012–The 14th International Meeting on Chemical Sensors, 2012, pp 1414–1417.

Reference

Assoc. Prof. Dr. Akira Baba

E-mail: ababa@eng.niigata-u.ac.jp , Center for Transdisciplinary Research Niigata University 8050 Ikarashi 2-nocho, Nishi-ku, Niigata 950-2181 JAPAN

Assoc. Prof. Dr. Sukon Phanichphant

E-mail: sphanichphant@yahoo.com, Office location: CB1 Building,

Department of Chemistry, Faculty of Science, Chiang Mai University, 239 Huaykaew Rd., Tambon Suthep, Amphoe Muang, Chiang Mai. 50200 THAILAND.

REFERENCES

1. Guimard, N. K., Gomez, N. and Schmidt, C. E., Conducting polymers in biomedical engineering, *Prog. Polym. Sci*., 2007, **32**, 876–921.
2. Shirakawa, H., Louis, E. J., MacDiarmid, A. G., Chiang, C.K. and Heeger, A. J., Synthesis of electrically conducting organic polymers: halogen derivatives of polyacetylene, $(CH)_x$, *J. Chem. Soc,. Chem. Commun*., 1977, 578–580.
3. Hikmet, R. A. M., New lithium–ion polymer battery concept for increased capacity, *J. Power Sources*, 2001, **92**, 212–220.
4. Mortimer, R. J., Dyer, A. L. and Reynolds, J. R., Electrochromic organic and polymeric materials for display applications, *Displays*, 2006, **27**, 2–18.
5. Cater, S. A., Angelopoulos, M., Karg, S., Brock, P. J. and Scott, J. C., Polymeric anodes for improved polymer light–emitting diote performance, *Appl. Phys.Lett*., 1997, **70**, 2067–2069.
6. Baba, A., Mannen, T., Ohdaira, Y., Shinbo, K., Kato, K., Kaneko, F., Fukuda, N. and Ushijima, H., Langmuir, Detection of adrenaline on poly(3–aminobenzylamine) ultrathin film by electrochemical–surface plasmon resonance spectroscopy, *Langmuir*, 2010, **26**, 18476–18482.
7. Sriwichai, S., Baba, A., Phanichphant, S., Shinbo, K., Kato, K. and Kaneko, F., Electrochemically controlled surface plasmon resonance immunosensor for the detection of human immunogloblin G on poly(3–aminobenzoic acid) ultrathin films, *Sens. Actuat. B-Chem.*, 2010, **147**, 322–329.

8. Janmanee, R., Baba, A., Phanichphant, S., Sriwichai, S., Shinbo, K., Kato, K. and Kaneko, F., Detection of human IgG on poly(pyrrole–3–carboxylic acid) thin film by electrochemical–surface plasmon resonance spectroscopy, *Jpn. J. Appl. Phys.*, 2011, **50**, No. 1, 01BK02–06.

9. Tian, S., Baba, A., Liu, J., Wang, Z., Knoll, W., Park, M. K. and Advincula, R., Electroactivity of polyaniline multilayer films in neutral solution and their electrocatalyzed oxidation of β–nicotinamide adenine dinucleotide, *Adv.Funct. Mater.*, 2003, **13**, 473–479.

10. Raffa, D. L. and Battaglini, F., Novel conducting polyaniline bearing functional groups, *J. Electroanal.Chem.*, 2001, **54**, 120–124.

11. Epstein, A. J.and MacDiarmid, A. G., Polyanilines: from solutions to polymer metal, from chemical currosity to technology, *Synth. Met.*, 1995, Issues 1–3, 179–182.

12. Salaneck, W. R., Friend, R. H. and Brédas, J. L., Electronic Structure of Conjugated polymers: consequences of electron–lattice coupling, *Phys. Rep*., 1999, **319**, 231–251.

13. Bakhshi, A. K., Electrically conducting polymer: from fundamental to applied research, *Bull. Mater. Sci.*, 1995, **18** 469–495.

14. Oh, T., Characteristic of organic thin film depending on carbon content by furier transform infrared spectra and X–ray diffraction pattern, *Bull. Korean Chem. Soc*. 2007, **28**, 1588–1590.

15. Groenendaal, L., Jonas, F., Freitag, D., Pielartzik, H. and Reynolds, J. R., Poly(3,4–ethylenedioxythiophene) and its derivatives: past, present, and future, *Adv. Mater.*, 2000, **12** (7), 481–494.

16. Brédas, J. L. and Street, G. B., Polarons, bipolarons, and solutions in conducting polymers, *Accounts Chem. Res.*, 1985, **18**, 309–315.

17. Blatchford, W. and Epstein, A. J., Resource letter: electronic polymer and their applications, *Amer. J. . Phys.*, 1996, **64**, 120–135.

18. Wilbourn, K., and Murray, R. W., The D.C. redox versus electronic conductivity of the ladder polymer poly(benzimidazobenzophenanthroline), *J. Phys. Chem.*, 1988, **92**, 3642–3648.

19. Mark, J. E. (Ed.), *Physical Properties of Polymers Handbook*, AIP Press, New York, 1996.

20. Skotheim, T., (Ed.), *Handbook of Conducting Polymers*, Marcel Dekker, New York, 1986.

21. Brédas, J. L. and Silbey, R., *The Novel Science and Technology of Highly Conducting and Nonlinear Optically Active Materials*, Kluwer, Dordrecht, Netherlands. 1991.

22. Guimard, N. K., *Biodegradable Electroactive Materials for Tissue Engineering Applications*, The University of Texas at Austin, 2008.

23. Baba, A., Tian, S., Stefani, F., Xia, C., Wang, Z., Advincula, R. C., Johannsmann, D. and Knoll, W., Electropolymerization and doping/dedoping properties of polyaniline thin film as studied by electrochemical–surface plasmon spectroscopy and by the quartz crystal microbalance, *J. Electroanal. Chem.*, 2004, **562,** 95–103.

24. W.S. Huang, B.D. Humphrey and A.G. MacDiarmid, Polyaniline, a novel conducting polymer. morphology and chemistry of its oxidation and reduction in aqueous electrolytes, *J. Chem. Soc., Faraday Trans. 1*, 1986, **82** 2385–2400.

25. Yánez–Heras, J., Planes, G. A., Williams, F., Barbero, C. A., and Battaglini, F., Sequential electrochemical polymerization of aniline and their derivatives showing electrochemical activity at neutral pH, *Electroanal.*, 2010, **22** (23), 2801–2808.

26. Huanga, L. M., Chena, C. H., and Wen, T. C., Delopment and characherization of flexible electrochromic devices based on polyaniline and poly(3,4–elethylenedioxythiophene)–poly(styrene sulfonic acid), *Electrochimica Acta*, 2006, **51**, 5858–5863.

27. Stejskal, J., and Gilbert, R. G., Polyaniline. preparation of a conducting polymer (IUPAC Techincal Report), *Pure Appl. Chem.* 2002, **74**, 857–867.

28. Vidal, J. C., Garcia–Ruiz, E. and Castillo, J.R., Recent advances in electropolymerized conducting polymers in amperometric biosensor, *Microchim. Acta*, 2003, 143, 93–111.

29. Adhikari, B. and Majumdar, S., Polymer in sensor applications, *Prog. Polym. Sci.* 2004, **29**, 699–766.

30. Lee, J. W., Serna, F., Nickels, J. and Schmidt, C. E., Carboxylic acid–functionalized conductive polypyrrole as a bioactive platform for cell adhesion, *Biomacromolecules,* 2006, 7, 1692–1695.

31. Pual, M. and Monk, S., *Fundamentals of Electro–Analytical Chemistry*, John Wiley, New York, 2001.

32. Christian, G. D., *Analytical Chemistry*, 5th ed., John Wiley, New York, 1994.

33. Plambeck, J. A., *Electroanalytical Chemistry*: *Basic Principle and Applications*, John Wiley, New York, 1982

34. Newman, J. S., *Electrochemical System*, Prentice–Hall, Englewood Cliffs, 1973.

35. Bard, A. J., and Faulkner, L. R., *Electrochemical Methods*: *Fundamentals and Applications*, 2nd ed., John Wiley, New York, 2000.

36. Heinze, J., *Electronically Conducting Polymers*. *In Topics in Chemistry*, Springer–Verlag,Berlin, 1990.

37. Chun, T. C., Kaufman, J. H., Heeger, A. J. and Wudl, F., Charge storage in doped poly(thiophene): optical and electrochemical studies, *Phys. Rev. B*, 1984, **30**,702–710.

38. Brédas, J. L. Chance, R. and Silbey, R., Comparative theoretical study of the doping of conjugated polymers: polarons in polyacetylene and polyparaphenylene, *Phys. Rev. B*, 1982, 26, 5843–5854.

39. Knoll, W., Interface and thin film as seen by bound electromagnetic waves, *Annu. Rev. Phys. Chem*., 1988, **49**, 569–638.

40. Hickel, W., Rothenhausler, B. and Knoll, W., Surface plasmon microscopic characterization of external surfaces, *J. Appl. Phys*., 1989, **66**, 4832–4836.

41. Baba, A., Advincula, R. C. and Knoll, W., In situ investigations on the electrochemical polymerization and properties of polyaniline thin films by surface plasmon optical techniques, *J. Phys. Chem. B*, 2002, **106**, 1581–1587.

42. Advincula, R. C., Aust, E., Meyer, W. and Knoll, W., In situ investigations of polymer self–assembly solution adsorption by surface plasmon spectroscopy, *Langmuir*, 1996, **12**, 3536–3540.

43. Xia, C., Advincula, R. C., Baba, A. and Knoll, W., *In situ* investigations of the electrodeposition and electrochromic properties of poly(3,4–ethylenedioxythiophene) ultrathin films by electrochemical–surface plasmon spectroscopy, *Langmuir*, 2002, **18**, 3555–3560.

44. Raitman, O. A., Katz, E., Buckman, A. F. and Wilner, I., Integration of polyaniline/poly(acrylic acid) films and redox enzymes on electrode supports: an in situ electrochemical/surface plasmon resonance study of the bioelectrocatalyed oxidation of glucose or lactate in the integrated bioelectrocatalytic systems, *J. Am. Chem. Soc*., 2002, **124**, 6487–6496.

45. Gardner, D. G. and Shoback, D., *Greenspan's Basic & Clinical Endocrinology*, 9th ed., McGraw-Hill, New York, 2011.

46. Purves, D., Augustine, G.J., Fitzpatrick, D., Hall, W. C., Lamantia, A. S., McNamara, J. O. and White, L. E., *Neuroscience*, 4th ed., Sinauer Associates, Sunderland, 2008.

47. Moghaddam, H. M. and Beitollahi, H., Simulataneous volatmmetric determination of norepinephrine and acetaminophen at the surface of a modified carbon nanotube paste electrode, *Int. J. Electrochem. Sci*., 2011, **6**, 6503–6513.

48. Joh, T. H. and Hwang, O., *Dopamine Beta–Hydroxylase: Biochemistry and Molecular Biology*, Annals of the New York Academy of Sciences, New York, 1987.

49. Manor, I., Tyano, S., Mel, E., Eisenberg, J., Bachner-Melman, R., Kotler, M. and Ebstein, R. P., Family-based and association studies of monoamine oxidase and attention deficit hyperactivity disorder (ADHD): preferential transmission of the long promoter-region repeat and its association with impaired performance on a continuous performance test (TOVA), *Mol. Psychiatr.*, 2002, **7**, 626–632.

50. Brunner, H. G., MAOA Deficiency and abnormal behaviour: perspectives on an association, *Ciba Foundation Symposium*, 1996**, 194**, 155–164, discussion 164–167. (http://europepmc.org/abstract/MED/8862875)

51. http://www.wisegeek.com/what-is-adrenaline.htm (November, 13 2012).

52. Cannon, W. B., Organization for physiological homeostasis, *Physiol. Rev.*, 1929, 9, 399–431.

53. Bennett, M., One hundred Years of Adrenaline: the Discovery of Autoreceptors, *Clin. Auton. Res.*, 1999, 9, 145–159.

54. http://www.unc.edu/~rowlett/units/scales/clinical_data.html (November, 15 2012).

55. http://www.amamanualofstyle.com/oso/public/jama/si_conversion_table.html (November, 15 2012).

56. Malik, V. S., Popkin, B. M., Bray, G. A., Després, J. P., Willett, W. C. and Hu, F. B., Sugar-sweetened beverages and risk of metabolic syndrome and type 2 diabetes: a meta-analysis, *Diabetes Care*, 2010, **33**, 2477–2483.

57. Pak, C. Y., Medical stone management: 35 years of advances, *J. Urology*, 2008, 180, 813–819.

58. Toncev, G., Therapeutic value of serum uric acid levels increasing in the treatment of multiple sclerosis, *Vojnosanit.Pregl.*, 2006, **63**, 879–882.

59. Lachapelle, M. Y. and Drouin, G., Inactivation dates of the human and guinea pig Vitamin C genes, *Genetica*, 2010, **139**, 199–207.

60. Aboul-Enein, H. Y. and Al-Duraibi, I. A., Analysis of L– and D–ascorbic acid in fruits and fruit drinks by HPLC, *Seminars in Food Analysis*, 1999, **4**, 31–37.

61. Musso, N. R., Vergassola, C., Pende, A. and Lotti, G., Simultaneous measurement of plasma catecholamine (norepinephrine, epinephrine, and dopamine) and free n-ethyl dopamine (epinine) levels, by HPLC with electrochemical detection, *J. Liq.Chromatogr*., 1990, **13**, 2217–2228.

62. Takahashi, M., Morita, M., Niwa, O. and Tabei, H., Highly sensitive high-performance liquid chromatography detection of catecholamine with interdigitated array microelectrodes, *J. Electroanal. Chem*., 1992, **335**, 253–263.

63. Nohta, H., Yukizawa, T., Ohkura, Y., Yoshimura, M., Ishida, J. and Yamaguchi, M., Aromatic glycinonitriles and methylamines as pre-column fluorescence derivatization reagents for catecholamines, *Anal. Chim. Acta*, 1997, **344**, 233–240.

64. Ragab, G. H., Nohta, H. and Zaitsu, K., Chemiluminescence determination of catecholamines in human blood plasma using 1,2-bis(3-chlorophenyl)ethylenediamine as pre-column derivatizing reagent for liquid chromatography, *Anal. Chim. Acta*, 2000, **403**, 155–160.

65. Kang, X., Cheng, G. and Dong, S., A novel electrochemical SPR biosensor, *Electrochem. Commun.*, 2001, **3**, 489–493.

66. Baba, A. and Knoll, W., Properties of poly(3,4-ethylenedioxythiophene) ultrathin films detected by in situ electrochemicalsurface plasmon field-enhanced photoluminescence spectroscopy, *J. Phys. Chem. B*, 2003, **107**, 7733–7738.

67. Wu, K., Fei, J. and Hu, S., Simultaneous determination of dopamine and serotonin on a glassy carbon electrode coated with a film of carbon nanotubes, *Anal. Biochem.*, 2003, **318**, 100–106.

68. Zhang, Y., Jin, G., Wang, Y. and Yang, Z., Determination of dopamine in the presence of ascorbic acid using poly(acridine red) modified glassy carbon electrode, *Sensor*s, 2003, **3**, 443–450.

69. Raj, C. R., Okajima, T. and Ohsaka, T., Gold nanoparticle arrays for the voltammetric sensing of dopamine, *J. Electroanal. Chem*., 2003, **543**, 127–133.

70. Peter, K., Nilsson, R. and Inganäs, O., Chip and solution detection of DNA hybridization using a luminescent zwitterionic polythiophene derivative, *Nature Mater*., 2003, **2** 419–424.

71. Baron, R., Zayats, M. and Willner, I., Dopamine-, L-DOPA-, adrenaline-, and noradrenaline-induced growth of Au nanoparticles: assays for the detection of neurotransmitters and of tyrosinase activity, *Anal. Chem*., 2005, **77**, 1566–1571.

72. Ma, Y., Yang, C., Li, N. and Yang, X., A sensitive method for the detection of catecholamine based on fluorescence quenching of CdSe nanocrystals, *Talanta*, 2005, **67,** 979–983.

73. Damos, F. S., Luz, R. C. S. and Kubota, L. T., Investigations of ultrathin polypyrrole films: formation and effects of doping/dedoping processes on its optical properties by electrochemical surface plasmon resonance (ESPR), *Electrochim. Acta*, 2006, **51**, 1304–1312.

74. S. R. Ali, Y. Ma, R. R. Parajuli, Y. Balogun, W. Y. C. Lai, H. He, A nonoxidative sensor based on a self-doped polyaniline/carbon nanotube composite for sensitive and selective detection of the neurotransmitter dopamine, *Anal. Chem*., 2007, **79,** 2583–2587.

75. Dong, H., Cao, X. D., Li, C. M. and Hu, W. H., An in situ electrochemical surface plasmon resonance immunosensor with polypyrrole propylic acid film: comparison between SPR and electrochemical responses from polymer formation to protein immunosensing, *Biosens. Bioelectron*., 2008, **23**, 1055–1062.

76. Hu, W., Li, C. M. and Dong, H., Poly(pyrrole-*co*-pyrrole propylic acid) film and its application in label-free surface plasmon resonance immunosensors, *Anal. Chim. Acta*, 2008, **630**, 67–74.

77. Wang, J., Wang, F., Chen, H., Liu, X. and Dong, S., Electrochemical surface plasmon resonance detection of enzymatic reaction in bilayer lipid membranes, *Talanta*, 2008, **75**, 666–670.

78. Song, S., Gao, Q., Xia, K. and Gao, L., Selective determination of dopamine in the presence of ascorbic acid at porous-carbon-modified glassy carbon electrodes, *Electroanal.*, 2008, **20**, 1159–1166.

79. Jeong, H. and Jeon, S., Determination of dopamine in the presence of ascorbic acid by nafion and single-walled carbon nanotube film modified on carbon fiber microelectrode, *Sensors*, 2008, **8**, 6924–6935.

80. Chernyshov, D. V., Shvedene, N. V., Antipova, E. R. and Pletnev, I. V., Ionic liquid-based miniature electrochemical sensors for the voltammetric determination of catecholamines, *Anal. Chim. Acta*., 2008, **621,** 178–184.

81. Yogeswaran, U. and Chen, S. M., Multi-walled carbon nanotubes with poly(methyleneblue) composite film for the enhancement and separation of electroanalytical responses of catecholamine and ascorbic acid, *Sens. Actuat. B-Chem.*, 2008, **130,** 739–749.

82. Kato, K., Yamashita, K., Ohdaira, Y., Baba, A., Shinbo, K. and Kaneko, F., Electrochemical surface plasmon excitation and emission light properties in poly(3-hexylthiophene) thin films, *Thin Solid Films*, 2009, **518**, 758–761.

83. Shankar, S. S., Swamy, B. E. K., Chandra, U., Manjunatha, J. G., Sherigara, B. S., Simultaneous determination of dopamine, uric acid and ascorbic acid with CTAB modified carbon paste electrode, *Inter. J. Electrochem. Sci.*, 2009, **4**, 592–601.

84. Manjunatha, R., Suresh, G. S., Melo, J. S., D'Souza, S. F. and Venkatesha, T. V., Simultaneous determination of ascorbic acid, dopamine and uric acid using polystyrene sulfonate wrapped multiwalled carbon nanotubes bound to graphite electrode through layer-by-layer technique, *Sensor. Actuat. B-Chem.*, **2010**, 145, 643–650.

85. Chuekachang, S., Kruefu, V., Phanichphant, S. and Chaisit, S., Fabrication of modified SWNTs/glassy carbon electrode for the determination of dopamine, *Mol. Cryst. Liq. Cryst*., 2011, **538**, 292–297.

86. Binning, G., Quate, C. F. and Gerber, Ch., Atomic force microscope, *Phys. Rev. Lett*., 1986, **56**, 930–933.

87. http://en.wikipedia.org/wiki/Atomic_force_microscopy (November, 16 2012).

88. Baba, A., Kaneko, F., Advincula, R. and Knoll, W., *Electrochemical-Surface Plasmon Resonance Methods for Polymer Thin Films, Functional Polymer Films*, Wiley-VCH Verlag GmbH & Co. KGaA, New York, 2011.

89. Liu, J., Tian, S. and Knoll, W., Properties of polyaniline/carbon nanotube multilayer films in neutral solution and their application for stable low-potential detection of reduced β-Nicotinamide adenine dinucleotide, *Langmuir*, 2005, **21**, 6696–5599.

90. Yamaguchi, M., Ishida, J. and Yoshimura, M., Simultaneous determination of urinary catecholamines and 5–hydroxyindoleamines by high-performance liquid chromatography with flourescence detection, *Analyst*, 1998, **123**, 307–311.

91. Fujino, K., Yoshitake, T., Kehr, J., Notha, H. and Yamaguchi, M., Simultaneous determination of 5–hydroxyindoles and catechols by high-performance liquid chromatography with fluorescence detection following derivatization with benzylamine and 1,2–diphenylethylenediamine, *J. Chromatogr. A*, 2003, **1012**, 169–177.

92. Norde, W. and Lyklema, J., Why proteins prefer interfaces, *J. Biomater. Sci. Polym*. Ed., 1991, **2**, 183–202.

93. Umpley II, R. J., Baxer, S. C., Ranpey, A. M., Rushton, G. T., Chen, Y. and Shimizu, K. D., Characterization of the heterogeneous binding site affinity distributions in molecularly imprinted polymers, *J. Chromat. B*, 2004, **804**, 141–149.

94. Sauerbrey, G., Verwendung von schwingguarzen zur wägung dünner schichten und zur mikrowägung, *Z. Phys. A*, 1959, 155, 206–222.

95. Polewski, K., Spectroscopic detection of adrenaline-quinone formation in resonance micelles, *Biochim. Biophys. Acta*, 2000, **1523**, 56–64.